Fine Sediment Pathways and Connectivity in San Francisco South Bay

L. van Gijzen

TU Delft Delft University of Technology

Deltares Enabling Delta Life

SFEI AQUATIC SCIENCE CENTER
SAN FRANCISCO ESTUARY INSTITUTE & THE AQUATIC SCIENCE CENTER

Sediment Pathways and Connectivity in San Francisco South Bay

by

L. van Gijzen

to obtain the degree of Master of Science
at the Delft University of Technology,

Student number:	4324064	
Project duration:	April 15, 2019 – March 16, 2020	
Thesis committee:	Dr. ir. B. van Prooijen,	TU Delft
	Prof. Dr. ir. P. Herman,	TU Delft; Deltares
	Dr. ir. M. van der Wegen,	Deltares; UNESCO IHE
	Ir. S. G. Pearson,	TU Delft ; Deltares

An electronic version of this thesis is available at `http://repository.tudelft.nl/`.

In collaboration with:

TU Delft Delft University of Technology

Deltares Enabling Delta Life

SFEI AQUATIC SCIENCE CENTER
SAN FRANCISCO ESTUARY INSTITUTE & THE AQUATIC SCIENCE CENTER

Preface

Writing a thesis is a bit like following a rainbow to find a bag of gold for 10 months. You know which direction you want to go, but sometimes the path seems long and unclear. Yet, something great is waiting for you in the end. Luckily, while you walk the meandering road alone, there are always people along the way to help you and to point you in the right direction. Now that I have finally found the bag of gold in the end, I would like to take this opportunity of acknowledging all the people who have helped me in the process.

First of all, this thesis builds on the studies of previous students who worked on this model. Thank you Silvia Pubben, Oxana van Kempen, Michelle Gostic and Sienna White for paving the way. I want to thank Vincent van Zelst at Deltares for you guidance, the help with the DELWAQ model and the general issues with Deltares technology. You were my mentor during my first week in of study Delft and now during my thesis. We can say "de cirkel is weer rond". Thanks to all my fellow-students at Deltares for the lunches, coffees and well-needed breaks. Many thanks to Arjen Markus, without whom I would not have been able to deal with the different model versions that came my way. To the people at San Francisco, thank you for providing me with the local knowledge, additional data and encouraging interest in my work.

Then of course, thank you to my committee, - Bram van Prooijen, Peter Herman, Mick van der Wegen and Stuart Pearson. Mick, thank you for providing me with the opportunity to work on this cool and interesting topic, all the advise, suggestions, fun side stories about the Bay Area and for checking-in if I was still having fun during the process. Thank you Stuart for all the tips on thesis writing, for introducing me to Sediment Connectivity, your constant support in my research and most importantly, your contagious enthusiasm for everything related to coasts and sediments. Thank you Bram and Peter for pointing out the interesting results to further analyse and for all the guidance in how to transform my model results into an interesting scientific report.

Although this is the preface of the thesis I completed at Deltares, this work was not possible without the support and sometimes well-needed distraction from my family and friends. First of all, I want to thank all the people who made my life at TU Delft better by studying together but most importantly simply by being my friends. Of course Tessa, you've been my companion since the first 10 minutes that I walked into the civil building, to Canada and back, up until my repetition for my thesis presentation and hopefully for many more years to come. To Wilmine and Kate, and all the hours hard-work spend together in our first master year, I was really happy to be your minion. And of course a special mention for Camila, Irene and Tessa with whom I roamed the Canadian roads in the ice-cold, looked out over staggering snowy mountains, walked over the most beautiful Pacific beaches and not to forget broke through the Canadian peace and quiet by singing along to our playlist on the top of our voices. Thank you Jip for all the distraction(sometimes a bit too much) and encouragement you provided during my thesis.

Thank you to my family, who has always been so interested in everything what I've been doing over here. I very much enjoyed the all texts, every time a beach, San Francisco, sea-level rise or anything likewise was in the news(which is quite often). I even received texts when a TU professor was in the news to ask if I knew them, which usually wasn't the case. And of course a special thanks to my Mum, Dad and brother who were always ready to help me over the last years whenever I needed it and were so interested they even paid an (in the family infamous) visit to my fieldwork at the Sand Engine.

Laurie van Gijzen
Delft, March 2020

Executive Summary

San Francisco Bay is one of the largest estuaries of the US Pacific Coast with an area of 4000 km2. Within two centuries the estuary has developed into a highly urbanized area with over 7 million inhabitants. It has impacted the coastal-estuarine system to a high degree by causing severe alterations to the Bay's geomorphology and water quality. South Bay is a sub-embayment of a unique character. It does not experience the freshwater flushing typical for estuaries as both saline as freshwater enter through the same inlet. South Bay is dealing with increased risk of inundation due to the combination of sea level rise and land subsidence and a deteriorating water quality.

Most of South Bay's coastal communities will eventually be at risk of flooding under current sea-level rise predictions. Next to that, the Bay's ecosystem is under increased stress due to toxic algae blooms in Spring which have become more frequent over the last decades. Understanding sediment pathways within South Bay and sediment exchange at its entrance can support the development of management strategies dealing with turbidity depended algae blooms and the development of salt marshes as a measure against sea level rise. Additionally, by understanding the current factors controlling fine sediment dynamics, future implications of climate change can be better predicted. Though San Francisco Bay is the topic of much research, a process-based model with a model domain covering the entire Bay is a novel approach to analyse fine sediment dynamics in South Bay.

A Delft3D-DELWAQ buffer layer model was calibrated against a newly available combination of local high-frequency suspended sediment concentration (SSC) measurements and two-monthly, depth varying SSC measurements across the entire 145 km length of the Bay. Subsequently the method of Sediment Connectivity was applied to analyse sediment pathways and net sediment fluxes in South Bay. Sediment Connectivity is an approach that uses network analysis to quantify sediment fluxes based on a schematization of San Francisco Bay into 17 segments. Large data sets of spatial and temporal output were reduced to a 17x17 adjacency matrix permitting a more straightforward analysis and the application of different statistical metrics unavailable in more traditional approaches.

Calibration efforts in this study have enabled the model to better capture seasonal and episodic variations in SSCs across the Bay. Modelled SSCs in South Bay during Spring were increased to the measured values. Furthermore, a higher vertical gradient in the water column was modelled which increased the amount of sediment available for resuspension during energetic episodes.

Connectivity analysis uniquely revealed key dominant pathways, with strongest fluxes being exchanged within the northern part of South Bay and with Central Bay. Southern flats are most in connection with Lower South Bay, but these fluxes are at least an order of magnitude smaller. Strongest fluxes in South Bay are observed during Spring and Summer when the summer sea breeze causes resuspension at the eastern flats, which agree well with literature.

Additionally, intra-Bay net-transports, net-exchange of sediment at the inlets and regions of erosion and sedimentation were found. While Lower South Bay showed a steady rate of import during the year, the rate of exchange at the South Bay entrance showed seasonal variations, though ended up to being importing by the end of the year. While South Bay was of a well-mixed nature from October-December it was gradually importing with peak imports during winter storms. During the regime of reverse circulation import halted, but showed a steep increase during the classic circulation in March. From April until July waves and residual currents generated by summer breezes led to export for South Bay. During calmer conditions in August and September South Bay gradually started importing again.

While keeping the limitations of the DELWAQ-Model and the Sediment Connectivity in mind, the research results can be used to predict the impact of current sediment dynamics on the issues of South Bay. Understanding of this impact can help to develop current management strategies and future policies to acquire and retain a healthy and safe estuary. It can for instance help identify regions of accretion or erosion, and therefore identify regions that are favourable for salt marsh restoration, or regions that require more attention. Additionally, by revealing the main sediment pathways it also provides an indication of pathways of contaminants such as mercury. Lastly, this study acts as a proof of concept for the Sediment Connectivity method that could be implemented to study fine sediment dynamics in other estuaries.

Contents

1

Introduction

San Francisco Bay (SFB) is part of one of the biggest estuaries of the North West Pacific Coast of the US with a surface area of about 4000 km2. It is a complex estuarine system and consists out of the two hydrologically distinctive sub-embayments North Bay and South Bay, separated by Central Bay which is connected with the Pacific Ocean at Golden Gate (Gartner, 2004). North Bay experiences a significant freshwater input from the confluence of the regionally important Sacramento River and San Joaquin River, which is also known as “The Delta" (Figure 1.1). Most parts of San Francisco Bay are dealing with eroding shores, increased risk of inundation due to the combination of sea-level rise and land subsidence and a deteriorating water-quality.

Within two centuries the estuary has developed into a highly urbanized area with over 6.1 million inhabitants (Cox, 2019). The urban development over the last centuries has impacted the coastal-estuarine system to a high degree (McKee et al., 2013). The Californian Gold Rush caused severe alterations to the Bay’s geomorphology and water quality, with an increase of 150% in yearly sediment input from the Delta in peak years of the main period of hydraulic mining (1852–1884) with respect to preceding volumes. The mercury used for hydraulic mining has found its way to the Bay through the river discharge from the Delta resulting in poor water quality throughout the Bay. Over the years the water quality declined further as a result of chemical disposal and sewer input into the Bay due to industrial and urban activities. Motivated by the Bay’s deteriorating condition and poor water quality, the San Francisco Bay coastal system has been the topic of sediment transport research for nearly 100 years (Barnard et al., 2013a). This results in the availability of data records which can go back decades.

Historically, the largest part of the Bay consisted of salt marshes and tidal mudflats. Many mudflats disappeared in the previous century as much of the land was reclaimed for industrial or residential purposes. The loss of mudflats caused a decline in unique habitats and subsequently a decrease in animal populations and vegetation. Over time human interventions such as river dams have altered the sediment budget of the Bay causing additional erosion along its coast. Analysis of sediment input from the Delta has shown a decreasing trend of -1.3%/year during the second half of the 20th century (Wright and Schoellhamer, 2004). Bathymetric volume change studies show that both North Bay (Jaffe et al., 2007) and Central Bay (Fregoso et al., 2008) experience sediment losses while only South Bay shows net sediment import (Jaffe and Foxgrover, 2006). The overall volume change in San Francisco Bay shows an eroding trend (Barnard et al., 2013c), which corresponds with the coastal erosion and shrinkage of mudflat areas.

Conceptual overviews of hydrodynamics (Conomos, T. J. Walters and Cheng, 1985) and sediment dynamics (Barnard et al., 2013c) together with the bathymetric studies give insight into general trends in sediment dynamics and can generate hypotheses for potential causes. Yet as these studies are not physical process-based it is hard to identify the precise impact and responsible processes of the change in sediment transport. The study of Barnard et al. (2013a) uses a processed based model, but focusses on sand transport and was run in depth-averaged mode (2D), which is not suitable for fine sediment studies in seasonally stratified areas. Other studies in San Francisco Bay were based on the linking of single-point measurements of hydrodynamic conditions and suspended sediment concentrations while considering only a single part of the Bay. A significant part of this type of research work has focused on the northern part of the Bay (e.g., McKee et al. (2006);

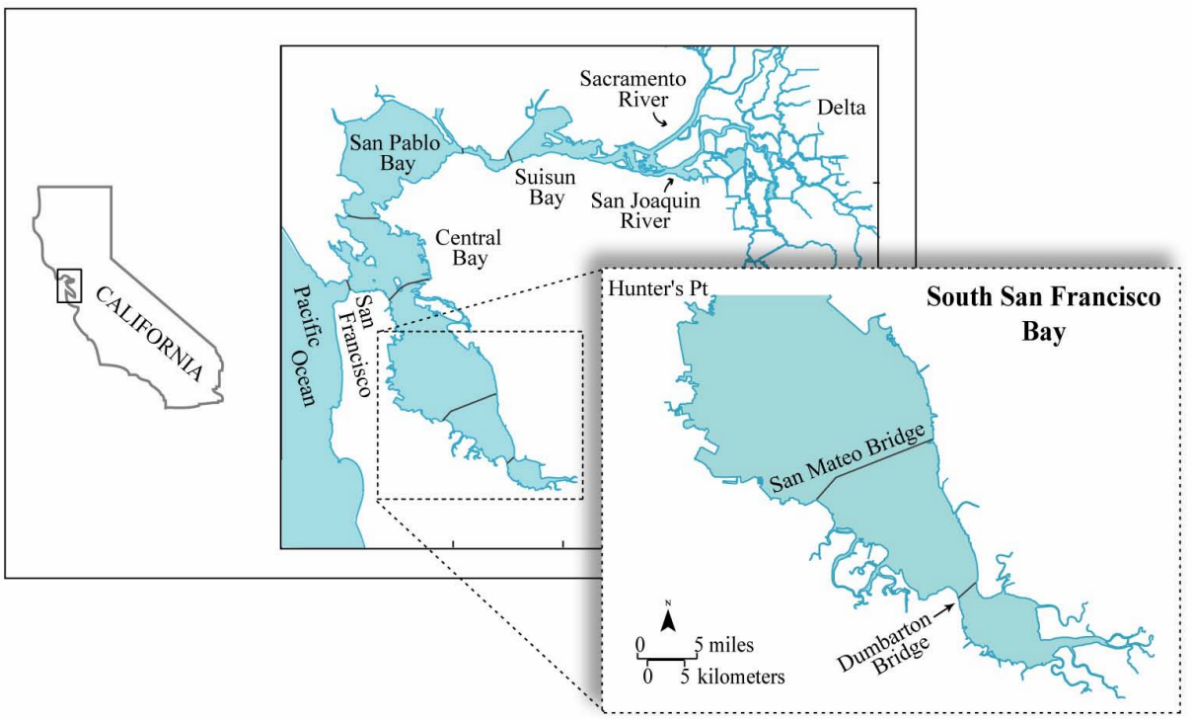

Figure 1.1: Overview of the topographic location of San Francisco Bay and its sub-embayments (from: Foxgrover et al. (2004))

Higgins et al. (2007); David et al. (2009)). Only a few studies were dedicated to the understanding of sediment dynamics in South Bay (eg. Egan et al. (2019),Lacy et al. (2017a) and Brand et al. (2010)).

1.1. Problem Definition

South Bay is dealing with water quality issues and local erosion like the rest of the Bay. South Bay extends from the Oakland Bay Bridge to the south-eastern tip of the Bay at San Jose (Figure 1.1). The sub-embayment is of a funnel shape with its narrowest point at the Dumbarton Narrows. South of the Dumbarton Narrows the cross-section widens again and it's referred to as Lower South Bay. South Bay is unique as both saline as freshwater enter from Central Bay through the same entrance. The main source of freshwater input for South Bay is traced back to the Delta (Barnard et al., 2013a). South Bay also experiences some freshwater input from local tributaries, though the amount is significantly smaller. This implies that South Bay does not experience the freshwater flushing typical for estuaries. Especially Lower South Bay experiences long residence times and sewage input, which makes it vulnerable to water quality issues such as (toxic) algae blooms.

Although the previously mentioned study of Jaffe and Foxgrover (2006) reported a net accretion of sediment in South Bay, a study by Schoellhamer (2011) shows a decreasing trend in mean SSCs south of Dumbarton Bridge. This may increase the risk of toxic algae blooms, which have previously damaged the Bay's ecosystem. Starting this millennium, San Francisco Bay has transformed from a low-productivity estuary to one having primary production typical of temperate-latitude estuaries. This shift is hypothesized to be the result of a decreasing trend in turbidity levels in South Bay, but this suspected relation is still a topic of research. Further information on suspended sediment concentrations and sediment exchange at the Dumbarton Narrows is needed to develop management decisions regarding water quality management.

South Bay is found to be relatively muddy (<63μm) with respect to the other sub-embayments. While local tributaries are an important source of sediment to South Bay, the contribution from Delta sediments is also hypothesized (Barnard et al., 2013a). Yet it is uncertain which processes are responsible for the exchange of sediment between Central Bay and South Bay, which part of the Bay is the main source of the sediment for the net import found by Jaffe and Foxgrover (2006). In literature, tidal asymmetry is identified to be responsible for a net-import most of the year with most sediment accretion at the flats. Net import hypo-

thetically increases during periods of high Delta discharge in Winter (Barnard et al., 2013a), while summer breezes cause resuspension at the flats. The sediment transport pathways within South Bay itself are mostly unknown, as are the sediment transport budgets. Understanding sediment pathways within South Bay and sediment exchange at its entrance can support the development of management strategies dealing with turbidity dependent algal blooms and the development of salt marshes as a measure against sea-level rise. This information can help identify zones of sedimentation and erosion within South Bay. Zones of sedimentation could be selected as favourable for salt marsh restoration and zones of erosion might need more attention as it may increase local flood risk and lead to the release of mercury buried in deeper bed layers. Additionally, a net export for South Bay might result in a further decrease of turbidity and a higher probability of turbidity depended algae blooms. Lastly, by understanding the current factors controlling fine sediment dynamics, future implications of climate change can be better predicted.

1.2. Research Objective

Pathways of sediment within South Bay are barely understood. Furthermore, the available information on sediment transport found in literature is not substantiated by a large scale process-based research. In this research, the fine sediment pathways within South Bay are aimed to be identified and quantified for an entire year. Additionally, sediment pathways are aimed to be identified and quantified separately for every season during the year, to investigate if distinct seasonal patterns can be observed. Furthermore, this study seeks to identify and quantify intra-Bay and extra-Bay net-transports during the year and for each season respectively. Finally, this study aims to learn more about the controlling forcings of sediment exchange at the South Bay and Lower South Bay entrances, while focussing on wind, tide and baroclinic processes.

There are a few model-based studies dedicated to specific parts of South Bay (eg. Brand et al. (2015): interpretation of sediment concentrations and vertical flux measurements and Mick van der Wegen; Bruce Jaffe; Johan Reyns; Amy Foxgrover: bed evolution at Alviso Slough). This research is novel as this level of coverage of the model domain by measured data is rarely seen and it will enable us to form a more complete overview of the model performance in the entire model domain, compared to previous researches. Furthermore, this research can form an intermediate link between the more conceptual Bay-wide studies and single location physical process focused studies.

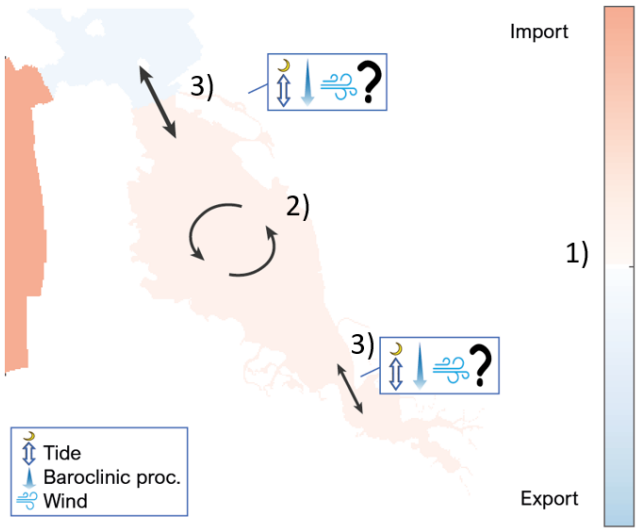

Figure 1.2: Conceptual Diagram of the knowledge gaps in the fine sediment dynamics in South Bay, with 1) presumptively export in Central Bay and import in South Bay and the Ocean 2) the unknown exchange mechanisms at the Dumbarton Narrows and Bay Bridge (the interface of South Bay and Central Bay) and 3) the unknown main sediment pathways within South Bay.

1.2.1. Research Approach

A process-based numerical model has been applied to deal with the knowledge gaps described in the previous section (Figure 1.2). Numerical modelling studies function as an adequate tool to improve our understanding of the driving physical processes of fine sediment transport, erosion, and deposition across the entire model domain. The Delft 3D modelling efforts of the San Francisco Bay Delta goes back to 2006. The first Community Model dates from 2013 and the hydrodynamics were validated and calibrated by Martyr-Koller et al. (2017) and salinity fields were validated by Pubben (2017). The sediment transport model was developed by Pubben (2017), and further calibrated by Gostic (2018) for a single measurement station in South Bay. This research will further calibrate the sediment transport model applying updated wind forcing and testing the model performance against additional measurement data with increased spatial coverage through the Bay both in depth and in the horizontal.

As the model is calibrated it will be used to answer the research questions with the help of the method of Sediment Connectivity. In other scientific disciplines such as neurology, ecology and social studies the concept of connectivity has been applied to analyse complex structures. Pearson et al. (2020) developed a framework for assessing coastal sediment connectivity, where large data sets of spatial and temporal output are reduced to an adjacency matrix permitting a more straightforward analysis and the application of different statistical metrics unavailable in more traditional approaches. This study could act as an additional case study and provide extended proof of concept to the work of Pearson et al. (2020).

Research Goals

The research objective to answer the described knowledge gaps can be summarized in the following research goals.

- Collect and analyse data of measured suspended sediment concentrations(SSCs) throughout South Bay for for WY2013, including High-Frequency SSCs measurements, Polaris Cruise Data and satellite imagery.
- Calibrate the DELWAQ-model of San Francisco Bay for WY2013 with collected measured data.
- Identify and quantify sediment transport pathways in San Francisco South Bay.
- Quantify net transport in South Bay and identify regions of sedimentation or erosion
- Quantify net sediment exchange at Bay Bridge, Dumbarton Narrows and between South Bay and the Ocean.
- Indicate the influence of respectively wind, tide and baroclinic processes on the net sediment exchange at Bay Bridge, Dumbarton Narrows.

The outline of the approach is displayed in Figure 1.3.

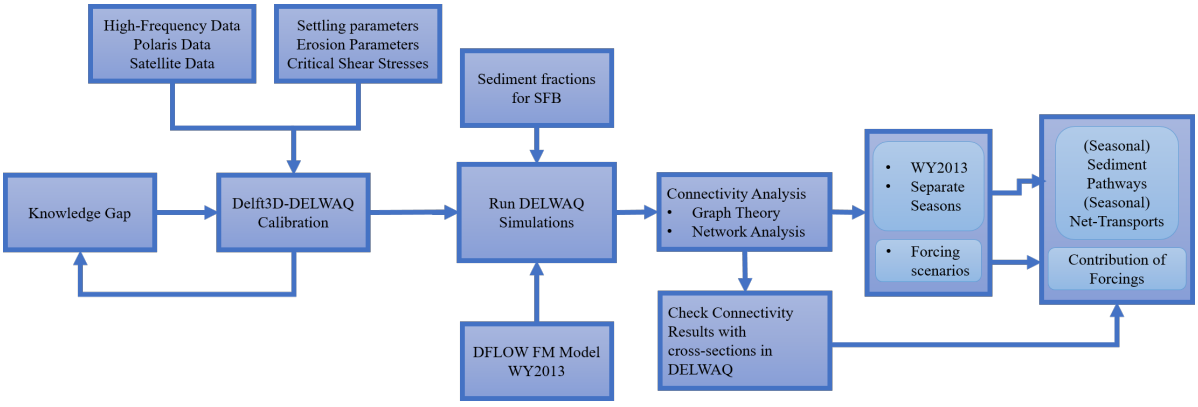

Figure 1.3: Work Flow Diagram

2

San Francisco Bay, history and physical processes

This chapter provides the required information for studying sediment dynamics in San Francisco South Bay. In this system overview, a more elaborate description of the geographical and historical context is given, followed by the current knowledge in science of fine sediment dynamics in the SFB system. To understand the sediment transport in South Bay in more detail, it is important to be aware of the current understanding of the forces which control sediment resuspension and transport, particularly in the shallower parts. The second section explains the complex 3D circulation patterns found in San Francisco Bay.

2.1. Geographical context

The San Francisco Bay is located in the middle of the Californian coast and well-known cities as San-Francisco, Oakland and San Jose are situated along its shores. It has a length of approximately 90 km and a varying width of 5-16 km. San Francisco Bay is a special estuary as the inlet is located in the centre of the Bay. The inlet divides the Bay into northern and southern sections with significantly different hydrodynamical features. North Bay consists of three sub-embayments. The Delta flows in Suisun Bay, which is connected to the San Pablo Bay through the narrow Strait of Carquinez. The San Pablo Strait flows into Central Bay where the estuary is connected to the ocean at the Golden Gate Inlet.
South Bay extents from the Oakland Bay Bridge to the south-eastern tip of the bay at San Jose (Figure 2.1. South Bay has a funnel shape with its narrowest point at the Dumbarton Narrows, where it slightly widens again. It has a channel-shoal morphology with the flood channel located slightly west of the middle flanked by two large tidal flats. The area south of the Dumbarton Narrows is very shallow and is prone to water quality issues due to the limited refreshing it experiences through the Narrows. Besides, the periphery is densely populated and both chemical and sewage discharge ends up in the Bay. The area is surrounded by operating salt ponds and former salt ponds in transition to salt marshes.

2.2. Historical Background

The San Francisco Bay aquatic ecosystem has deteriorated over the past centuries as a result of the population growth and industrialization of the region in the previous centuries. Urban development really took off in the mid-19th century due to the Californian Gold Rush in 1849, experiencing another boom after the end of the Civil War in 1865. The main business of the region was mining and San Francisco functioned as a financial centre (Walker, 2001). In the 1860s, agriculture began to develop rapidly in the valleys surrounding the Bay. By the 20th century also the region of Oakland would urbanize, creating the greater Bay metropolis it is today.
The hydraulic gold-mining resulted in an exceptionally high influx of loose Delta sediments to the Bay during the late 19th century. This enormous sediment input led to a significant seaward migration of the coasts and the development of substantial tidal flats and salt marshes (Barnard et al., 2013a). Attached to the inflowing sediments, mercury used in hydraulic gold mining dispersed throughout the Bay, in severe water quality problems. Though the main pulse of mining-related sediments passed Sacramento by the 1950s(Meade,

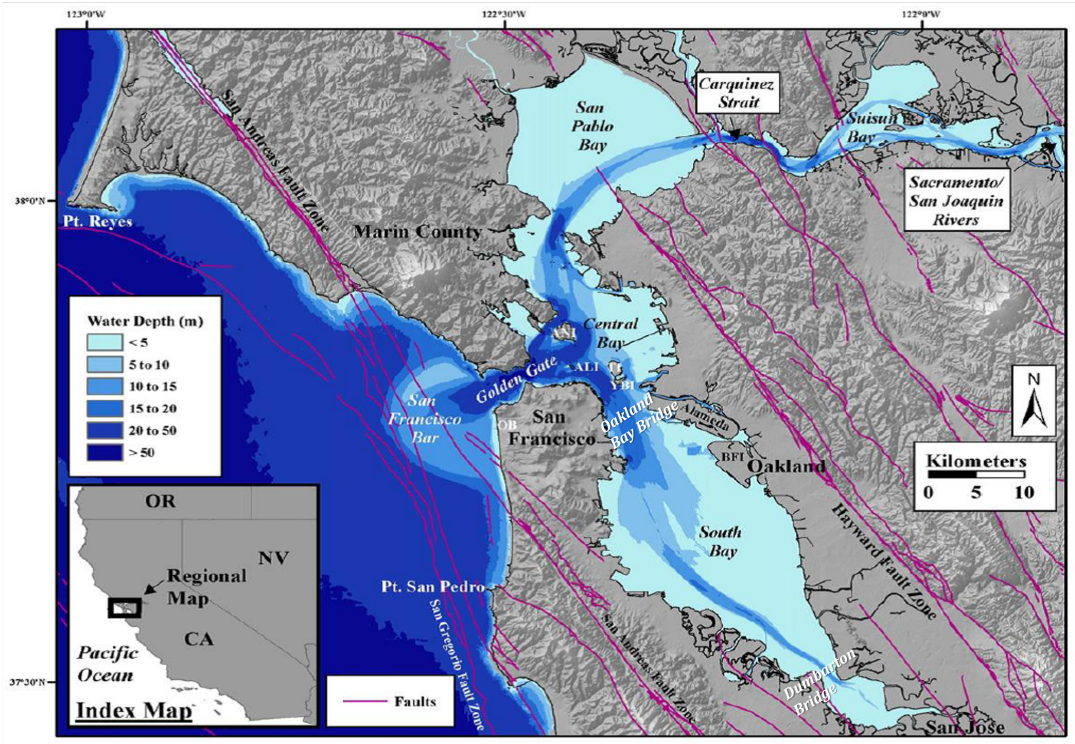

Figure 2.1: Overview of San Francisco Bay, the local bathymetry and its surrounding cities and mountain areas.(from: Barnard et al. (2013a))

1982), recent research of sediment cores has shown contaminated sediments are still actively redistributed. Therefore, mercury contamination is still causing concern for water quality in San Francisco Bay(David et al., 2009).

While gold-mining became legally prohibited by the 20th century, the estuarine system was altered by extensive civil construction projects. In response to inundation problems and salt intrusion in both the Sacramento as the San Joaquin watershed several dams were created. River dams trap sediment and the bank protection in the rivers prevents the erosion of river banks (Wright and Schoellhamer, 2004). These developments in the region have resulted in a decreasing trend in the sediment yield.

Historically, a large part of SFB consisted out of salt marshes and tidal flats. Over the last century, 91 % of the tidal wetlands have been lost to reclamation for farmland, residential areas, salt ponds and industrial areas (Miles, 2007). Salt production has been one of San Francisco's largest industries since 1854 (San Francisco Bay Comission, 2005). Recently, the area has been sold to both Federal as State governments and private foundations who make efforts to restore the salt ponds to their historical function.

2.3. Hydrodynamics and fine sediment dynamics of South Bay

In this section an overview of the main hydrodynamic forcings in SFB is given. This information is suplemented with information on the influence of the forcings on fine sediment dynamics if this impact is understood or hypothesized. First some general information on fine sediment in San Francisco Bay is provided.

2.3.1. Fine sediment in San Francisco Bay

Fine sediment found in San Francisco Bay mainly consists of mud mixed with some sand and is of cohesive nature. Mud is dominantly present in South Bay and in the shallower parts (<5m) of the estuary. The main source of incoming sediment for the Bay is the Sacramento–San Joaquin Delta system with sediment input ranging from 1-1.2 Mt/year (McKee et al., 2006) to 4 Mt/year (Shvidchenko et al., 2004). The highest importing fluxes occur during the wet season, from late fall-early springLewicki and McKee (2010). In addition, over 450 local tributaries flow into San Francisco Bay and their merged sediment inflow may exceed the sediment contribution from the Delta (Barnard et al. (2013a); Lewicki and McKee (2010)). Yet, there is a high uncer-

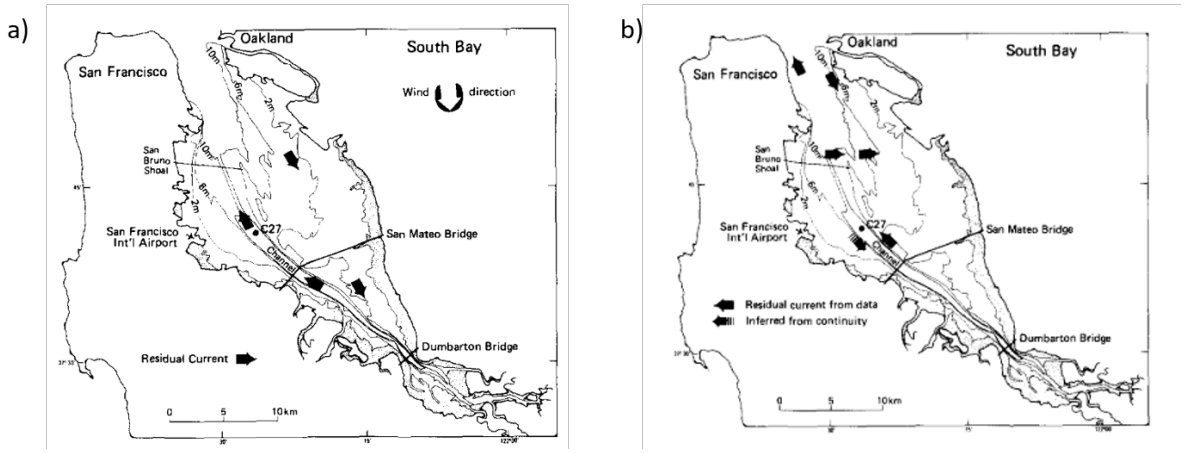

Figure 2.2: Figures by Conomos, T. J. Walters and Cheng (1985) with a) residual currents during a wind event coming from the north and b) residual currents during a tidal cycle

tainty in the precise volume of sediment inflow from each tributary.

2.3.2. Tide & Fine Sediment Dynamics

The tide propagates into SFB through the narrow Golden Gate inlet, locally generating very fast currents. The tidal signal is mixed diurnal and semi-diurnal, with two highwaters a day with varying tidal amplitude and has a strong spring-neap variance. Tidal influence can be found as far upstream as Sacramento, which is located 155 km from the Golden Gate. Tidal currents are more powerful than the freshwater inflows except during peak flows during the winter season. The tidal prism exceeds the volume of freshwater inflow by one to two orders of magnitude (Hanes and Barnard, 2007). Tidal currents cause most of the mixing (Cheng and Smith, 1998) and the generated turbulence is responsible for resuspension of sediments at many locations of the Bay. Schoellhamer (1996) found that the highest SSCs in South Bay were observed during the lowest spring tides. He ascribed the peak SSCs to advection from the turbid waters at the flats and concluded that advective transport due to tidal currents was the dominant process affecting SSC during spring tides. Flood asymmetry of the South Bay tide leads to an import (Figure 2.2.b) Furthermore, the tidally-driven vertical mixing was found to prevent settling sediments to form a thick mud layer in South Bay by Brand et al. (2010).

2.3.3. Wind-induced waves and residual currents

The ocean swell penetrating through the Golden Gate only reaches local exposed parts and the eastern mudflat in Central Bay. Therefore, waves found in the Bay are mainly generated by local winds, which play a minor role in the deeper channels but can induce significant turbulence and sediment transport in the shallow, fetch-exposed mudflats (Schoellhamer, 1996). Winds are commonly north-westerly to westerly, particularly during the fall months, making the eastern mudflats of South Bay particularly fetch-exposed. In this case the residual current at the flats is in southern direction (Figure 2.2.a).
A south to south-westerly landward wind shear develops during summer sea breezes in the afternoon leading to the highest sediment concentrations in South Bay found during the year, when the generated waves bring a vast amount of shoal sediments in resuspension. The sediment resuspension at the flats is found to play an important role in the overall sediment budget in the South Bay (Barnard et al., 2013a). Surface currents are wind-driven across coasts of the eastern flats towards the Southeast, as sediment fluxes follow the currents the net transport is in this direction during the Spring/Summer season (Schoellhamer, 1996). Highest sediment concentrations are found when wind and tidal forcing occur together. Most resuspension events in South Bay occurred during flood tides following strong wave events in the preceding low water phase (Brand et al., 2010).

2.3.4. Baroclinic circulations

The San Francisco Bay tends to be of a well-mixed nature throughout most of the year. Although tidal energy causes strong estuarine mixing (Cheng and Smith, 1998), freshwater inputs during peak winter discharges from the Delta can occasionally lead to strong stratification events and an interface between fresh and saline water can be observed in North Bay (Pubben, 2017). South Bay experiences little freshwater input during most of the year, during which it is a well-mixed estuary. Every tidal cycle South Bay experiences an inflow of salt ocean water strongly exceeding the amount of freshwater inflow from the local tributaries. During peak winter discharges from the Delta, North Bay and San Francisco Bay become significantly fresher, inducing a positive salinity gradient landward from Central Bay to South Bay. During this period a reverse circulation can be observed as South Bay is saltier than Central Bay (Figure 2.3). As Delta discharges reduce in February, the incoming tide will make Central Bay saltier than South Bay inducing a negative salinity gradient landward leading to a classic estuarine circulation. This salinity gradient diminishes in time, making South Bay well-mixed for the remainder of the year. Vast volumes of sediment enter the system during the peak discharges in Winter, making Central Bay sediment-rich relative to the rest of the year. Hence, the baroclinic circulations make a significant contribution to sediment exchange at Bay Bridge.

2.3.5. Knowledge Gaps

As mentioned, the sediments from the Delta are likely to be a source for South Bay. Sediment particles would need to travel down from North Bay to Central Bay and brought into South Bay by exchanging sediments at Bay Bridge. The contributions of different forcings as tide, wind and baroclinic processes are uncertain. Little is known about the sediment pathways within South Bay during the year. Furthermore, Lower South Bay is found to be very turbid, yet does not experience a significant sediment input from local tributaries. Hence, most of this sediment must originally have passed through the Dumbarton Narrows, yet there is uncertainty in the processes governing this exchange.

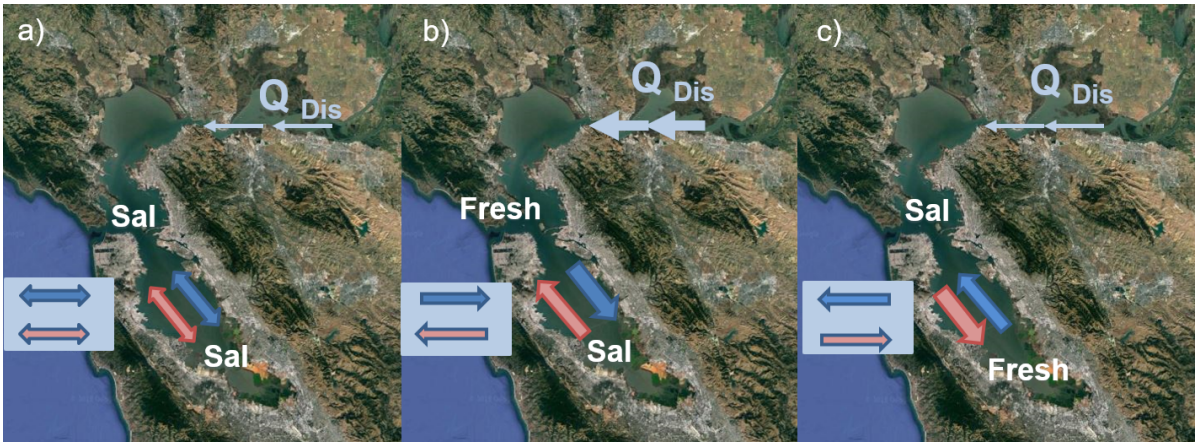

Figure 2.3: Different circulations patterns occurring in SFB during the year with a) a well-mixed situation with a weak circulation current, b) a residual circulation during high discharges as the Delta in Winter and c) a classic circulation occurring after the discharges return to the values prevailing in the course of the remainder of the year. The classic circulation regime will evolve into a well-mixed regime in time.

3

DELWAQ-Model Setup

Numerical models function as an adequate tool to investigate the sediment dynamics in SFB. This study uses the Delft Water-Quality Module (DELWAQ) of Delft 3D. DELWAQ simulates the transport of one or more substances within the model area by solving the diffusion-advection equation (Deltares, 2019). In this model, only the transport of fine suspended sediment is modelled. The DELWAQ model has used the hydrodynamical simulations of the D-Flow FM model of San Francisco Bay as input. DELWAQ was offline-coupled with the D-Flow FM model, so the computational intensive D-Flow FM model only needed to be run once. As a downside, there was no morphological feedback on the hydrodynamics. However, as it only concerns fine suspended sediment, the influence of changes in morphology on the hydrodynamics were not likely to be significant. Interest in sediment dynamics in the San Francisco Bay is long-standing and modelling efforts started in the previous decade. Recent studies developed a Delft3D Flexible Mesh D-FLOW model (Pubben, 2017) to simulate the Bay's hydrodynamics, a DELWAQ model (van Kempen, 2017) and an improvement of this model (Gostic, 2018) for South Bay specifically. The latter study added a so-called Buffer Layer to the model, more information can be found in Section 3.2.1. This study builds upon these modelling efforts to improve our understanding of the sediment paths within South Bay. The set-up of the DELWAQ model will be described more elaborately further in this section. First, the set-up of the D-Flow FM model will be described.

3.1. Hydrodynamics

DELWAQ uses the hydrodynamical output of the D-FLOW FM Model developed and validated by the San Francisco Estuarine Institute(SFEI) (Holleman et al., 2017). Their work builds upon previous model versions developed by Martyr-Koller et al. (2017) and improved by Pubben (2017). Recently, the wind input for this model was revised by King (2019). The hydrodynamic model was validated for the Water Year 2013 (WY2013) due to the availability of a vast set of measured data. WY13 spans from October 2012 to October 2013 to capture one discharge pulse from the Delta during winter in one simulation. The simulation time starts in August 2012 to enable the model to spin-up before the actual water year starts in October 2012.

The model domain includes San Francisco Bay as well as parts of Coyote Creek and Guadalupe River flowing into South Bay and extents northward until the rivers of the Delta. The western boundary of the model domain is situated in the ocean at a 20 km distance from shore. The horizontal grid resolution varies from 20 m in a few sloughs of Lower South Bay, to over 2 km in the ocean. In the vertical dimension, the σ-approach is applied, so the grid size and shape vary proportionally to the local depth for 10 layers in the vertical. The height of each layer can vary from the order of decimetres in shallow areas to ten meters in the ocean (Holleman et al., 2017).

3.1.1. Hydrodynamical Boundary Conditions and Forcings

The used version of the hydrodynamical model of San Francisco Bay includes an updated wind input with respect to previous studies of modelling hydrodynamics in San Francisco Bay (Achete et al. (2015), Martyr-Koller et al. (2017)) and (Nuss et al., 2018). Where previously the Ludwig Wind Model was used (Ludwig et al., 1991; Ludwig and Sinton, 2000), a new wind model for San Francisco Bay was developed at the San Francisco Estuarine Institute (King, 2019). Data from 52 wind stations located near the water in the SFB-Delta were in-

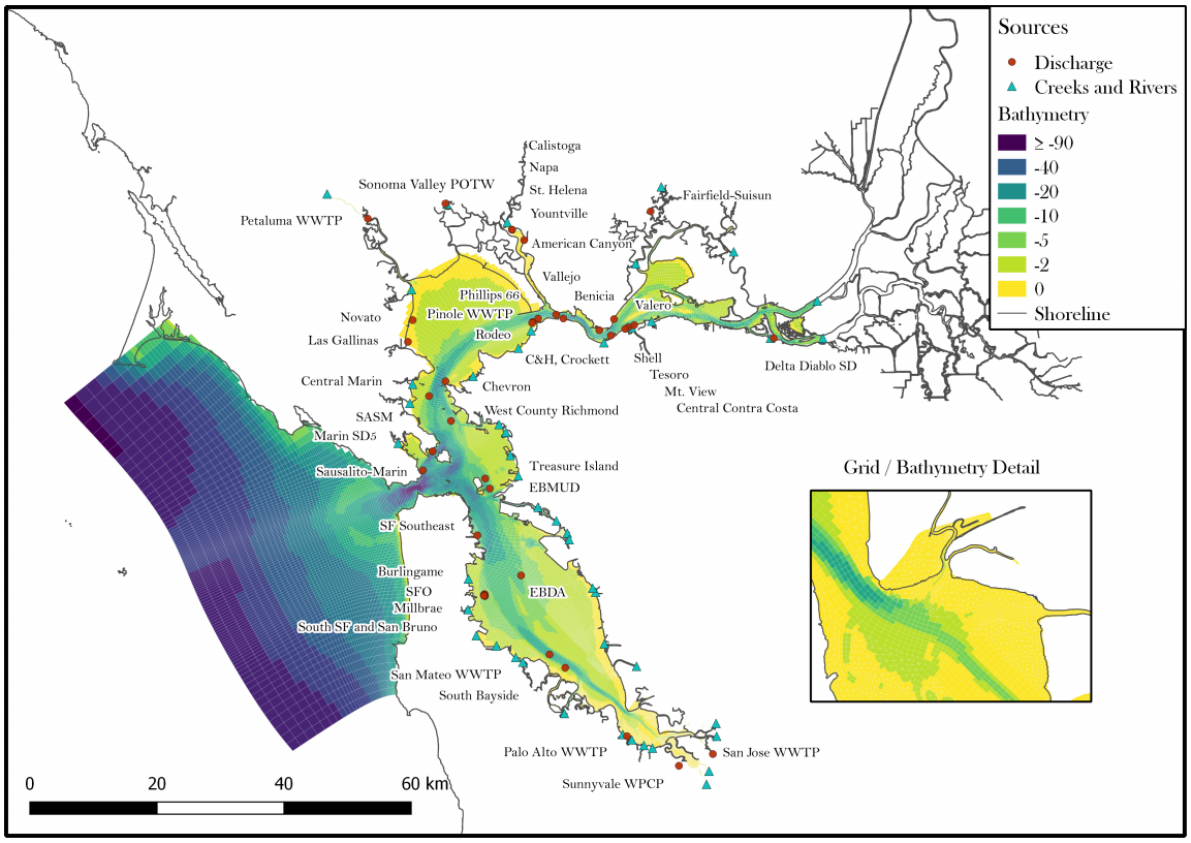

Figure 3.1: Overview of the D-FLOW Model grid, bathymetry and discharge locations by Holleman et al. (2017).

cluded. Wind input for the DFLOW-Model was created by natural neighbour interpolation of hourly averaged 10 m winds at the 52 stations. This new method is simpler in use and in addition validation showed that it was 30% more accurate than the Ludwig model across the Bay Area (King, 2019).

The tidal forcing at the western open ocean boundary was derived from measurements at Point Reyes from NOAA (National Oceanic and Atmospheric Administration). The western and southern ocean boundaries are closed. Freshwater inflow from local rivers and creeks were computed by the Bay Area Hydrology Model. Exceptions are the inflows from the Sacramento and San-Joaquin Delta which were determined from measurements at the USGS stations at Rio Vista (Sacramento) and Jersey Point (San-Joaquin). The Sacramento River and the San Joaquin River are responsible for respectively 90% and 9% of the total run-off from the Delta (Figure 3.3). Next to creeks and rivers 42 water treatment plans discharge into San Francisco Bay which are included as freshwater inflows. An overview of inflows from rivers, creeks and discharges can be found in Figure 3.1.

3.2. Sediment definitions and processes

In order to model the suspended sediment concentration, the 3D-Mass Balance equation needs to be solved. In the vertical, the boundary fluxes at the bed are governed by erosion and sedimentation processes at the bed. For a sandy bed with fine particles, the classical model by Partheniades and Krone is often applied. Recently, a different approach has been developed called the Buffer Layer Model (van Kessel et al., 2011). It introduces a new buffer layer consisting of fines. The thin layer can store fines during calmer conditions, which then erode easily when hydrodynamic conditions increase.

3.2.1. Buffer Layer Model

The climate in San Francisco Bay has a seasonal variability, hence the wave and wind forcing varies seasonally. Furthermore, sediment supply may vary during different seasons as peak discharges in Winter also lead to peak sediment input. The zeroth-order calculation of erosion in the classical erosion-deposition model of

Partheniades and Krone does not account for the variability of sediment in the bed. The concept of equilibrium mass per unit area based on the local bed shear stresses and sediment availability does not exist in the conventional model. This leads to excessively high erosion values at locations with high bed shear stresses and insufficient deposition at locations with low bed shear stresses (van Kessel et al., 2011). As a consequence, the classical model shows some deficiencies while capturing the seasonal variations of suspended sediment concentrations. To better capture this variability an alteration was made to the classical model and a second layer was introduced. The first layer of the bed exists of a fluffy layer which consists of fluid mud. Fine sediment accumulates in this layer during slack time, forming a thin layer of unconsolidated mud on top of the solid bed. The fine particles of the fluffy layer are resuspended again as tidal currents increase. The buffer layer underneath the fluffy layer is a mix of infiltrated mud with sand. In this buffer layer fines can reside during calmer periods and are only resuspended during more severe conditions such as storms or spring tides. Therefore direct sediment exchange between the buffer layer and the water column does not occur often and residence times can become significant (van Kessel et al., 2011). The sediment exchange between the layers and the water column is described by the equations below.

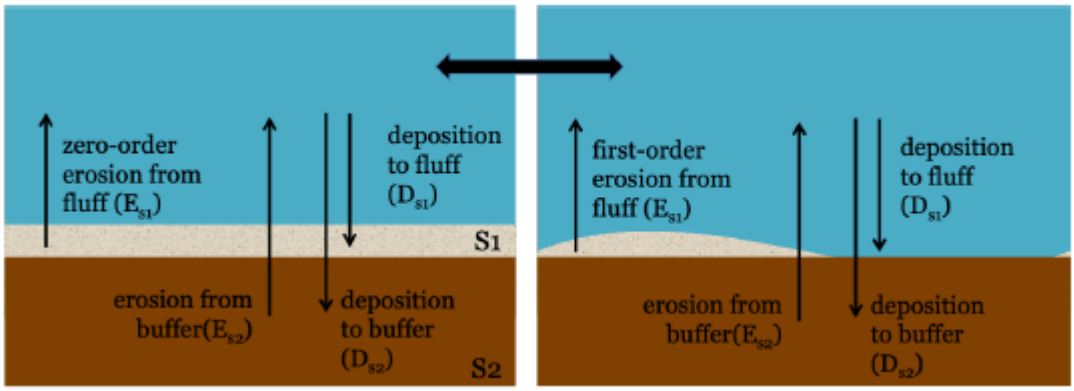

Figure 3.2: Schematization of the Buffer Layer Model by White (2019). Layer S1 represents the thin Fluffy Layer and S2 represent the Buffer Layer. The left picture shows a well covered buffer layer and the zeroth-order resuspension regime is prevailing. In the right diagram the amount of sediment in the fluff layer has decreased significantly and the model is in first-order regime by White (2019).

$$D_1 = (1-\alpha)\, w_s * C D_2 = (\alpha)\, w_s * C \tag{3.1}$$

$$D_2 = (\alpha)\, w_s * C \tag{3.2}$$

Parameter α determines the fraction of the deposition flux contributing to the buffer layer, w_s is the settling velocity, C is the near-bed suspended sediment concentration. Following Winterwerp(2007), it is assumed that there is no threshold in bottom shear stress to allow for settling, hence settling will occur continuously and simultaneously with erosion. This assumption is expanded to the fluff layer and buffer layers by assuming deposition occurs for both layers simultaneously. The ratio of deposition between the two layers is determined by α and can be adjusted as a measure of calibration.

The resuspension flux is calculated by the formulas 3.3 and 3.4. Initially, the bed will be covered by the mud in the fluff layer (S1) and the zeroth-order resuspension regime will be active. Over time, the fluff layer will contain less sediment and the lower buffer layer will become exposed. During moderately energetic conditions sediment from the buffer layer will not be resuspended as it has a higher critical shear stress due to the presence of sand. As less sediment is present in the fluff layer, the resuspended flux is expected to decrease as well. To account for this process the first-order resuspension regime was introduced. From this moment onwards, the resuspension flux will be scaled with $m_1 * M_1$ instead of M_0. The formula for erosion from the fluff layer is described below.

$$E_{S1} = min(m_1 * M_1, M_0)(\frac{\tau_b}{tau_{cr,1}} - 1) \tag{3.3}$$

Where $\tau_{cr,1}$ is the critical shear stress for the fluff layer, M_0 the zeroth-order resuspension parameter,M_1 the first-order resuspension parameter and m_1 is the sediment mass/unit area.

The second layer represents a sand matrix infiltrated with mud and has a user-defined thickness. This thickness is related to the mixing depth of mud into the sandy layer over which the mud is distributed more or less homogeneously over the vertical by i.e. bioturbation (van Kessel et al., 2011). The buffer layer only erodes during periods of high hydrodynamic energy such as spring tides or storms. The formula for erosion from the buffer layer is described below.

$$E_{S2} = p_2 * M_2 * (\frac{\tau_b}{tau_{cr,2}} - 1)^{1.5} \tag{3.4}$$

Where $\tau_{cr,2}$ is the critical shear stress for the buffer layer, M_2 the resuspension parameter for the buffer layer and p_2 is the fraction of fines in the Buffer Layer. An overview of all variables in the formulas can be found in Table 3.1.

Table 3.1: Overview of the variables in the deposition and erosion formulas in the Buffer Layer Model.

Overview calibration scenarios Parameter	Symbol	Unit
Settling Velocity	ws	mm/s
Critical Shear Stress S1	Tc1	N/m^2
Critical Shear Stress S2	Tc2	N/m^2
Fraction Deposition to S2	alpha	-
Zeroth-Order Resuspension Parameter S1	M0	kg/m2/s
First-Order Resuspension Parameter S1	M1	kg/m2/s
Resuspension Parameter S2	M2	kg/m2/s

3.2.2. Boundary Conditions

When applying a sediment model implementing accurate boundary conditions for the incoming sediment from the local tributaries and rivers is essential to compute reliable sediment concentrations in the Bay. However, from the over 75 tributaries and rivers flowing into SFB, only 7 are monitored by USGS-gauges (White, 2019). Previous versions of the DELWAQ model (Gostic, 2018) only took into account sediment inflow from the biggest contributing rivers and tributaries (Figure 3.3 and 3.4. The research of White (2019) developed a method to estimates sediment concentrations for all tributaries flowing into SFB during Water Year 2013 and concluded the role of the sediment supply from minor tributaries was significant. Hence this version of the DELWAQ model will implement these estimates as boundary conditions. The reader is directed to this research for more information on the used methods White (2019).

3.2.3. Initial Conditions

At the beginning of a simulation, an initial bed needs to be defined, specifying the mass of each sediment class present at each bed layer. This initial distribution of sediment in the model domain should resemble the dynamic equilibrium of sediment distribution as closely as possible. Larger quantities of mud are found at low-dynamic locations such as the shallow shoals whereas the mud at channels will be swept away due to higher shear stresses. If this is not the case the system will try to restore this equilibrium and the time it takes for the model to restore its balance is called the spin-up time. During spin-up time the model does not produce realistic results as the bed tries to adjust to the dynamic equilibrium. This spin-up time can be minimized by letting the initial bed composition approach the equilibrium composition closely.

For this model, the initial bed was generated by starting with an initial guess for the bed composition and run the model for two years with a parameter set obtained from the study of Gostic(2019). After this period most irregularities in the bed should be obviated. As an initial guess, an amount of 500 g/m^2 was included in the fluff layer with equal fractions of both sediment classes at locations with a depth below 5m. Together with a uniformly distributed buffer layer with equal fractions for both sediment classes the initial bed composition is displayed in Figure 3.5a. After two years of simulation, much of the mud is relocated and a new bed composition is formed (Figure 3.5b). In Figures 3.5c and 3.5d the composition of both the fluff layer (S1) and the buffer layer (S2) can be observed. In comparison with the sediment distribution of Figure 3.5a the

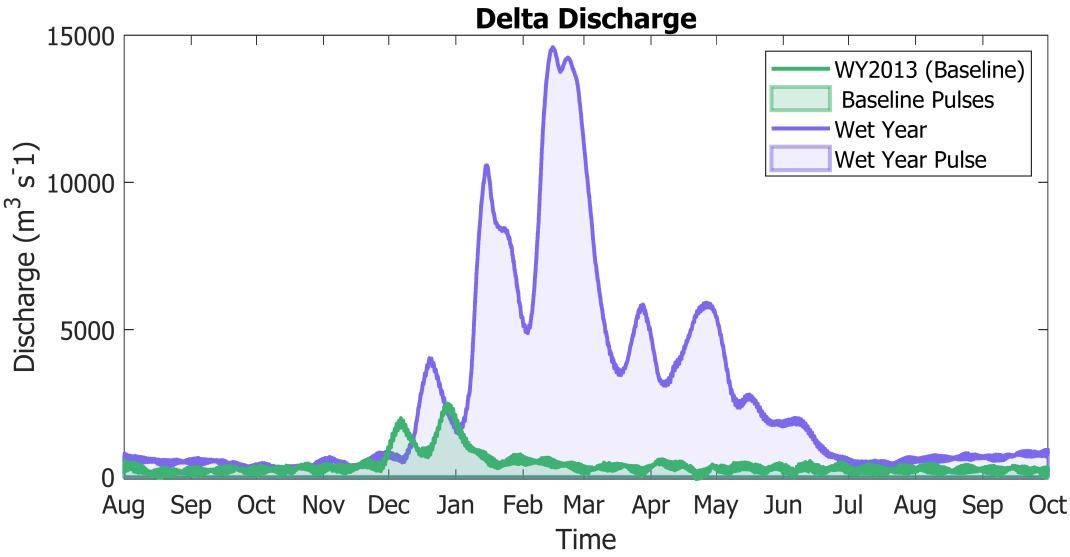

Figure 3.3: Plot of the model's boundary conditions: combined Delta Discharge of the Sacramento River and the San Joaquin River for both the representative water year of 2013 and the wet water year of 2017.

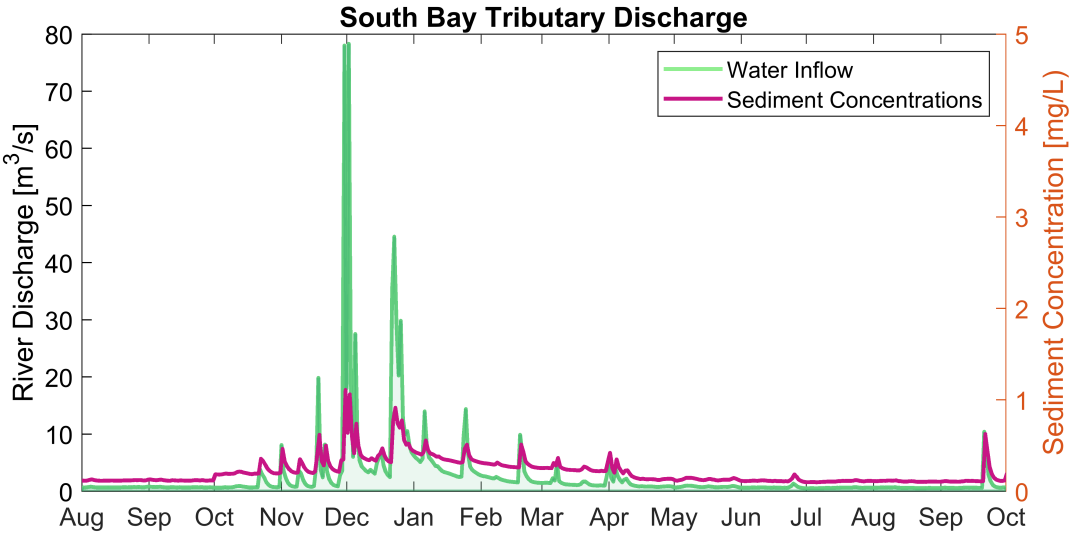

Figure 3.4: Plot of the model's boundary conditions: the water discharge and combined sediment concentrations of tributaries entering South Bay: Coyote Creek, San Lorenzo River, Alameda River

channels have been flushed out and larger amounts of mud have settled at the flats. This bed composition will be used in the model calibration.

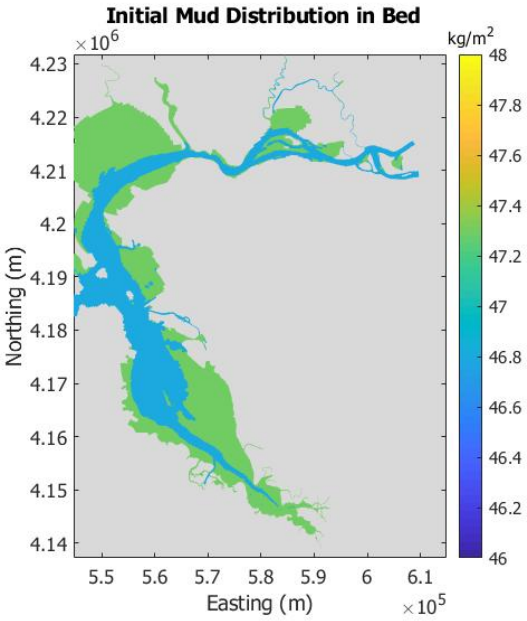

(a) Initial guess of the bed composition with mud added in the fluff layer at locations of a depth below 5m

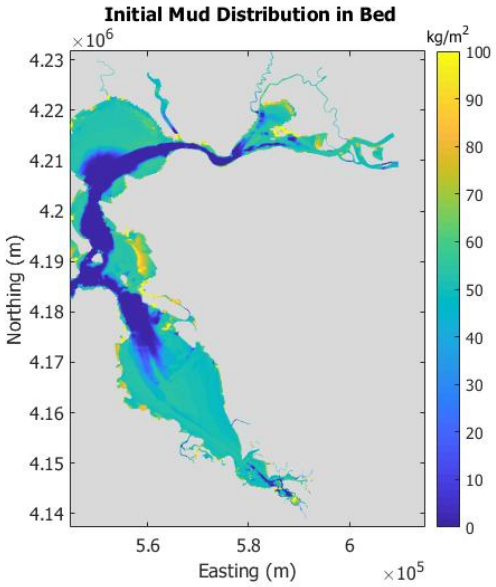

(b) Initial bed composition after a two year simulation

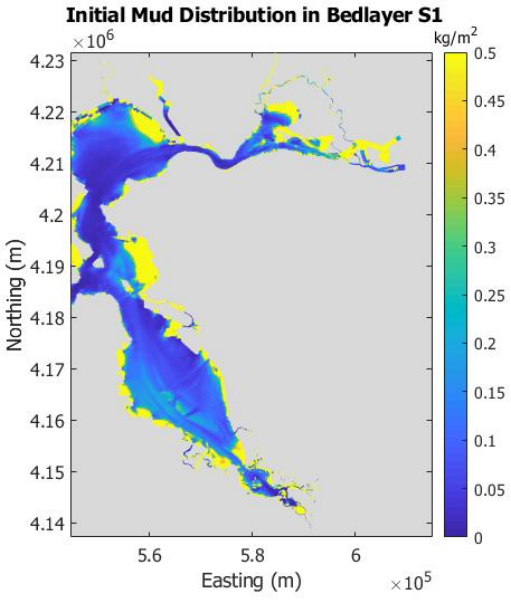

(c) Initial Bed Composition for the fluff layer (S1) after a two year simulation

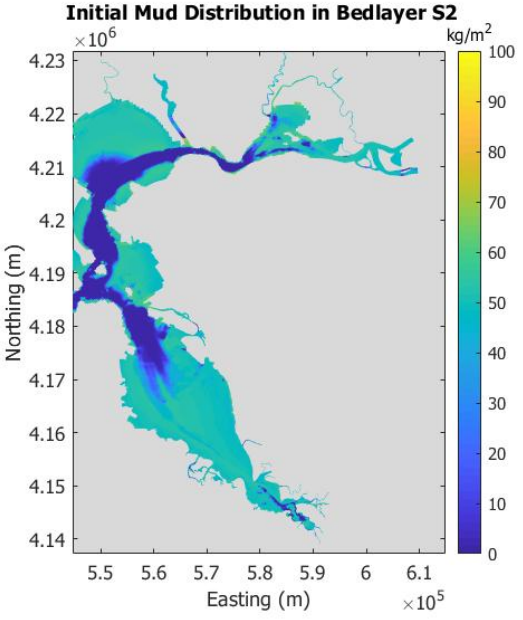

(d) Initial Bed Composition for the buffer layer (S2) after a two year simulation

Figure 3.5: Several plots of the initial bed compositions with a) initial bed composition of the combined fluff layer and buffer layer before spin-up, b)initial bed composition of the combined fluff layer and buffer layer after spin-up, c)initial bed composition of the fluff layer after spin-up d) initial bed composition of the buffer layer after spin-up

4

Model Calibration

In a previous study of Gostic (2018), the model was calibrated against measured suspended sediment concentrations of WY2015 at the single location of Dumbarton Bridge and for the unrevised wind input. In this study, the model has calibrated with the hydrodynamic forcing of the updated hydrodynamic output of WY2013. This updated version included waves and an updated wind forcing from King (2019). The suspended sediment concentrations in the Bay have been calibrated against local measurements of the suspended sediment concentration measurements and the estimated SSCs derived from remote sensing data. The Baseline run resulted from the early sensitivity study of the model, after which the model performance was assessed with both a more subjective visually oriented approach and a more objective quantitative approach by the use of statistics. After the analysis of the Baseline Run, two different areas of focus were identified where the model underperforms. Different scenarios were developed and applied to the model in order to improve the model output. Parameter scenarios were set based on the gained knowledge of the sensitivity of the model to certain parameters. Analysis of the different scenarios resulted in a final parameter set with improved model performance compared to the measured data.

4.1. Data Review and Analysis

Before a developed model can be used to model scenarios of sediment transport it must be validated and calibrated with the in situ measured data. In many regions of the world, developers of sediment transport models are challenged by the lack of data of local sediment concentrations and bathymetry as this kind of information requires long and costly measurement campaigns (Van Der Wegen et al., 2011). Fortunately, the San Francisco Bay is an exception as data on hydrodynamics have been collected by the USGS since 1969. Three different data sources on sediment concentrations in the Bay have been used to assess the model performance during calibration. All sources vary strongly in temporal and spatial coverage. A combination of all three can add to the comprehension the model performance, both spatially and in time. The three different sources of data included the Polaris cruises, conducted, high-frequency SSCs data measured at 8 different USGS stations (Figure4.1a) and satellite imagery.

4.1.1. Polaris Cruise Data

San Francisco Bay has been dealing with poor water quality since the mercury used for hydraulic mining has found its way to the SFB through the river discharge from the Delta. The water quality has deteriorated over the years as industrialization and urbanisation increased the amount of sewer discharge and chemical depositions in the Bay. To investigate the water quality in the Bay, the USGS designed a measurement program to describe the changes in water quality in the Bay. Continuous measuring started in 1969 with the use of the research vessel Polaris, changing to the R/V David H. Peterson vessel in 2016. Measurement campaigns are executed every month following a fixed series of measurement stations (Figure 4.1b). The sailed transect varies from Full Bay transect in some months to only the South Bay part of the transect in other months. During the cruise-information, on salinity, temperature, Suspended Particulate Matter (SPM), Dissolved Oxygen, light penetration, and chlorophyll concentration is collected. In this research, the main interest lies with the data of SPM, which has been measured since 1993.

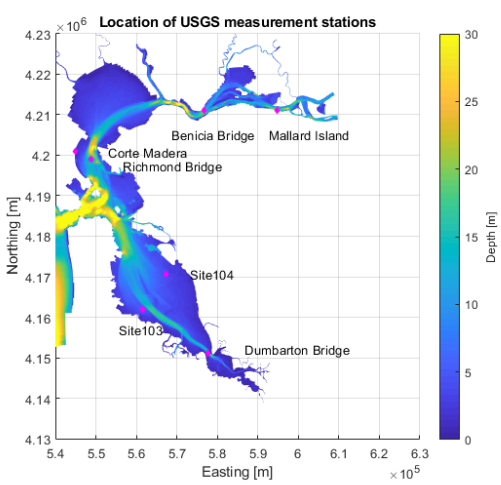

(a) Location of USGS-stations in SFB

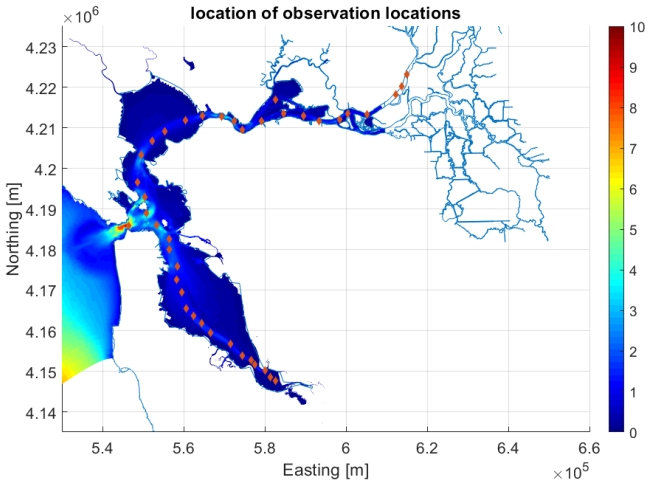

(b) Overview of the measurement locations during the Polaris Cruises while sailing the transect from North to South Bay every once or twice a month

Figure 4.1: Two main sources of measured SSCs used for calibration

4.1.2. High-Frequency USGS Data

The USGS has employed several measurement stations throughout San Francisco Bay measuring water levels, velocities, temperature and different dissolved and particulate matters. Eight USGS stations have recorded the suspended sediment concentrations during the period of interest. The locations are distributed over both North Bay and South Bay (Figure 4.1a). Though they only give information on specific locations in the Bay, the high frequency of the measurements makes it an important data source in obtaining information over tidal cycles and spring-neap cycles.

4.1.3. Comparison of USGS Data and Polaris Data

Though the High-Frequency USGS Data and the Polaris Cruise data are different in spatial and temporal coverage, we attempted to compare their outcomes. Four USGS Stations are located nearby Polaris measurement points. In Figure 4.2 the high-frequency SSC signal is plotted with the monthly measured Polaris SSC as scattered dots. The level of agreement between the two data sources differs both per station and during the year. In general, the Polaris cruise seems to measure values of the same order as the USGS-stations do, though Polaris tends to measure lower compared to USGS. At Dumbarton Bridge the values of USGS were higher than the measured values of Polaris except for Spring. At Richmond Bridge, consistently lower valued measurements are observed for Polaris. Few measurements were taken at Benicia Bridge for the Polaris Cruise at sufficient depth, yet the measurements compare. Measurements at Mallard Island seem to compare well visually, though Polaris tends to measure slightly lower values. With the help of a scatter plot and statistical metrics, both data sources are compared quantitatively. The scatter plot includes a line of best fit which indicates a bias of 0.29 of the USGS measurements with respect to the Polaris Data, hence USGS measured values tend to turn out higher than the Polaris values. Yet the coloured dots show this mainly applies to the measurements at Mallard Island and Dumbarton Bridge. The R-Squared score of 0.18 generally qualifies as a weak relationship between the two data sources. However, most measured values below 50 mg/L are located around the 1:1 slope while the higher values start to show a deviation, leading to a tilted best-fit line based on which R-squared is calculated. The lower measured values deviate from the best-fit line while contributing to a lower r-squared. Nonetheless, they are located near the 1:1 line, indicating a good relationship between the two data sources for measured values below 50 mg/L. Whereas if measured values exceed 50 mg/L the USGS data tends to measure higher values than the Polaris Data.

4.1.4. Satellite Imagery

A new approach to data collection in San Francisco Bay is deriving suspended sediment concentrations from satellite imagery. The water reflection retrieved from the images indicates the turbidity near the surface, which is related to the suspended sediment concentration near the surface. The mathematical relation between the turbidity and suspended sediment concentration is not validated yet and still under development.

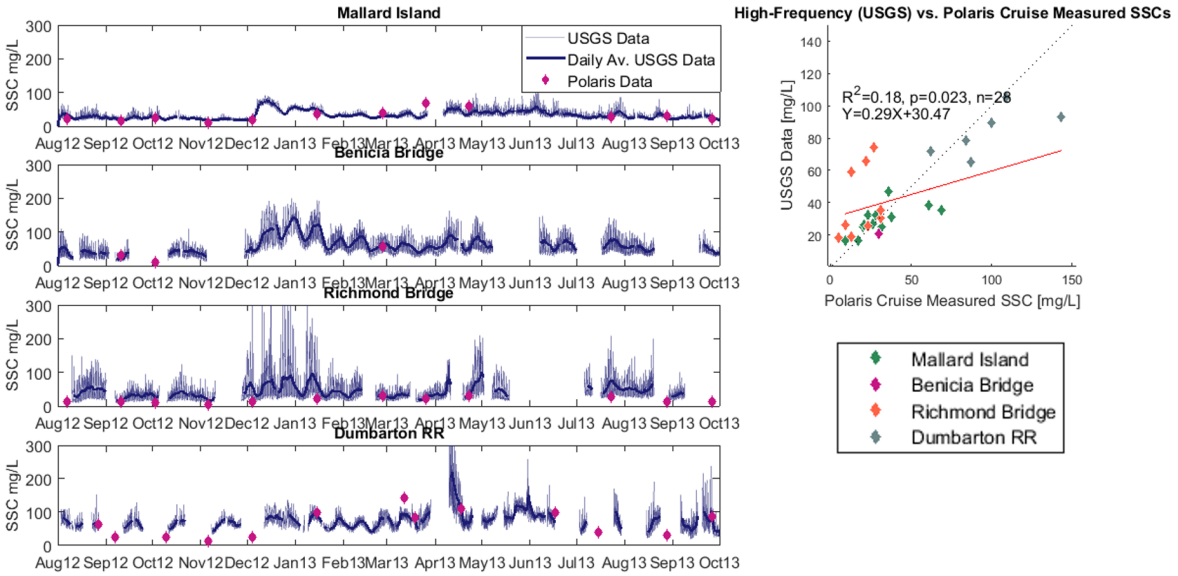

Figure 4.2: Comparison of measured data of the High-Frequency USGS Data and the Polaris Data for 4 USGS stations located in the channel near measurement locations of Polaris. The USGS is plotted in blue and the Polaris measurements are plotted as magenta dots. In the scatter plot measured data of the USGS stations is plotted against the Polaris data. A best-fit line is shown in red.

Hence, the data has not been used to check the model performance statistically. Though it was used to provide a qualitative indication if the general trends in SSC are captured in the model. As it is the only data source that provides data on the sediment concentrations at the shoals it provides valuable information, but it has been kept in mind that it has not been validated yet.

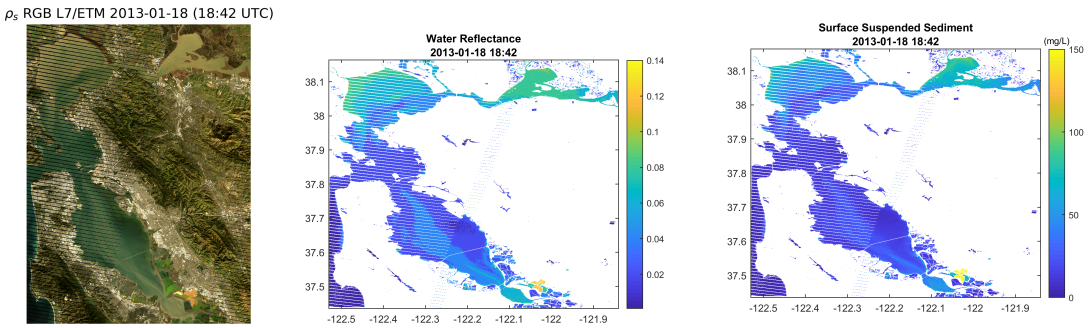

(a) Satellite Image from San Francisco Bay on 18th of January 2013

(b) Water Reflectance derived from satellite image

(c) Suspended Sediment Concentrations derived from the water reflectance

Figure 4.3: Suspended Sediment Concentrations were derived from satellite imagery, by first estimating the water reflectance from the satellite image and subsequently computing the SSCs.

4.2. Sensitivity Analysis and prior calibration efforts

These calibration efforts build on earlier calibration efforts by Gostic (2018) and White (2019). As a first start, the sediment parameter set from Gostic (2018) and White (2019) was used. Compared to the DELWAQ model calibrated by Gostic (2018) the simulation period changed from WY2015 to WY2013 during the calibration process and the hydrodynamical simulation in DFLOW was forced with a different wind model. Compared to the DELWAQ model calibrated by White (2019) for WY2013, river inputs were corrected and wave forcing was included during the calibration process, which will be further discussed in the next subsections. The sensitivity analysis consisted of the adjustment of several parameters so the parameter sensitivities and response of the model could be discovered. With this information suitable calibration scenarios could be developed in subsection 4.3 to eventually improve the model performance. The variation in parameters was based on system information in literature (Lacy et al. (2017a), Allen et al. (2019), Schoellhamer (1996), Schoellhamer et al. (2018)) and values applied in numerical modelling studies (Van Der Wegen et al. (2011), Ganju and Schoellhamer (2006)).

Initially, the model tended to underestimate the measured SSCs from both the High-Frequency USGS Data and Polaris Cruise Data and did not capture SSC variations over the semi-diurnal tidal cycle , nor the spring-neap tidal cycle. Attempts were made to increase sediment concentrations in SFB by decreasing the fall velocities, which decreases the sedimentation flux. Additionally, zeroth- and first-order resuspension parameters were increased and the critical shear stress for the fluff and buffer layer was decreased. Both these measurements increase the resuspension flux. This in combination with a decreased sedimentation flux will lead to a higher sediment concentration the water column. Decreasing the fall velocities only had a noteworthy impact when the settling velocity of the larger sediment fraction (IM1) was decreased by a factor 2 or more. The variation of settling velocities did influence the average level of SSCs, but did not influence the tidal variations as much. Furthermore, the variation of the resuspension parameters had little effect. The model turned out to be most sensitive to the decrease of the critical shear stress of the buffer layer, which gave positive results in both North and South Bay. The average level of SSCs increased and the variation over the spring-neap tidal cycle improved as well.

Furthermore, the effect of increasing vertical dynamics in the model was tested. Both fall velocity and resuspension parameters were increased proportionally, as more deposition will increase sediment availability during energetic periods. North Bay and South Bay tended to respond oppositely to most changes of the spatially uniform parameters. Applying separate values for sediment parameters in North and South Bay resulted in better model performance.

Most important conclusions to be made from the varying sediment parameters in the model are: 1) North Bay and South Bay respond differently to a sediment parameter alteration constant in the entire model domain. 2) only varying a sediment parameter in the targeted area gave a positive model response, without decreasing model performance in the rest of the model domain. 3) SSC variations over the spring-neap cycle were most sensitive to the variation of the critical shear stress of the buffer layer and less to the variation of the critical shear stress of the fluff layer. 4) Variation of settling velocities mainly shifted average SSC levels, but did not increase SSC variability over a daily or spring-neap tidal cycle. Supporting figures of this sensitivity analysis are included in Appendix A.

4.2.1. Changing Forcings and Boundary Conditions

In the shallow parts of an estuary, the interaction between currents and waves is responsible for the resuspension of sediments. Especially waves can induce significant resuspension of cohesive sediment in shallow waters. As most of San Francisco Bay is sheltered against ocean swell, waves are generally wind-driven and locally generated with a limited fetch. Especially winter storms and strong summer breezes can generate waves up to 0.6 meters in San Pablo Bay (Barnard et al., 2013c). Particularly in shoal-channel estuaries like San Francisco Bay, many regions are shallow enough for wind waves to interact with the muddy bottom (Brand et al., 2010). Shallow shoals comprise a significant part of South Bay and San Pablo Bay and field measurements in South Bay show the highest levels of suspended sediment concentrations during flood tides combined with a low tide with high wave events. Hence, wave resuspension is considered an important process to incorporate in the simulation of sediment transport in San Francisco Bay.

The first version of the hydrodynamical output of WY2013 provided by SFEI did not include the computa-

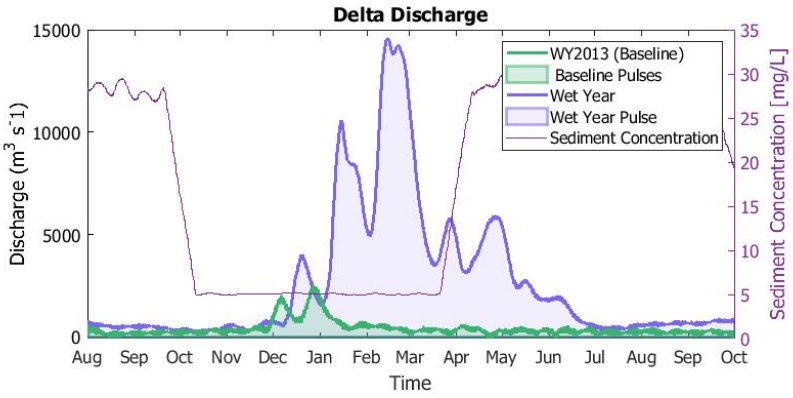

Figure 4.4: Depiction of the faulty input-file of sediment concentrations of the incoming rivers near the Delta, against the background of the incoming water discharges from the Delta during the simulation period. The sediment concentrations tend to follow the signal of water discharges as higher velocities increase the amount of sediment that is brought in suspension. In this signal of sediment concentrations instead of an increase, a decrease is observed from October 2012 until April 2013.

tion of wave-induced bottom shear stresses. Therefore, also the DELWAQ simulations did not comprise wave forcing, while the model version of Gostic (2018) did. Therefore, the set of parameter settings did not fit the hydrodynamic forcing. SSCs values only increased to former values by decreasing *Taushields* parameter by a third compared to previous parameter settings. Waves were found to be very important to include in the hydrodynamic forcing and a new hydrodynamic simulation for WY2013 was run that included waves. After the incorporation of waves, the initial bed was spun-up again for the new hydrodynamical forcing and the sediment settings from Gostic (2018) performed well again.

All conducted simulations showed a lack of high sediment concentrations in North Bay during the peak of river discharges and the accompanying sediment input from the Delta. Significant volumes are expected to enter during this period, yet it was not observed in model results. This led to an inspection of the provided boundary condition files for the sediment concentrations of the Sacramento River and the San Joaquin River. Analysis showed the files for WY2013 were flawed. New input files were generated for the two rivers with a local relationship between river discharge and suspended sediment concentrations in the river. This relationship is derived from the records of discharge and sediment concentrations in WY2015. More details can be found in Appendix A. Furthermore, the modelled wind forcing was revised by King (2019), by developing a new simpler method for generating wind fields. In previous studies, the Ludwig wind model was applied to generate spatial and temporally varying wind inputs. As it was cumbersome to acquire and convert wind data sets in the required format a new method was developed. Wind fields resulting from the new method by King (2019) are more accurate by 30 percent compared to hourly measured wind speeds.

4.2.2. Conclusions

The sensitivity analysis has revealed that the two hydrodynamically distinct sub-estuaries of North Bay and South Bay respond differently to a sediment parameter alteration if it is applied in the entire model domain. Setting separate parameters to the different parts of the Bay gave a positive model response in the targeted area, without decreasing model performance in other parts. Furthermore waves are found to be of importance and are advised to be included in the hydrodynamic model. Extra bottom shear stresses generated by wind waves stir up sediments at the extensive flats of the Bay. Waves should be included to enable the model to capture these peaks in concentrations.

4.3. Calibration Method

A Baseline Run resulted from this early sensitivity study of the model after which two different areas of focus where identified. As a first step the measurements of the USGS stations are compared to the model output. The model performance is described in a quantitative manner by computing the Mean Absolute Error and the Brier Skill Score. Calibration scenarios are developed to improve model performance with respect to the measured data.

4.3.1. Statistical metrics for model performance

MAE is the average of the absolute difference between the predicted values and observed value. The Mean Absolute Error (MAE, Equation 4.1) is chosen instead of the more popular Root Mean Square Error(RMSE) as the presence of outliers is emphasized for an RMSE. When modelling suspended sediment concentrations errors occurring during certain episodes of high concentrations should not detract from the overall quality of the modelling. The MAE is not biased towards higher deviations as is a linear score indicating that all the individual differences are weighted equally in the average.

Another commonly used metric for the assessment of model performance is the Mean-Squared Error Skill Score (MSESS), also known as the Brier Skill Score(BSS), described in equation 4.2. The skill score is the mean square difference between the model forecast and the observed value weighted by the squared sum of the observed values, with y_i denoting the model forecast and i_i denoting the observed values. The skill score ranges from 1 for an impeccable score to -∞, with scores lower than zero implying the error between the modelled and observed value is bigger than the values of the measurements itself.

$$MAE = \frac{1}{n}\sum_{n}^{i=1} \left| y_i - x_i \right| \tag{4.1}$$

$$BSS = 1 - \frac{\sum_{n}^{i=1} y_i^2 - x_i^2}{\sum_{n}^{i=1} x_i^2} \tag{4.2}$$

4.3.2. Baseline Model

After prior calibration efforts and the sensitivity analysis of the model parameters, a parameter set was defined as the Baseline Run. The model was run for WY2013 with a simulation time of 01-08-2012/01-10-2013 for which the first two months are regarded as spin-up time. The parameter settings used for the Baseline Run can be found in Table 4.2. Hereafter, the modelled SSCs will be compared to the USGS Data, Polaris Cruise Data, and the Satellite Imagery.

Six locations in the Bay with high-frequency(15-min) SSC measurements spread throughout SFB and two DFW Cruise locations at the South Bay East Flat and West Flat were used to compare the performance of the model in time. Figure 4.5 shows the results for the Baseline Run. The model seems to capture the daily averaged SSC trend relatively well in most stations in both North Bay (Benicia Bridge & Richmond Bridge) and South Bay (Dumbarton RR and Shoal 103 and 104) during most of the year. Only the station Mallard Island located near the Delta shows a structural underestimation of the modelled SSC.

The underestimation of the SSC in South Bay during spring (April-July) stands out especially at the shoals at Site 103 and 104, though also at Dumbarton Bridge SSCs are underestimated. Representative stations for North Bay (Richmond Bridge) and South Bay (Dumbarton Bridge) were selected to investigate the behaviour of the tidal signal in the SSC. In Figure 4.6 the model results for two weeks representative for Autumn/Winter and Spring/Summer are plotted. Particularly Richmond Bridge shows a high amplitude in the SSC signal in Winter which is not captured by the model, while the daily averaged SSCs agree quite well. This high amplitude has disappeared completely in the SSC signal measured in Spring, which the model captures well. At Dumbarton Bridge, the amplitudes seem to agree in winter, though they are out of phase. The amplitude is much smaller than the amplitude measured at Richmond Bridge which is likely because Dumbarton Bridge is located further from the tidal inlet at Golden Gate Bridge. In spring the modelled amplitude is overestimating the measured amplitude.

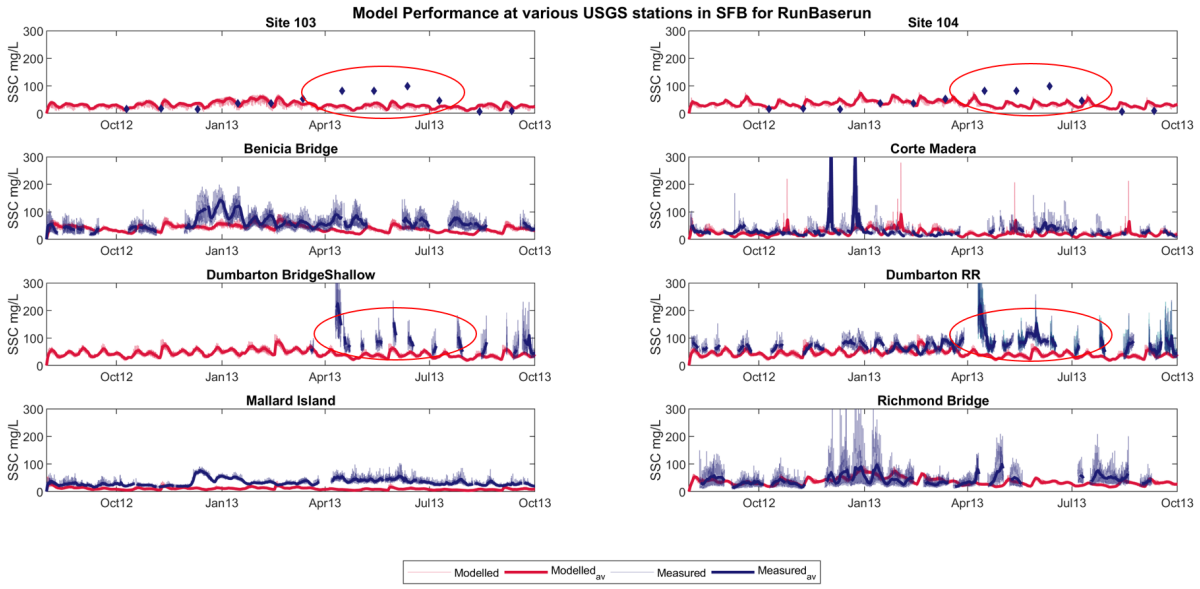

Figure 4.5: Results for the Baseline Run for the High-Frequency USGS-stations over the entire simulation period. With the daily averaged modelled SSCs in thick red lines red and the measured SSCs in blue for the 8 USGS stations. Instantaneous measurements are shown in the thinner transparent lines. Locations of all stations can be found in Figure 4.1a

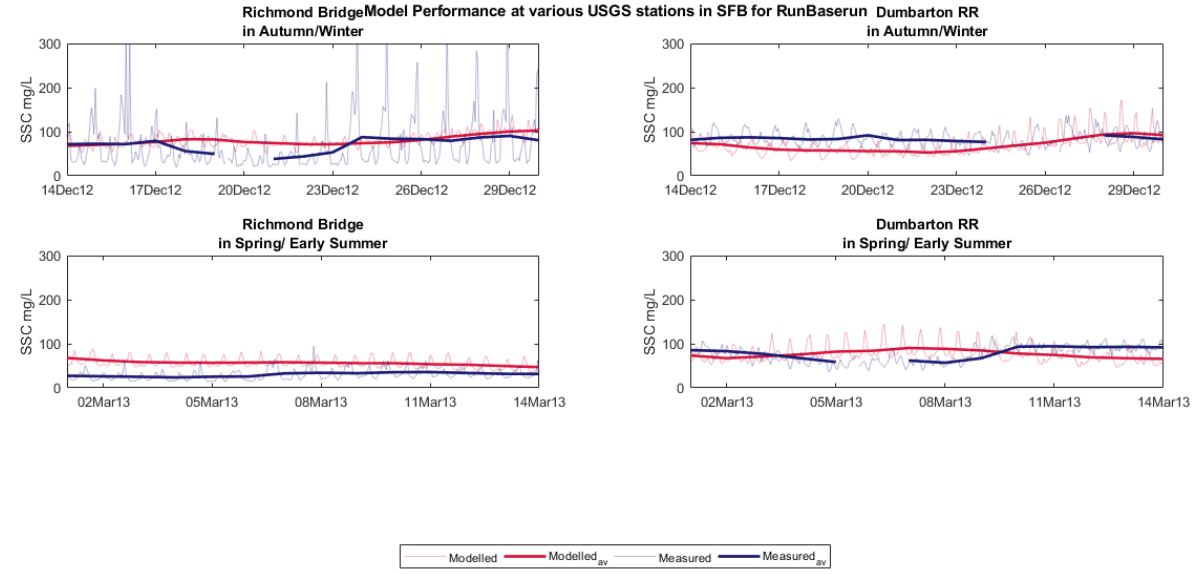

Figure 4.6: Results for the Baseline Run for the High-Frequency USGS-stations during Autumn/Winter and Spring/Summer for stations in North Bay (Richmond Bridge) and South Bay (Dumbarton Bridge). With the daily averaged modelled SSCs in thick red lines red and the measured SSCs in blue for the 8 USGS stations. Instantaneous measurements are shown in the thinner transparent lines.

A thalweg plot was created to compare the measured data with the modelled SSCs. Figure 4.7 shows the results for a cruise conducted on March 18th, 2013. At this specific moment in time, high sediment concentrations were measured at South Bay (mid-plot). The model results (top-plot) do show an increase in sediment for South Bay, yet the sediment concentrations are underestimated. In the entire transect, the model shows SSCs of 30-40 g/ml whereas only SSCs of 10-20 g/ml were measured, with exception for South Bay. The thalweg plot only shows the results for one cruise, though its results are representative for the other 23 conducted cruises. The model underestimates the SSCs at locations where peaks in SSCs were measured, indicating smoother gradients in the model than in the measurements.

As the thalweg plot only provides a comparison at one moment during the simulation period a time stack plot was created to indicate the model performance during the simulation period. The time stack plots in Figures 4.8a and 4.8b show the overestimation or underestimation of the model near the bottom and near the surface. The top or bottom depth layer the bottom-plot such as Figure 4.7 represents single column. In time stack plot, columns each representing one Polaris Cruise are stacked in time. The plots show an equal signal of over- or underestimation during a certain cruise, yet the signal is stronger closer to the bottom. Highest concentrations can be found near the bottom, which is why an over- or underestimation is likely to be higher than near the surface. The time stack plot shows an overestimation throughout the Bay during winter, but from December onwards higher concentrations are measured in both North as South Bay which the model does not capture. The model tends to overestimate the SSCs at Central Bay the entire year.

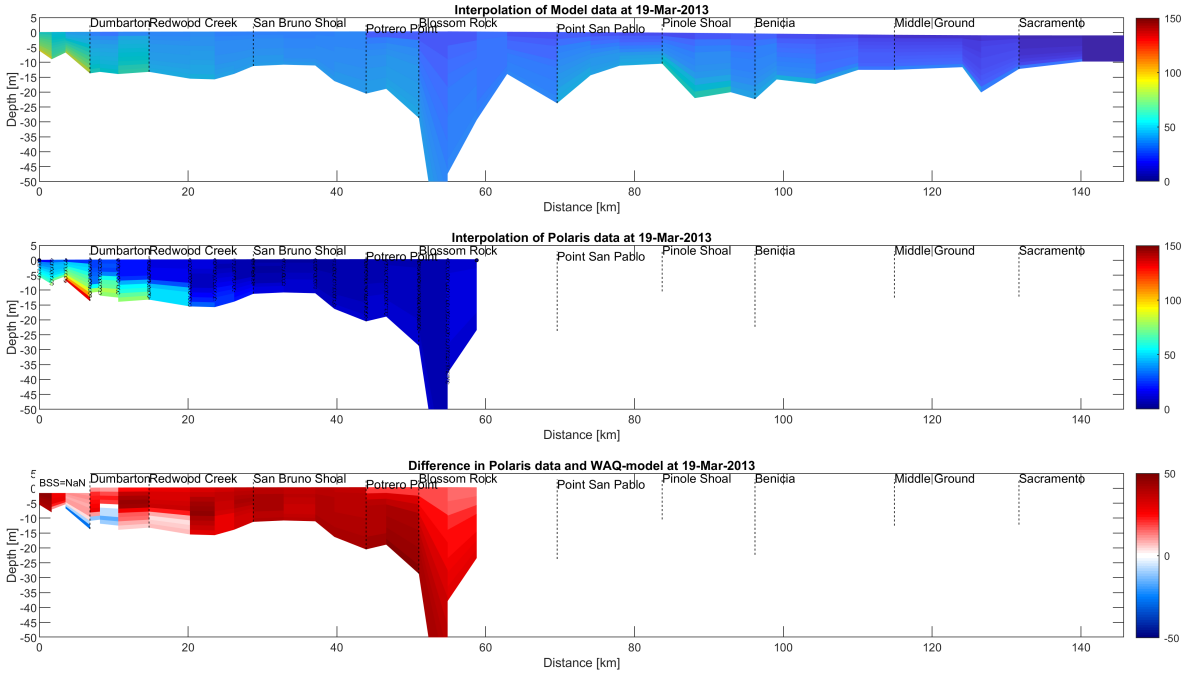

Figure 4.7: Comparison of modelled and measured SSCs along the transact sailed by the Polaris Cruise. This figure shows the results for one cruise at a certain date. Measurements were taken at 37 locations in the Bay Figure 4.1b between which was interpolated(mid plot). Model results were obtained for the same 37 locations and also interpolated(top plot). The measured SSCs were subtracted from the modelled SSCs in the bottom plot with an overestimation in red and an underestimation in blue.

As an additional data source, the indication of SSCs at the surface derived from satellite imagery is consulted. It is a valuable addition to the other data sources as it has high spatial coverage and gives information on SSCs at the shoals. The used relation between the turbidity and suspended sediment concentration to create the figures is not validated yet and still under development. Hence, the data was only be used to observe whether trends are captured by the model. According to Figure 4.9 the model shows similar trends in surface SSC in most of North Bay, with an increase in SSC at the flats and lower values in the channel. Only at Suisin Bay where the Delta rivers flow into SFB, the model underestimates the SSC. In South Bay, the order of magnitude of surface SSC is captured well in the channel, yet the observed SSC shows a decrease at the shoals, whereas the suspended sediment seems to be uniformly distributed over all South Bay according to the model. After comparing the model output of the Baseline Run to the various measured data a few discrepancies show up in all the sources. (1) There seems to be an underestimation in SSCs in South Bay during spring. (2) The amplitude in the SSC following the tidal signal is underestimated by the model North Bay according to the USGS data. This is compatible with the lack of high gradients and the absence of peak values in the model, which are found in the Polaris Data.

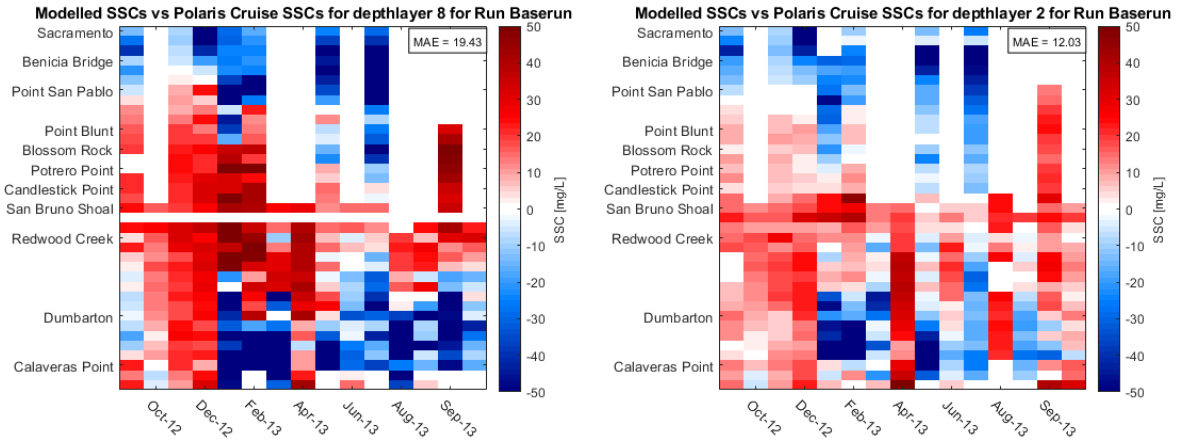

(a) (b)

Figure 4.8: These time stack plots show the overestimation or underestimation of SSCs by the model in absolute values compared to the measured SSCs of the Polaris cruises for the WY2013. Each column represents the results from a cruise expedition with the spatial location of the transact along the y-axis, with North Bay at the bottom and South Bay at the top. Figure a) shows the time stack plot for the depth layer near the bottom and b) shows the time stack plot for the depth layer near the surface.

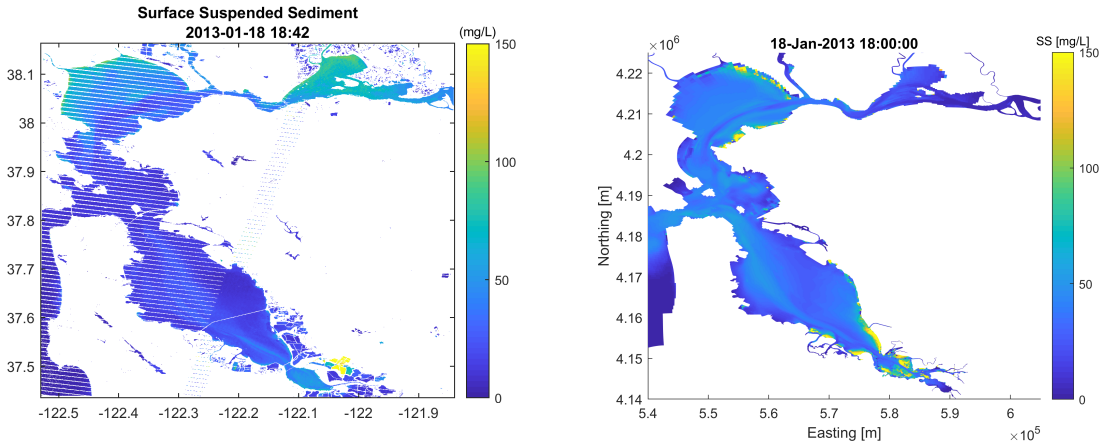

(a) Indication of suspended sediment concentrations at the surface derived from the satellite images (b) Modelled SSCs at the surface layer

Figure 4.9: Comparison of Modelled SSCs with Satellite imagery at January 18th 2013

4.3.3. Calibration Scenarios

As discussed in the previous section, the Baseline model run does not capture all observed characteristics of the measured SSCs. Two main focus points are increasing SSCs in South Bay in Spring and to increase gradients in the model to enable it to capture peak values when necessary. To improve model performance several calibration scenarios were developed, each influencing the model behaviour differently. As two distinctive discrepancies were identified, separate calibration scenarios have be developed to deal with it. The model calibration has focussed on increasing the SSCs in South Bay in Spring and the model's ability to capture high gradients and peak values, with thereby increasing the amplitude of the SSC following the tidal signal where needed.

Increasing SSC in South Bay during Spring

A comparison of the modelled results to the USGS measurements shows a distinct underestimation in Spring for SSCs in South Bay. Especially the stations at the shoals (Site 103 and 104) show a strong underestimation. Also the station at Dumbarton Bridge shows an underestimation. During this period (south-)westerly summer breezes are typical, which result in significant wave generation(Barnard et al., 2013c). Water depths at the South Bay shoals are sufficiently shallow for resulting wave motions to reach the bottom, where wave energy is dissipated. Figure 4.10 shows the modelled wind and bottom shear stresses at the two shoal locations

in South Bay. Bottom shear stresses at Shoal 104 have a wind wave induced component, while Site 103 does not show this signal as waves generated by westerlies are not fully developed at this location. Whereas wind speeds increase on average from April on, bottom shear stresses at Shoal 104 do not show this increase.
The shoals in South Bay have small slopes and at some locations extend for several kilometres, which has shown to lead to a wave height reduction of 50% at the shoals of San Pablo Bay located in North Bay(Lacy and MacVean, 2016), which are similar. Wave height reduction at shoal locations further from the channel might explain why the increase in wind speeds in Spring do not lead to an increase in bottom shear stresses. However, field measurements of bottom shear stresses at a nearby location at the SB East Flat by Brand et al. (2010) show that wave shear stresses contribute significantly to the bottom shear stresses during windy periods, both near the channel as further in the shoal. Also different field measurements of bottom shear stresses located at a shoal south of San Mateo Bridge performed by Egan et al. (2019) showed a dominant wave induced component. Perhaps this difference could be explained by the siltier nature of the buffer layer in South Bay, which attenuates waves better(Lacy and MacVean, 2016).

The adequate modelling of bottom shear stresses is an important factor in the modelling of mud resuspension and therefore sediment transport(Lacy and MacVean (2016), Egan et al. (2019)). The study of Egan et al. (2019) also attempted to characterize the mean and turbulent properties of the boundary layer for the location in South Bay. They observed canopy flow dynamics near the bed with a strong near bed wave-induced momentum flux in the case of strong waves and highlighted the importance of a correct characterisation of the bottom roughness. The measured shear stress in the study could not be approximated well by various estimation methods due to unresolved canopy flow dynamics and wave momentum fluxes. The bottom shear stresses in DFLOW were simply calculated by adding the bottom shear stresses due to currents and waves assuming the velocity profile follows the logarithmic profile. This more traditional approach is likely to overestimate mean current-induced shear stress, but to underestimate the total bed shear stress during strong waves.

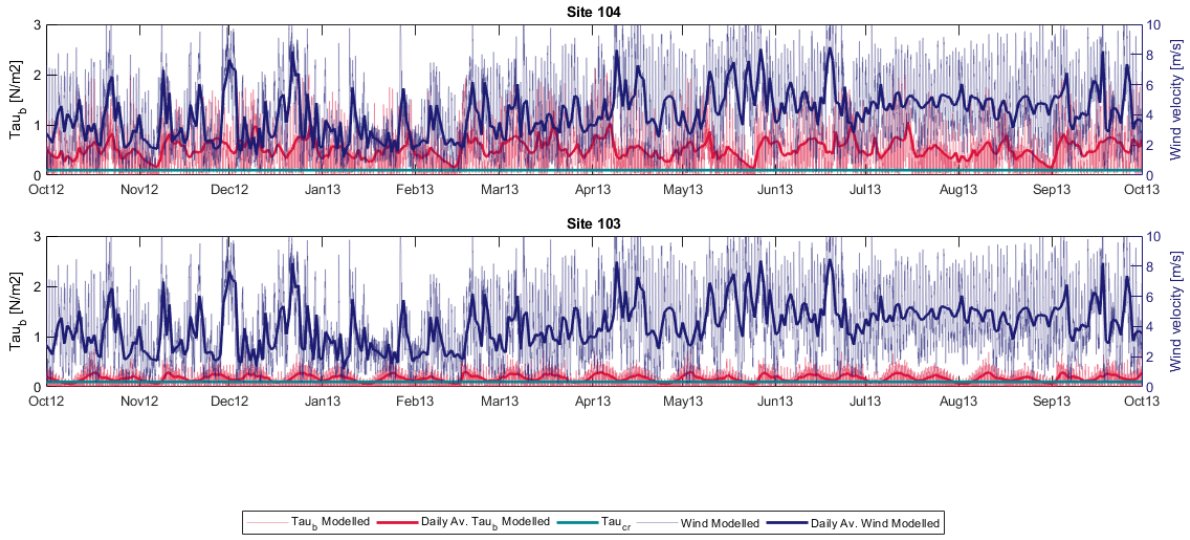

Figure 4.10: Two plots showing the local modelled wind speeds in blue and the local bottom shear stresses in red at the West Shoal (Site 103) and East Shoal (Site 104) in South Bay.

Furthermore, increased wind stress on the water surface during high wind events can influence flocculation of suspended particles. Due to the flocculation of the mud particles, the fall velocity imposed to the model represents the settling velocity of flocs, which depends on the floc size and shape (Chen Margeret, 2015). Turbulent motions can increase floc sizes as more individual particles can collide and form bigger flocs, yet when turbulent shear gets too high inter-particle bonds may break decreasing the average floc size. The process of flocculation and the effect of turbulent mixing due to waves is not included in the DELWAQ-model (Deltares, 2019). During the observed strong wind events turbulent shear at the shoals may get to the level of deflocculation, decreasing the floc settling rate. Also, in Spring temperature of the water increases, which is found to be favourable for the formation of spherical floc shape with lower settling rates (Chen Margeret, 2015). As

a final potential cause for the increased SSCs found in South Bay is the increase of bioactivity during Spring as temperature rises. During the field work of Egan et al. (2019) benthic worm species were found stirring up sediments. Many different species of invertebrates are found throughout the Bay (Mooi et al., 2007), which fecal pellets are more erodible than the cohesive bed. This can lead to increased erodibility (Austen et al., 1999).

Three potential causes for the increase in SSCs at the South Bay shoals in Spring are identified above and three scenarios were developed to take them into account in the DELWAQ model by altering the sediment parameters. While bottom shear stresses are found to increase in the field during strong wind events (Brand et al., 2010), bottom shear stresses computed by DFLOW do not show this increase. This is artificially compensated for in the calibration scenario S1 by lowering the critical bottom shear stresses for the buffer layer to bring more sediment in resuspension as would happen during higher wind events. It is preferred to deal with the issue by changing the calculation method for the bottom shear stresses themselves, yet this is not possible as the bottom shear stresses in the model are obtained from the DFLOW simulation and are not calculated in a DELWAQ simulation. In calibration scenario S2 the fall velocities are decreased to compensate for the increase of wind shear stress and mixing due to waves, of which the effects are not included in the model. In scenario S3 the erodibility of the bed is enhanced by increasing the first-order resuspension parameter to account for the presence of bioactivity. Table 4.1 shows the precise values for which the sediment parameters were altered in South Bay from 1-Apr/14-Jul in the simulation period.

Table 4.1: Overview of the scenarios and sediment parameters used to increase the SSCs in South Bay during Spring.

Calibration scenarios (SB in Spring) Parameter	Symbol	Unit	Baseline	S1	S2	S3
Settling Velocity (IM1/IM2)	ws	[mm/s]	0,5/0,1	0,125/0,025	0,5/0,1	0,5/0,1
Critical Shear Stress S1	τ_{c1}	[N/m^2]	0,1	0,1	0,1	0,1
Critical Shear Stress S2	τ_{c2}	[N/m^2]	0,9	0,9	0,9	0,75
0th Order Resuspension Flux S1	M0	0,0006	[g/m^2/s]	0,0006	0,0006	0,0006
1st Order Resuspension Flux S1	M1	0,00006	[g/m^2/s]	0,00006	0,00012	0,00006

Increasing gradients and peak values of SSC

Analysis of the Baseline run shows that the amplitude in SSC following the tidal signal is underestimated by the model at certain stations in North Bay according to the USGS data. This is compatible with the lack of high gradients and absence of peak values in the model, which are found in the Polaris Data. To increase the presence of high peaks and stronger gradients in the model three different scenarios where the sediment parameters have been adjusted were developed. Besides, the previously used numerical scheme in the computation was consulted as this can influence the level of gradients computed by the model.

First Scenario

In the first scenario the settling rates for both fractions are increased to enlarge the vertical gradients in SSC, which are observed in the measurements of Polaris. Yet, only increasing the fall velocity will not necessarily lead to higher concentrations near the bottom as it will also increase the total sedimentation flux and most suspended sediments will be taken up in the bottom. Furthermore, it results in an imbalance with the unadjusted resuspension flux leading to a decrease in average SSC over time. To compensate for the increase in settling rates and prevent the two resulting issues, the deposition efficiency is lowered equally to retain an equal sedimentation flux. Besides, decreasing the deposition efficiency will cause higher SSCs near the bottom as not all falling sediments are directly taken up in the bottom.

Second Scenario

The second scenario focuses on the influence of the initial availability of sediment in the fluff layer on the resuspension flux. After transition to the first-order regime the resuspension flux is the product of parameter M1 and the amount of mass in the fluff layer(see Equation **??**). The moment of transition from zeroth to first order is also influenced by the amount of sediment in the bed as it will transition earlier into a first order regime if the fluff layer is thinner. Thin fluff layers prevent high peaks in SSCs during energetic periods as there is not enough sediment available to get into suspension. More sediment was added artificially to the fluff layer and the first order resuspension parameter was decreased equivalently to retain an equal resuspension flux in calm conditions, yet during energetic conditions the fluff bed will not be depleted.

Third Scenario

In the third scenario, an attempt is made to enhance the gradients in the model by lowering the critical shear stresses of both the buffer layer and the fluff layer and the resuspension flux scales with the exceedance of the critical shear stress by the modelled bottom shear stress. This will create a higher resuspension flux during energetic periods. An overview of the applied sediment parameters in each calibration scenario can be found in Table 4.2.

Table 4.2: Overview of the scenarios and sediment parameters used to calibrate the model to enhance gradients and peaks where measurements show this

Calibration scenarios (Gradients & peak values) Parameter	Symbol	Unit	Baseline	C1	C2	C3
Settling Velocity (IM1/IM2)	ws	[mm/s]	0,5/0,1	2,0/0,4	0,5/0,1	0,5/0,1
Critical Shear Stress S1(NB/SB)	τ_{c1}	[N/m^2]	0,1	0,1	0,1	0,08/0.1
Critical Shear Stress S2 (NB/SB)	τ_{c2}	[N/m^2]	0,9	0,9	0,9	0,8
0th Order Resuspension Flux S1	M0	[g/m^2/s]	0,0006	0,0006	0,00012	0,0006
1st Order Resuspension Flux S1	M1	[g/m^2/s]	0,00006	0,00006	0,000012	0,00006
Deposition Efficiency	p_2	[-]	0,1	0,025	0,1	0,1
Bed Mass in fluff layer	[-]	[g/m^2]	x 1	x 1	x 5	x 1

4.3.4. Numerical Scheme

In addition to varying the sediment parameters, better model performance is pursued by changing the applied numerical scheme in DELWAQ. The analysis of the new measurement data of Polaris of Figure 4.7 has shown steep gradients in both the horizontal and vertical direction, which the model does not capture well. In all previous DELWAQ simulations, the implicit upwind-scheme was used in both the vertical and horizontal direction. An upwind scheme induces numerical mixing of steep gradients and is hence not recommended to use in case of steep gradients (Deltares, 2019). As steep gradients in SSC are measured by Polaris throughout the year, the upwind scheme is not suitable for this SFB DELWAQ-Model. Instead, the *Local-Theta Flux-Corrected Transport* scheme is applied. This scheme first solves the equations for a cell with an explicit method. If the CFL-criterium is met then no further processing is required. Otherwise, an implicit method is used where just enough numerical dispersion is added (Deltares, 2019). This approach reduces the amount of numerical mixing significantly, without increasing the computation time.
Results for this alteration can be observed in Figure 4.11 where the top-plot shows the modelled SSCs for the upwind scheme, the mid-plot shows the modelled SSCs for the new numerical scheme and the bottom plot shows the measured SSCs by Polaris. Though all sediment parameters and hydrodynamic forcing remained equal a clear difference can be observed between the results of both simulations. The simulation with the new numerical scheme shows steeper gradients and higher values and approaches more towards the measured SSCs.

4.4. Calibration Results

First, the results of the different scenarios developed to increase Spring SSCs in South Bay are discussed after which the results of the three scenarios dealing with enhancing gradients. Peak concentrations have been analysed based on the USGS data. The best results were combined to a final calibration run, which were again compared to USGS data, Polaris data and satellite data.

Increasing SSC in South Bay during Spring

The outcomes of the three different calibration scenarios (Table 4.1) are summarized in Figure 4.12. In this figure, the three stations located in South Bay are plotted for the simulation time in Spring for which the sediment parameters were adjusted. All three calibration results have resulted in an increase in SSCs in South Bay, yet some perform slightly better. Waves are most abundant at Site 104, which shows the highest increase in SSC with scenario S1 showing maximum modelled values following a spring-neap cycle. Based on the few points of measurements at the shoals it is difficult to pick the best performing scenario so the performance at Dumbarton Bridge is leading. Scenario S1 seems to follow the spring-neap cycle trend best visually, whereas both S2 and S3 tend to underestimate the signal in the first month and overestimate the signal in the last month. Based on statistical analysis scenario S3 is clearly the best performing scenario, with top scores in

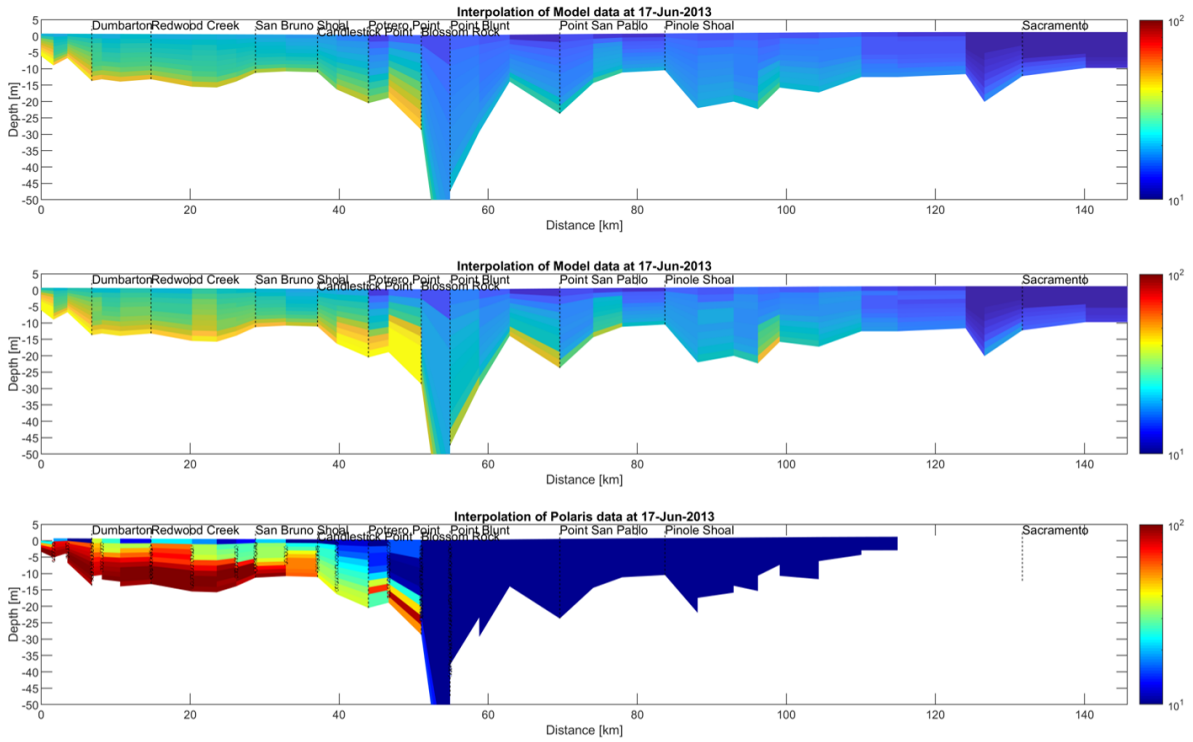

Figure 4.11: The difference in SSC depth profile for different numerical schemes. The top-plot shows the modelled SSCs on June 17th, 2013 for the upwind scheme. The middle plot shows the modelled SSCs at the same moment for a simulation with the local-theta flux-corrected transport scheme, which shows steeper gradients in the results as the scheme induces less numerical mixing. The bottom figure shows the measured SSCs at a Polaris Cruise conducted on June 17th 2013.

MAE and BSS (Figure 4.13b.b). As visual inspection of the three scenarios does not make any really stand out, both calibration scenarios S1 and S3 will be combined with the best performing scenario of the other calibration focus in Section 4.4.

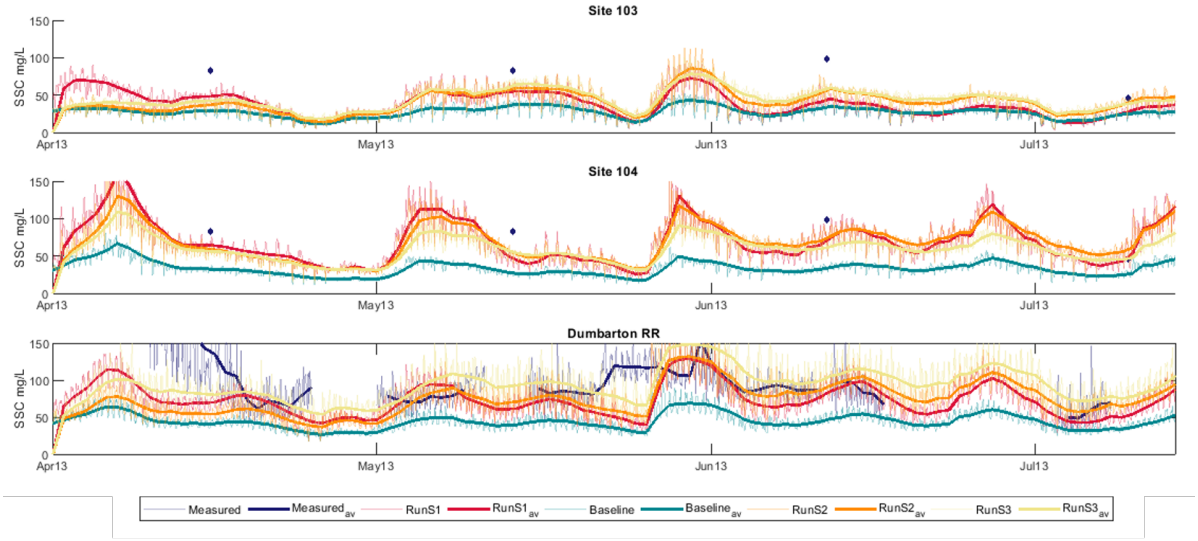

Figure 4.12: Results of the calibration runs plotted against the Baseline run (in green) for the stations in South Bay, respectively Site 103(West-Flat), Site 104(East-Flat) and Dumbarton Bridge.

Stations	MAE Base	C1	C2	C3	BSS Base	C1	C2	C3
3 - NB_BEN	11,7	11,83	48,57	11,62	0,82	0,85	-0,47	0,8
4 - NB_COR	9,7	9,4	40,06	8,83	0,31	0,36	-1,6	0,38
5 - SB_DUM	21,42	21,68	54,19	23,97	0,63	0,64	-0,55	0,58
6 - SB_DUMRR	15,54	17,78	84,79	19,14	0,76	0,72	-2,8	0,69
7 - NB_MAL	8,67	11,61	37,9	7,79	0,64	0,49	-2,2	0,7
8 - BN_RIC	10,45	9,09	40,94	8,53	0,7	0,74	-1,5	0,79
Total	77,48	81,39	306,45	79,88	3,86	3,8	-9,12	3,94
Total_NB	40,52	41,93	167,47	36,77	2,47	2,44	-5,77	2,67
Total_SB	36,96	39,46	138,98	43,11	1,39	1,36	-3,35	1,27

(a) Scenarios enhancing gradients and peak values in the model

Stations	MAE Base	S1	S2	S3	BSS Base	S1	S2	S3
3 - NB_BEN	15,8	15,76	14,53	16,59	0,71	0,72	0,72	0,69
4 - NB_COR	10,52	14,53	10,71	10,51	0,66	0,39	0,65	0,66
5 - SB_DUM	30,93	17,88	19,3	14,08	0,54	0,75	0,7	0,79
6 - SB_DUMRR	29,16	16,94	16,86	12,78	0,57	0,75	0,76	0,83
7 - NB_MAL	11,09	13,43	12,7	12,14	0,66	0,54	0,57	0,6
8 - BN_RIC	11,83	11,99	10,6	11,66	0,64	0,67	0,71	0,66
Total	3,86	90,53	84,7	77,76	3,78	3,82	4,11	4,23
Total_NB	2,47	55,71	48,54	50,9	2,67	2,32	2,65	2,61
Total_SB	1,39	34,82	36,16	26,86	1,11	1,5	1,46	1,62

(b) Increasing SSCs in South Bay during Spring

Figure 4.13: Overview of the model performance based on the MAE and the BSS for Suspended Sediment Concentrations measured at the USGS stations

Increasing gradients and peak values of SSC

In order to assess the performance the model results of the three calibration scenarios C1, C2 and C3 were plotted against the Baseline run (Figures 4.14, 4.15 and 4.16). The analysis is focused on the two stations in North Bay where the measured signal showed the highest amplitudes in the SSC signal and therefore initially the highest deviations of the model. Scenario C1 performs best based on visual assessment as Scenario C2 strongly overestimates the SSCs and does not show the right spring-neap signal. After the adjustment of the bed the scenario was run for 3 years as the bed needed to spin-up. The amplitude of SSCs following the tidal signal has improved though, so if more time is available to spin up the bed, this might be a more promising run. Scenario C3 also does not show the desired increase in amplitude, which scenario S1 does show. Statistical analysis shows mixed results as scenario C1 performs better based of the MAE, but scenario C3 performs best in the BSS with C1 not too far behind (Table 4.13b.a). However, the MAE and the BSS are calculated based on the daily averaged SSC and the daily amplitude in the signal of SSCs is not taken into account. As the enhancement of the amplitude of the daily SSC signal was the focus of these scenarios and as scenario C1 clearly performs better based on this aspect it is chosen as the best performing scenario.

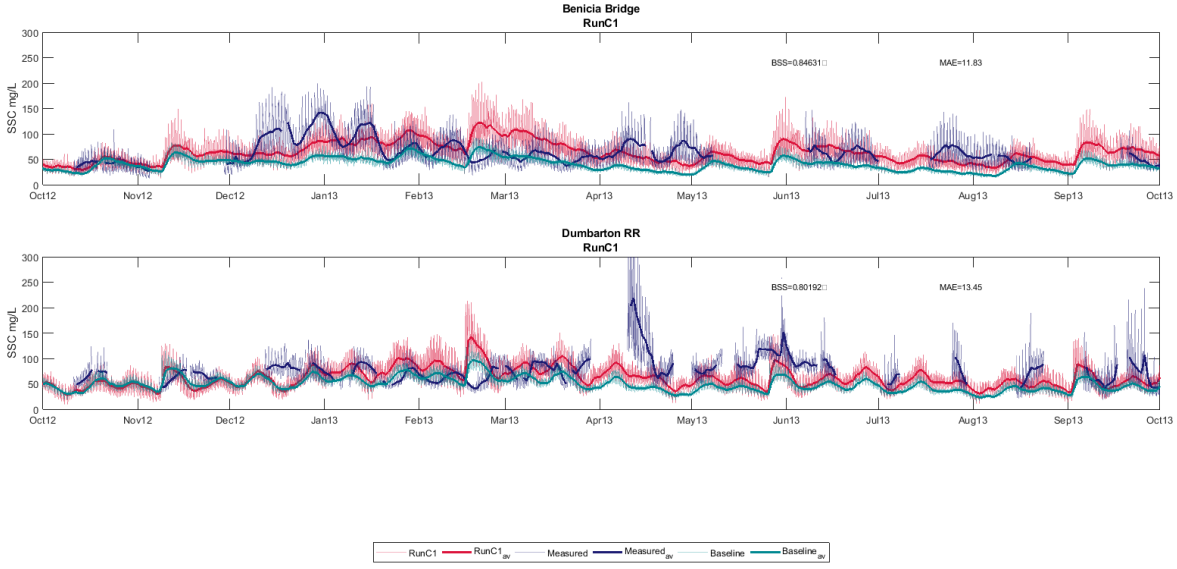

Figure 4.14: Results of the calibration scenario C1 (in red) plotted against the Baseline Run (in green) and the measured SSCs (in blue) for a station in North Bay (Benicia Bridge) and a station in South Bay (Dumbarton Bridge)

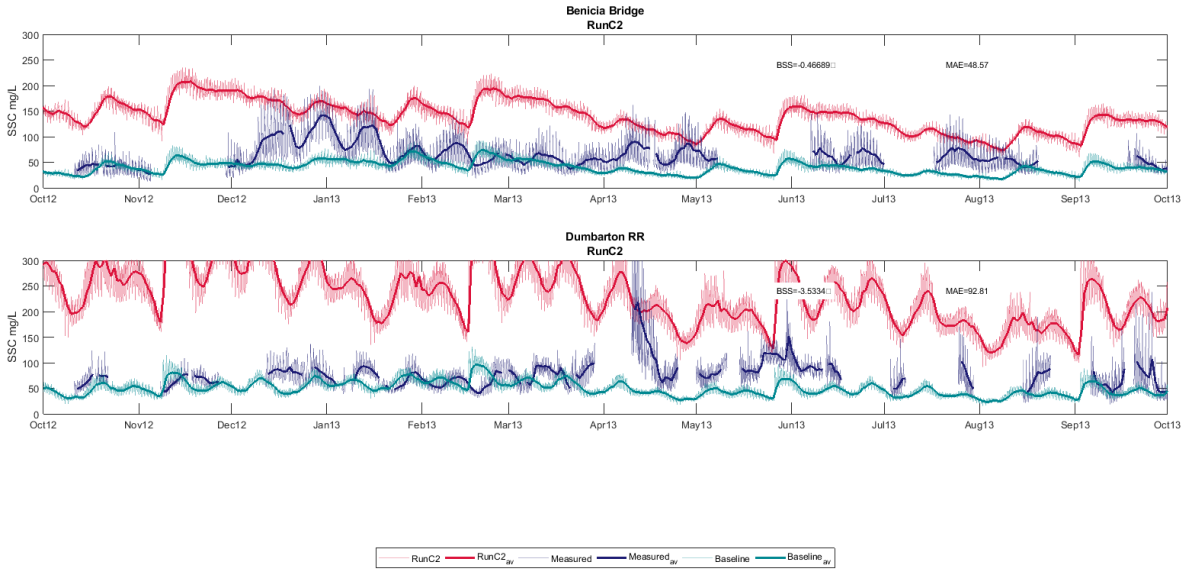

Figure 4.15: Results of the calibration scenario C2 (in red) plotted against the Baseline Run (in green) and the measured SSCs (in blue) for a station in North Bay (Benicia Bridge) and a station in South Bay (Dumbarton Bridge)

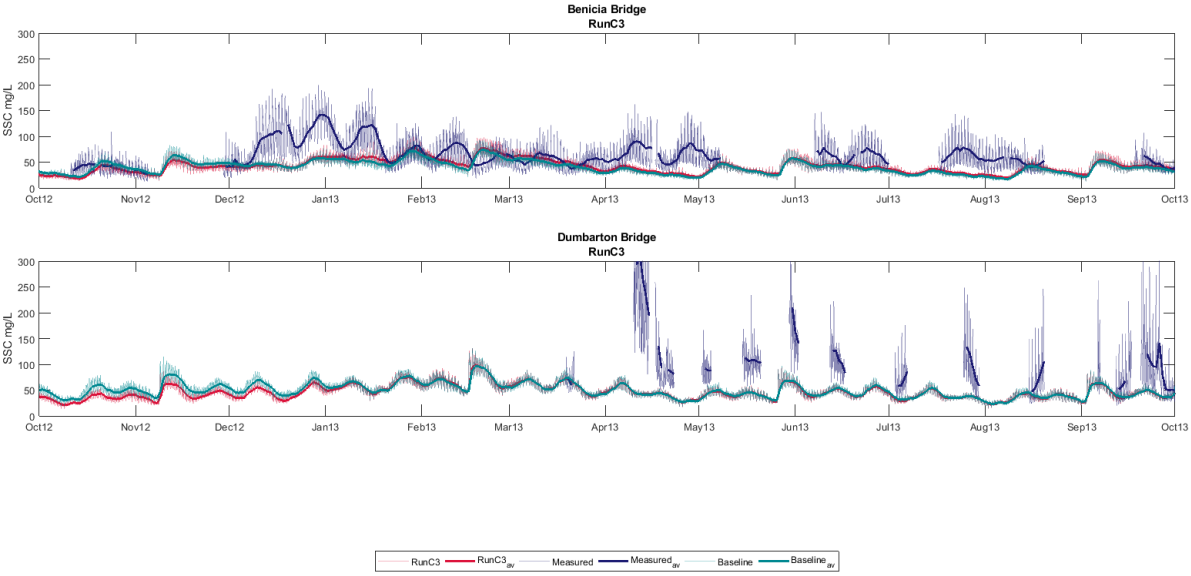

Figure 4.16: Results of the calibration scenario C3 (in red) plotted against the Baseline Run (in green) and the measured SSCs (in blue) for a station in North Bay (Benicia Bridge) and a station in South Bay (Dumbarton Bridge)

Final Calibration Run

For the final calibration step, the sediment parameter sets of run C1 and S3 were combined in order to let the model perform better on both the main discrepancies observed in the Baseline run in Section 4.3.2 with (1) the underestimation of SSCs in South Bay during Spring and (2) the lack of high gradients and peak values in the model. The sediment parameters of Run C1 were applied from 01-10-2012/01-04-2013, the parameters of Run C1 and S3 were combined during the period of 01-04-2012/14-07-2013 after which the parameters of only C1 were applied again until the end of the simulation period. In addition, the parameter sets of C1 and S1 were combined as combining S1/S3 with C1 might result in a different performance of the parameter sets. The Final Calibration runs have been analysed both visually as statistically, informing all three available data sources of USGS High-Frequency Data, Polaris Cruise data, and the satellite imagery.
Figure 4.17 shows the USGS results for the Final Calibration for the combination of Run C1 and S1. Although the scenario S3 performed best on the MAE and BSS in scenario 4.4, for the combination with run C1, S1

performed better than the combination of C1 and S3. The resulting sediment parameter set is shown in Figure 4.18.a. Compared to Figure 4.5 of the Baseline run the model results have improved significantly in different components. At both Site 103 and 104 at the shoals, the modelled SSCs signal is better able to follow the increase in Spring. However, the SSC concentrations are slightly underestimated at Site 103. In addition, average SSCs at Dumbarton have increased and approached the measured values better. Besides progress has been made in the second goal of the calibration efforts. The model shows a higher amplitude in the SSC signal on a daily scale when measurements show this same signal in comparison to the Baseline run. Higher peaks are observed in the model and stronger gradients in time are observed. Spatial gradients will be addressed when comparing model results to the two other data sources. The Final run statistically performs better in total, based on both MAE as BSS (Table 4.18). Performances on both metrics have improved significantly for the stations in South Bay (5 & 6). Statistical performance in North Bay varies per station, resulting in slightly lower performance in MAE and a slight increase in BSS score.

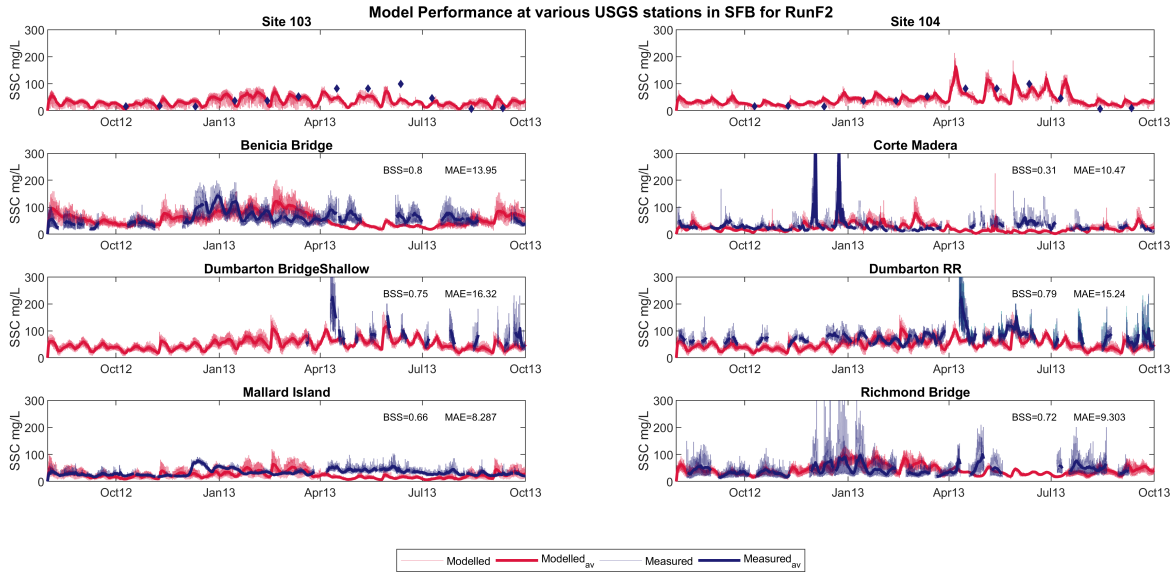

Figure 4.17: Results for the Final model calibration plotted against measured data of the High-Frequency USGS-stations over the entire simulation period. With the daily averaged modelled SSCs in thick red lines red and the measured SSCs in blue for the 8 USGS stations. Instantaneous measurements are shown in the thinner transparent lines. Locations of all stations can be found in Figure 4.1a

a)

Calibration scenarios Parameter	Symbol	Unit	Baseline	Final	$Final_{Spring}$
Settling Velocity (IM1/IM2)	ws	[mm/s]	0,5/0,1	2,0/0,4	0,25/0,05
Critical Shear Stress S1(NB/SB)	τ_{c1}	[N/m^2]	0,1	0,1	0,1
Critical Shear Stress S2 (NB/SB)	τ_{c2}	[N/m^2]	0,9	0,9	0,9
0th Order Resuspension Flux S1	M0	[g/m^2/s]	0,0006	0,00012	0,00012
1st Order Resuspension Flux S1	M1	[g/m^2/s]	0,00006	0,00006	0,00006
Deposition Efficiency	p_2	[-]	0,1	0,025	0,025

b)

Stations	MAE Base	MAE Final	BSS Base	BSS Final
3 - NB_BEN	11,7	13,95	0,82	0,8
4 - NB_COR	9,7	10,47	0,31	0,31
5 - SB_DUM	21,42	16,32	0,63	0,75
6 - SB_DUMRR	15,54	15,24	0,76	0,79
7 - NB_MAL	8,67	8,29	0,64	0,66
8 - BN_RIC	10,45	9,3	0,7	0,72
Total	77,48	73,57	3,86	4,03
Total_NB	40,52	42,01	2,47	2,49
Total_SB	36,96	31,56	1,39	1,54

Figure 4.18: a) Overview of the sediment parameter settings for the Baseline Run and the Final calibrated parameter set, with adjusted parameters for Spring. b) Overview of the model performance based on the MAE and the BSS for Suspended Sediment Concentrations measured at the USGS stations

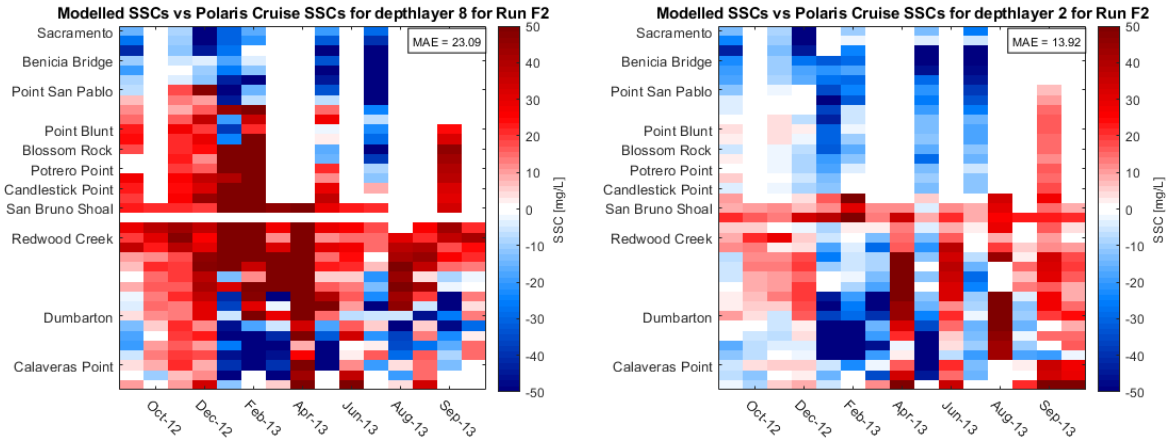

(a) Layer near the surface

(b) Layer near the bed

Figure 4.19: These timestack plot shows the overestimation or underestimation of SSCs by the Final Calibration model run in compared to the measured SSCs of the Polaris cruises for the WY2013. Each column represents the results from a cruise expedition with the spatial location of the transact along the y-axis, with North Bay at the bottom and South Bay at the top. Figure a) shows the timestack plot for the depth layer near the bottom and b) shows the timestack plot for the depth layer near the surface.

Secondly, the modelled results for the final calibration run are compared to the measured SSCs at the Polaris Cruises and the previous model results for the Baseline run. In Figure 4.20 the results for the cruise conducted on the 15th of July 2013 can be found in terms of a thalweg plot. At this moment in time, the Polaris Cruise shows some increased values of SSC in South Bay near the bottom. The Baseline run initially did not capture this signal, but the Final calibration run does show increased values near the bottom in South Bay. The peak values are not found at the exact same locations as in the Polaris Data, but the Final run simulates the signal better from a visual perspective. As Figure 4.20 only shows the results for a single conducted cruise a time stack plot was created to analyse the model performance compared to the Polaris Data over time. Figure 4.19 shows the time stack plot for a layer near the bottom and near the surface. Greater deviations from the measured data are found near the bottom. The model tends to overestimate the SSCs near the bottom compared to the surface, where more underestimation is observed. This is likely the result of the reduction of the deposition efficiency as this leads to higher sediment concentrations near the bottom. However, this adjustment has also led to increased gradients and peak values in the model as was the goal. Compared to the Baseline run, the Final Calibration run scores worse on the MAE both near the surface as near the bottom. As the calibration run aimed to increase peaks and gradients in the model SSC values have increased, which leads to bigger deviations when peaks do not occur at the exact location. Yet analysis of the individual Polaris cruises shows that the final calibration better captures the trends over depth and space, then the Baseline run.

In addition to the in situ measured SSCs, the model can be compared to sediment concentrations derived from satellite imagery. This gives an opportunity to analyse the model performance at shoals, which are less monitored in the other two data sources. Yet as the method of derivation of SSCs is still under development this data source is used to observe trends, but not to evaluate the absolute values of SSC. In Figure 4.21 the SSCs derived from a satellite image on January 18th were compared with the modelled SSCs at the surface layer for the final calibration run. The trend of high concentrations near the Delta is not visible in the model plot, yet there is more sediment present in the surface compared to the Baseline run (Figure 4.9). The sediment concentrations at San Pablo Bay show a clear gradient between the channel and the shoals, as is observed in the satellite image. Yet whereas the SSCs increase shoreward in the satellite image, SSCs seem to decrease shoreward in the model. Central Bay shows more turbid regions in the model. In South Bay the gradient between high SSCs in the channel compared to lower SSCs at the shoals are enhanced with respect to the more uniform distribution of the Baseline run. Nevertheless, the SSCs in the channel seem a bit too high. In Lower South Bay the model shows distinct peaks in SSC in different locations, whereas the satellite imagery shows a more uniform distribution.

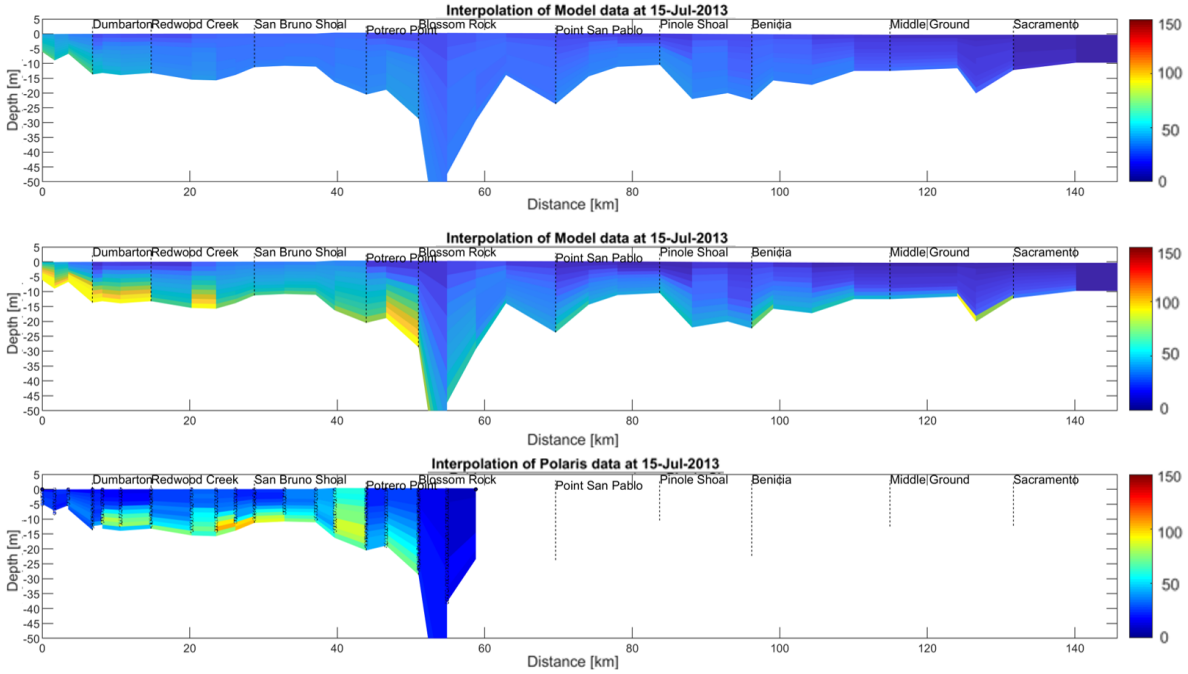

Figure 4.20: Comparison of modelled and measured SSCs along the transact sailed by the Polaris Cruise. This figure shows the results for one cruise at the 15th of July 2013. Measurements were taken at 37 locations in the Bay Figure **??** between which was interpolated(subplot). Model results were obtained for the same 37 locations and also interpolated. The top-plot shows the model results for SSCs of the Baseline run. The mid-plot shows the model results for SSCs in the Final run.

Model Results for a Wet Year Run

Calibration efforts have significantly improved the model performance for the DELWAQ simulation of WY2013 with increasing the variation in SSC over a tidal scale and increasing SSC values in Spring in South Bay. In addition, the model performance is tested for the relatively wet WY2017 when peak discharges from the Delta showed an increase of SSCs during Winter with respect to WY2013. Most remarkable is the very wet episode lasting from January to June where peak values increased by 400-600% (Figure 3.3). Two locations in San Francisco Bay have been selected in order to assess the model performance for WY2017. Richmond Bridge is located in North Bay, hence closer to the Delta river inflow and Dumbarton Bridge in South Bay. Richmond Bridge shows an increase in measured values, with peaks of an over 400% increase during the wet episode in WY2017 with respect to WY2013. The modelled SSCs follow the increased measured SSCs reasonably well from January until July. The model shows an increase in SSCs from mid-July Both WY2013 and WY2017 do not score well on the R-squared metric, yet as fine sediment values are hard to predict R-squared values below 0.50 are expected. Although there tends to be an underestimation in the model as measured values increase for WY2013, most measured values below 100 mg/L seem to be located around the 1:1 line. Modelled SSCs are significantly overestimated for all measured values and the model is considered to have a bad capability of prediction with only an R-squared value of 0.01.

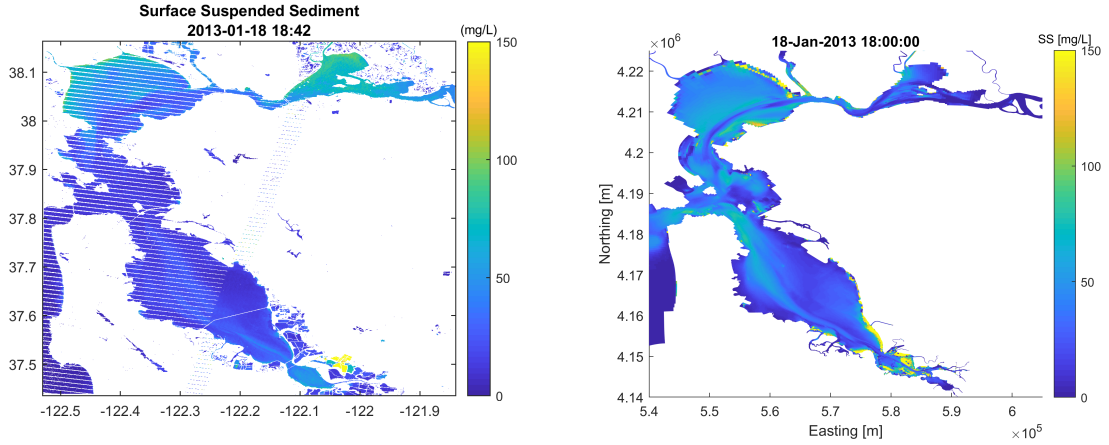

(a) Indication of suspended sediment concentrations at the surface derived from the satellite images

(b) Modelled SSCs at the surface layer

Figure 4.21: Comparison of Modelled SSCs with Satellite imagery at January 18th 2013 for the final calibration run

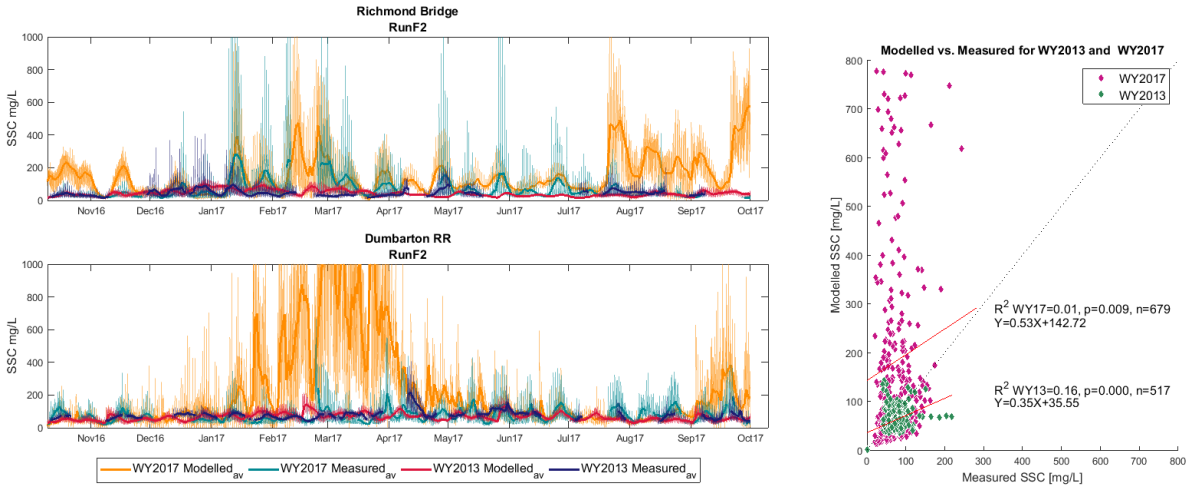

Figure 4.22: Results of model runs for WY2013 (in red) plotted with WY2017 (in orange) and the measured SSCs for WY2013 (in blue) and WY2017 (in green) for a station in North Bay (Benicia Bridge) and a station in South Bay (Dumbarton Bridge). Together with a scatter plot of the modelled SSCs plotted against the measured SSCs for WY2013 in green and WY2017 in pink.

5

Sediment Connectivity

San Francisco Bay is a large and complex estuarine system with several sub embayments of distinct character, complicating the exchange mechanisms between them. Hydrodynamics and subsequently sediment transport are subject to forcings of a different nature. Apart from the deterministic tide, stochastic forcings such as wind resulting in wind waves and river discharges introduce an uncertainty in the model, though some yearly repetitive patterns can be observed. Furthermore, a crucial challenge in sediment dynamics is the mismatch between the time and spatial scale of sediment processes such as deposition, sedimentation and advection and the resulting decadal and landscape-scale changes in morphology (Turnbull et al., 2018).
In other scientific disciplines, the concept of connectivity has been applied to analyse complex structures. In the discipline of neurology, connectivity is used to analyse connections in the brain Rubinov and Sporns (2010). Other scientific fields where connectivity is implemented include ecology, marine biology and social studies. Previous studies by amongst others Wainwright et al. (2011), Bracken et al. (2015) and Pearson et al. (2020) have explored the application of connectivity to sediment transport and developed frameworks for assessing (coastal) sediment connectivity. In these studies, the approach of sediment connectivity has shown promising results by providing a structured framework for analysing sediment pathways. In this framework, large datasets of spatial and temporal model output are reduced to an adjacency matrix, which enables the application of different statistical metrics. By adopting the approach of coastal sediment connectivity this study could act as an additional case study and provide extended proof of concept to the work of Pearson et al. (2020).

5.1. Hypothesis

According bathymetry studies, South Bay is the only net-importing sub-embayment in San Francisco Bay (Foxgrover et al., 2004). In addition, it is the only sub-embayment with a flood-asymmetry (Gartner et al. (1997), Barnard et al. (2013b)). Furthermore, persistent westerly to south-westerly winds are observed during Spring and Summer. Resulting surface currents drive sediments toward the southern land boundaries and in seaward direction at the channel(Walters, 1982). Hence, the sediment flux in the shallow part of the South Bay is expected to be directed toward the South-East (Schoellhamer (1996), Lacy and MacVean (2016)) during these seasons. Besides, calibration efforts of the previous chapter have shown that SSC levels increased at the South Bay shoals during Spring, which coincides with the period of strong consistent winds. Furthermore, South Bay is known to receive sediment input from local tributaries, yet it is suggested that sediment input from the Delta river system might be an important source for South Bay as well (Barnard et al., 2013c).

Based on literature and earlier calibration efforts four hypotheses on sediment pathways could be formulated. First, South Bay is expected to be importing during during WY2013. Secondly, it is predicted that the South Bay East Flat will erode during Spring due to strong resuspension. Thirdly, wind-induced resuspension and residual patterns are presumed to lead to seaward export and a south-easterly intra-Bay sediment flux. Lastly, it is hypothesized that sediments originating from the Delta river system are an important sediment source for South Bay.

Most of the literature on which these hypotheses are formulated are based on the results of local fieldwork

campaigns. Testing these hypotheses with a process-based model with a system-wide model domain will not only support the statements, further analysis of the model results can also provide more understanding of the underlying processes. This in turn can provide a more thorough understanding of sediment dynamics is South Bay, which can support the development of strategies to manage the issues facing coastal communities.

5.2. Methodology

5.2.1. Defining Sediment Connectivity

The word connectivity was simply defined as "a level of connectedness within a system, which corresponds to a set of relationships within spatially distinct entities" by Turnbull et al. (2018). In the field of sediment dynamics, it can be described as "the degree to which sediment can travel from point A to B" (Pearson et al., 2020). The route of sediment when travelling from point A to B are sediment pathways, thereby connecting different regions in the system. If these connections can be discovered and quantified, it can shed a light on the connectivity within the coastal system.

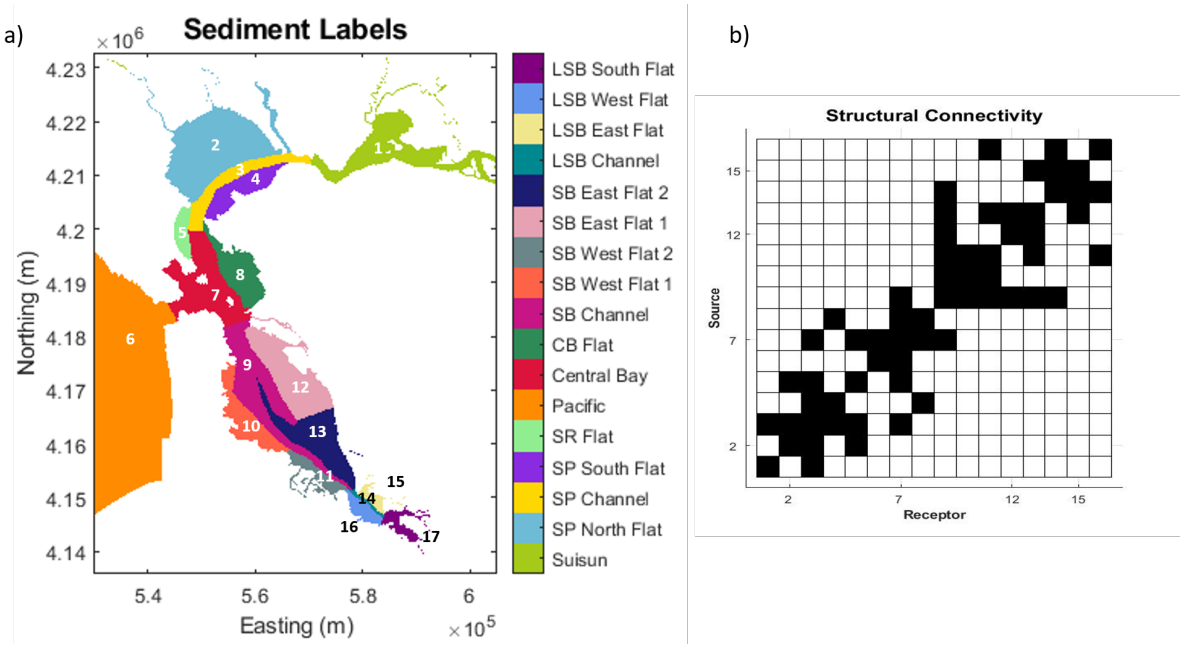

Figure 5.1: a) Division of San Francisco Bay into 17 segments for determining Sediment Connectivity, b) Structural Connectivity depicted in a adjacency matrix with a black cell for neighbouring segments

Setting up the graphical network

A first but very important step is to define the regions in the model domain between which the connections can develop. In literature, these regions are also known as morphologic cells. The way these morphologic cells are defined influences the connectivity that will be observed. When a complex estuarine system is reduced to a series of paths, inevitable simplifications can induce significant loss of information. Great attention should be paid to the division of the system to ensure that important patterns and signals will be captured (Pearson et al., 2020). At this moment, no general algorithm or guidelines are available to determine the optimal division in segments. General belief is that sediment transport and hydrodynamics within a unit should be relatively uniform. Furthermore, the number of segments should be sufficiently high to be able to observe the main distinct pathways in the system. Characteristics such as morphological function, depth, hydrodynamic energy and prior knowledge of sediment pathways can help define an optimal division.
When defining the morphological cells for San Francisco Bay, the first division was based on the morphological function by making a distinction between channels and shoals while applying a 5 meters depth threshold. Hydrodynamic energy and sediment transport is assumed to be relatively uniform within a shoal area or channel. In the end, a balance must be found in the determination of the total number of segments between a sufficient resolution and acceptable computation time (which increases with the number of segments). This

research focusses on South Bay and therefore a higher number of segments is defined in this area. Yet, this leads to a difference in surface area between the segments and perhaps a distorted result while identifying the important sediment pathways as larger segments are more likely to have strong gross fluxes. This effect is accounted for in the analysis by besides analysing gross fluxes, the sediment fluxes will be divided by the surface area of the originating segment. The resulting division of SFB is shown in Figure 5.1.a.

Structural and Functional Connectivity

A distinction can be made between two types of connectivity: structural connectivity and functional connectivity (Wainwright et al., 2011). In an estuary, structural connectivity can be defined as physical contact between adjacent segments. Functional connectivity represents the sediment fluxes between the segments or the exchange of sediment between segments. Sediment connectivity is based on the interaction between structural connectivity and functional connectivity (Figure 5.1.b). Both types of connectivity also impact each other. The functional connectivity is likely to have a strong relationship with the structural connectivity for shorter timescales as sediments are usually more likely to interact with neighbouring regions than distinct parts of the domain, yet this does not have to be the case. In return, functional connectivity can influence structural connectivity over time since unbalanced sediment fluxes can lead to morphological change, which in turn can change functional connectivity. However, this effect of interdependency is of less importance in our case as it particularly starts to play a role when time scales increase. In addition, a more practical reason is the fact that as we are working with a morphostatic model, the structural connectivity is not modified by the sediment fluxes (Newman, 2003).

5.3. Setting up the graphical network

Creating the Adjacency Matrix

Now that the different units in the model domain are defined, the complex system of San Francisco Bay can be viewed as a group of segments with sediment fluxes between them. This schematization can be framed as a network, following the approach of graph theory (Newman, 2003). In this approach, sources and receptors of sediment fluxes are defined as a series of n nodes connected by m links. Reducing the complex system of sediment dynamics in SFB to a series of nodes and links provides an opportunity to analyse the system mathematically and to assess the connectivity of different regions in the system.

The exchange of sediment between all morphologic cells will be traced by labelling all sediment in the model based on the segment where it is located in at the beginning of the simulation. So at the beginning of the simulation 17 sediment fractions are defined, corresponding to the 17 segments. This follows a similar approach as studies performed by Elias et al. (2011), Nienhuis and Ashton (2016), and Beck and Wang (2019). After the model simulation all redistributed sediment in the Bay can be traced back to the originating segment (Figure 5.2.a). For each fraction i the total amount of mass found in each separate segment can be summed (Figure 5.2.b). This information can be tabulated and the displacement of each fraction i corresponds to one single row. The rows for all sediment fractions can be assembled to a n x n matrix (Figure 5.2.c).

Once the model output is tabulated, the connectivity of a single segment(i) is represented in a single row i and its connectivity to any other segment (j) can be found in cell (i,j). If cell (j,i) does not show a similar value as cell (i,j) this might indicate that sediment travels from segment (i) to segment (j), but the same amount does not necessarily travel in the reverse direction. Hence this asymmetry in the matrix can be interesting when analysing sedimentation and erosion patterns in a system. However this is only the case for a matrix filled with values of gross mass transport.

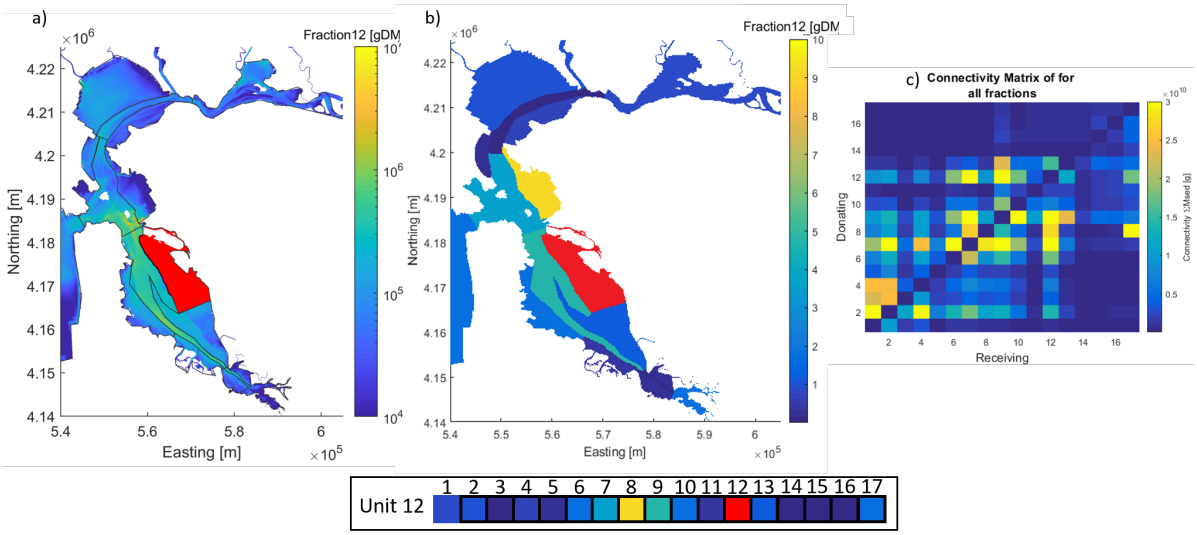

Figure 5.2: Example for segment 12 (East-Flat SB)of the creation of the adjacency matrix from model output. a) Running the model and tracing sediment from segment 12 (in red). b) Compute sum of all sediment mass from segment 12 found in each other segment. The mass found in each segment from segment 12 can be tabulated and compiled to row 12. a) This procedure can be repeated for each segment and the rows can be assembled into the adjacency matrix.

5.3.1. Analysing Connectivity with Network Analysis

Once the large data sets of model output are schematized into the network of nodes and links and an adjacency matrix is created, the network can be analysed mathematically with the use of analytical metrics and visually by displaying it in a network diagram. A full year simulation of WY2013 will be analysed to reveal the overall transport patterns throughout the year. Besides, sediment distribution in the Bay can be computed for different seasons or for the timescale of a single tidal cycle. This analysis of connectivity during different timescales can unveil different levels of connectivity with respect to the connectivity observed for the entire year and therefore give more insight into the seasonal variability of sediment pathways throughout the year.

Analytical Metrics

Once the adjacency matrix is created many different types of metrics can be applied to analyse the information in the matrix. The abundance of available analysing metrics and statistics when using the graphical framework is the advantage of using connectivity over other approaches (Pearson et al., 2020). The metrics included in the connectivity analysis can be divided into a category applied to analyse the system-level behaviour and a category applied to focus on individual segments. The analytical metrics have been applied to analyse a full year simulation of WY2013 in order to reveal the overall structure of pathways, net transport patterns, key-pathways throughout the year and to identify groups of segments with significant interconnectivity.

Analysing the connectivity on a system level will give important insight into the complex structure of sediment patterns in San Francisco Bay. Bigger patterns are essential to understand as they largely determine the large-scale processes and influence the sediment dynamics occurring on a smaller scale in between individual nodes.

Asymmetry

As long as the adjacency matrix is symmetric, an equal amount of sediment is exchanged between each pair of segments. Asymmetry in an adjacency matrix implies that sediment exchange between two segments is unequal and implies a net flux in one direction. A segment is receiving more sediment from a given segment than donating to it, or vice versa. Computing asymmetric connectivity is essential when predicting future morphological changes (Pearson et al., 2020) as a net flux leads to erosion or sedimentation at a certain location.

Modularity

Modules are defined as clusters of segments that are densely interconnected or have external connections in common. The modularity of the segments in San Francisco Bay is divided into sediment-sharing communi-

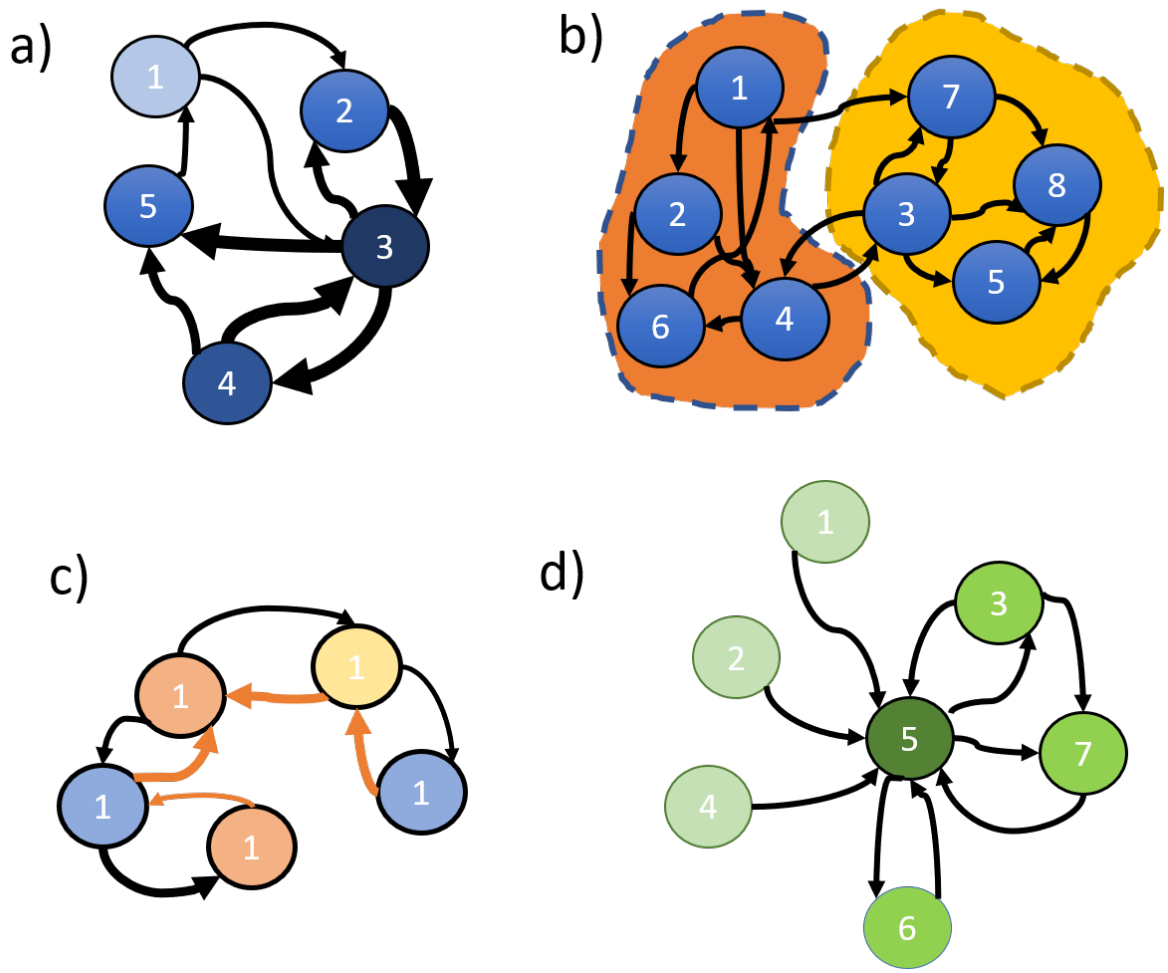

Figure 5.3: Schematic display of the used analytical metrics inspired by Pearson et al. (2020) with a) Strength; Through which node pass the most and strongest pathways, b) Modularity; Can a the network be divided into separate modules, that consist out of highly interconnected nodes? c)Asymmetry; Are stronger fluxes going in or out of each node? And d) Betweenness Centrality; which node is most interconnected in the network.

ties by using the Louvain Community Detection algorithm (Rubinov and Sporns, 2010). Some segments are more likely to share sediment due to advantageous topology, morphology or similar hydrodynamic forcing. When analysing a coastal system it is important to understand the influence of a single node to the bigger picture. Analysis of single nodes can identify bottlenecks in transport pathways and indirect pathways in between non-adjacent units. Understanding local behaviour is essential when designing a coastal intervention to prevent unexpected responses.

Betweenness Centrality

Centrality indicates how many other nodes are connected to a given node, or how 'central' a node is located in the system. Betweenness centrality is computed by determining the portion of all paths that go through a certain node (Phillips et al., 2015). Nodes with a high betweenness centrality are important for the system as they may be more efficient in transferring sediment than other nodes. Hence, information on centrality can be used to identify potential bottle necks in the system.

Strength

Strength of a certain node is computed by taking the sum of all fluxes in and out of a given node. Taking into account the size of the fluxes in stead of only analysing the amount of connections can give more information on the structure of a coastal system, especially if fluxes are unequally distributed in the domain (Pearson et al., 2020).

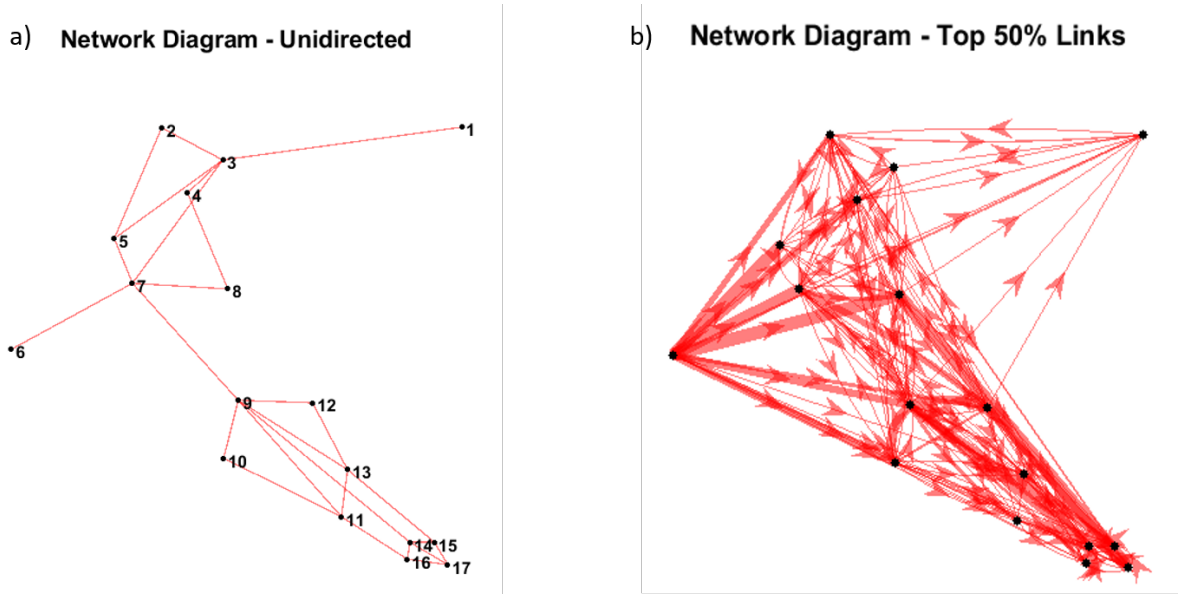

Figure 5.4: Representation of the adjacency matrices as a) A undirected network diagram based on the structural connectivity matrix of Figure 5.1.b and b) A representation of 50 % of all possible connections in between all nodes.

Network Diagram

As each cell represents sediment fluxes between each segment, they can be visualized in a network diagram. The network diagram can be created for the entire adjacency matrix, incorporating all links present in the system. The uni-directed network diagram based on the structural connectivity of San Francisco Bay in Figure 5.4.a shows the connection between all adjacent segments. Of course, sediment fluxes are also possible between non-adjacent segments and the representation of 50% of all possible links in the network is shown in Figure 5.4.b. The visualization of all active links in the network will be quite chaotic, therefore only the top 5% percent fluxes will be displayed in the research results. The network diagram can show gross fluxes between two nodes, but can also be used to visualize the net flux between two nodes. Both gross fluxes and net fluxes give important information as while the net flux might be small, two segments might exchange big gross fluxes and be very dynamic.

5.4. Results

In this section, sediment pathways are investigated by analysing the adjacency matrix and network diagram for a full-year simulation visually and substantiated with a variety of statistical metrics. Seasonal pathways are studied by creating network diagrams for each season. Asymmetry of the adjacency matrix is analysed to compute net fluxes across the South Bay inlet (Bay Bridge) and the Lower South Bay inlet (Dumbarton Narrows). Furthermore, the influence of the different forcings on the net fluxes at the inlets is analysed by comparing the net fluxes for different periods when a forcing is either weak or dominant. Lastly, a correlation analysis was conducted that supported earlier observed seasonal patterns in sediment transport and unveiled new relations.

No literature is available about the fate of fine sediments once it leaves the Bay during ebb. Yet, according to conventional belief, only a little amount of sediment is suggested to re-enter the Bay at flood, after it exited the Bay at ebb. Therefore, the amount of sea originating sediment that is found in the Bay in the model results is likely too high compared to reality. The connectivity study shows significant cumulative fluxes on the order of 10^7 kg from the ocean to the other segments within the Bay. As these fluxes represent transport of sediment that is not there in reality, sediment labelled as segment 6 (ocean) at t=0 entering the Bay are excluded in the analysis.

5.4.1. Sediment Pathways in South Bay

To obtain an overview of important sediment pathways in San Francisco Bay an adjacency matrix was created, showing the connectivity between all morphologic cells for all fractions (Figure 5.5.a), the sediment fraction IM1 (higher falling velocity,Figure 5.5.b) and fraction IM2 (Figure 5.5.c). A clear signal is the large sediment fluxes from the ocean (column 6) to nearly all segments from the ebb-tidal delta formed in the mode. However, in reality, the ebb-tidal delta has disappeared. Therefore in further results row 6 will not be taken into account. Two other segments acting as important sediment donators are the South Bay channel (segment 9) and the South Bay East Flat (segment 12). The blue cells in the bottom right and upper left corners indicate little sediment is exchanged from North Bay to The eastern flat of Central Bay (column 8) is receiving a lot of sediments to nearly all segments except Lower South Bay (14-17). The histograms show the sum of donated or received sediment mass for each segment to/from all other segments. The bottom histogram highlights the North-Eastern flat in South Bay as an additional segment receiving a significant amount of sediment. Furthermore, fraction IM2 shows a higher level of connectivity as more mass is found in other segments and distribution over greater distances than IM1.

The sediment connectivity is further evaluated into detail in Figure 5.6. Figure 5.6.c shows the evolution in time of the number of connected cells in the system. The entire network has a link density of 94.1% at the end of the simulation time, meaning 94.1% of all possible connections are in use. Most connections (75%) are established within the first four weeks of the simulation after which the number of connections increases asymptotically. The main links are explored in the first tidal cycles, after which sediment is required to travel larger distances. In 5.6.a the adjacency matrix of Figure 5.5.a is visualized topographically by creating a network diagram showing the top 5% strongest gross fluxes within or connected to South Bay (Figure 5.6). The strongest fluxes are between Central Bay, the South Bay channel and the East Flat. The tidal channel has the strongest outgoing fluxes towards the Ocean. Within South Bay, strongest fluxes are directed eastwards. Southwards, the gross fluxes are smaller and are not included in the top 5% strongest fluxes in South Bay. To account for the variation in surface area between the segments, the top 5% strongest fluxes divided by originating area are shown in Figure 5.6.b. This shifts the focal area to Lower South Bay, which turns out to be dynamic relative for its size with most fluxes going southwards.

The main connections observed in Figure 5.6 are supported by the statistical metrics strength, betweenness centrality and modularity in Figure 5.7. Modularity of the segments in San Francisco Bay was computed and four sediment-sharing communities or modules could be formed. The modules are Ocean-West Flat (light-blue), Central Bay-East Flat (dark-blue), South Bay Channel-West Flat (orange), Lower South Bay-West Flat (yellow) and Lower South Bay-Central Bay Flat (purple). Although external sediment fluxes exist between each of these communities, the majority of fluxes occur inside of them and/or the segments have comparable exchange patterns with the external modules. Thus, Central Bay and the South Bay East Flat are relatively strongly connected. Strength is the sum of all in and outgoing fluxes of a given node for weighted networks

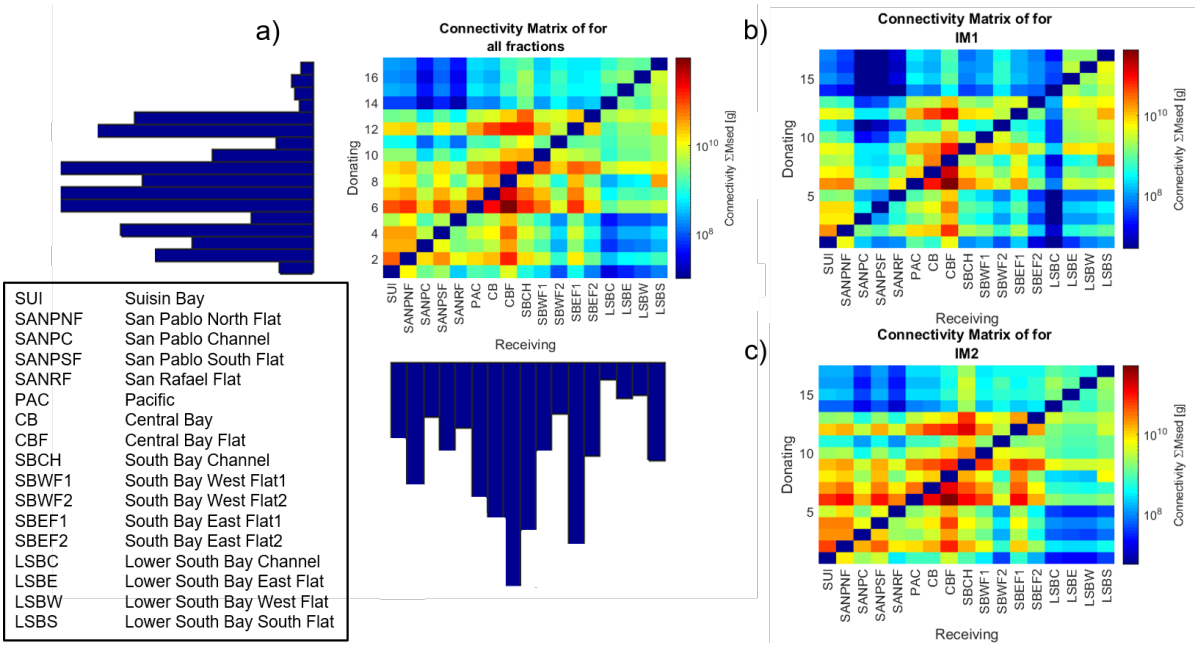

Figure 5.5: Adjacency matrices for the distributed sediment mass found in the bed and in suspension for all or individual sediment fractions, with rows representing the donating units and columns the receiving units. With a) the connectivity matrix for all fractions IM1 and IM2 with histograms where each bar represents the sum of the corresponding row/column, b) the connectivity matrix for the larger fraction IM1 and c) the connectivity matrix for the smaller fraction IM2. A clear emerging pattern is the net transport from the ocean (column 6). The eastern flat of Central Bay is receiving most sediments.

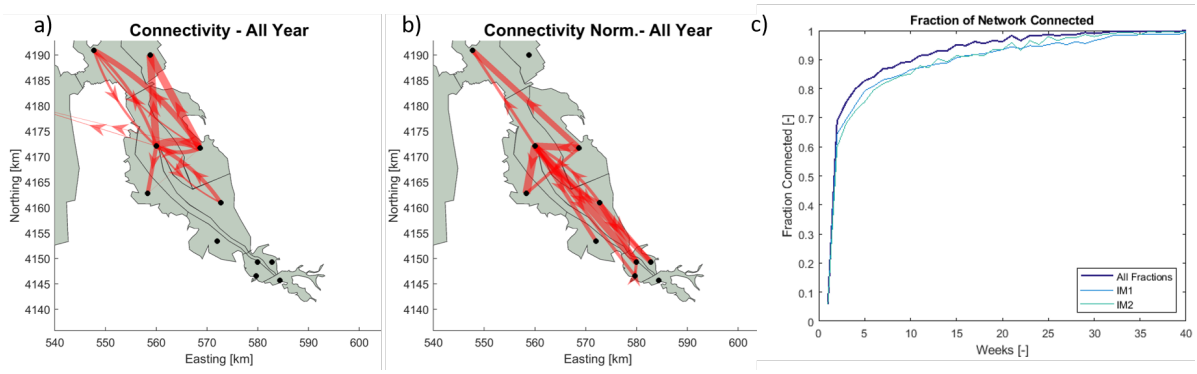

Figure 5.6: a) Network Diagram of the Connectivity showing the top 5% sediment fluxes in the network within South Bay. Their relative magnitudes are indicated by the thickness of the red arrows. b) Network Diagram of the Connectivity of the top 5% sediment fluxes where the fluxes are normalized by the area of the originating segments, which makes the emphasis of the main fluxes shift southwards, indicating the smaller segments are relatively dynamic for their size. c) Evolution of the fraction of the network that is connected in time, ending with a link density of 94.1%. Meaning 94.1% of all possible connections are operative.

(Pearson et al., 2020), while the western part of South Bay is more connected to the ocean. Figure 5.7 shows that the nodes with the highest strength are located near the inlet and flood channel, with the South Bay channel as the strongest node. Centrality assesses how "central" a certain node is positioned in a system. Betweenness centrality alludes to the percentage of all paths in the system that pass through a certain node (Phillips et al., 2015). The high score of betweenness centrality of the South Bay channel in Figure 5.7.c indicates the node is located in the centre of the South Bay flux network and points out the channel serves as a transport bottleneck within the system.

Special attention is paid to the pathways linking South Bay with the Delta, as the Delta sediments are hypothesized to be an important source of sediment to South Bay (Barnard et al., 2013a). To investigate whether this hypothesis can be confirmed, only the distribution of sediment located at t=0 in segment 1 was analysed (Figure 5.8.a). The network diagram of Figure 5.8.b shows a network diagram of the fluxes of sediments to

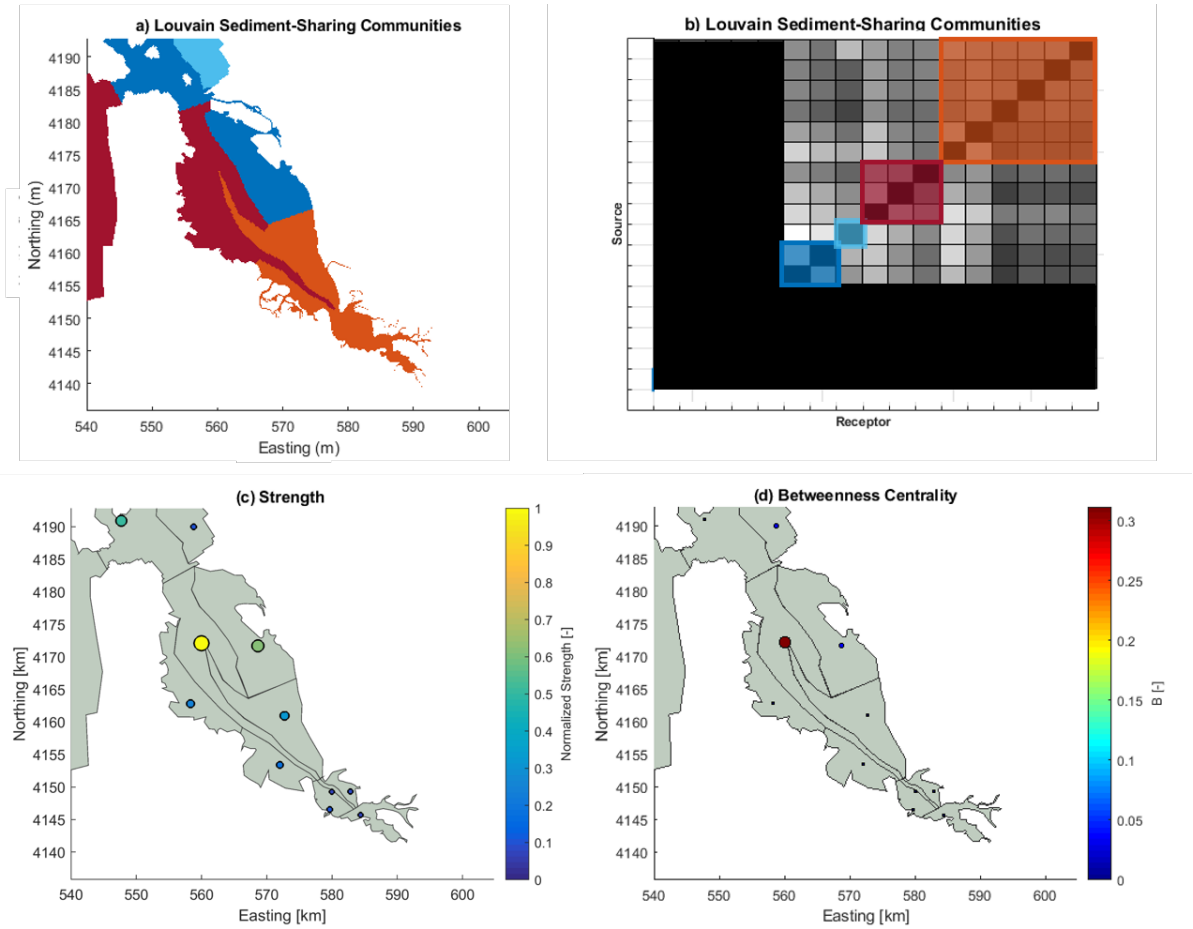

Figure 5.7: a) Modularity of the segments in San Francisco Bay is shown by dividing the segments in sediment-sharing communities also known as modules using the Louvain Community Detection algorithm. Each coloured square corresponds to a module that has strong connectivity with other nodes in that module and weaker connectivity with nodes outside it. b) The sorted adjacency matrix into sediment sharing communities or modules corresponding to figure a. The fluxes from and to North Bay segments are not taken into account and are therefore blackened. c) Strength of each connection; lighter colours and larger dots indicate that greater fluxes are passing into or out of a given node. d) Betweenness/Centrality; Lighter colours and larger dots indicate that more other nodes are connected to a given node, either as sources or receptors. This can be used to identify potential bottle necks in the system.

other segments after a one-year simulation from the Delta/Suisin Bay. Strongest fluxes are observed towards the North Bay flats. Furthermore, Delta sediments are also transported towards the South Bay and Central Bay segments to a lesser extent. The bed composition at the last time step of the simulation is portrayed in Figure 5.8.c and complies with the patterns observed in the network diagram. Most sediment from the Delta is deposited at the flats of San Pablo Bay, yet some of it is found in South Bay (mostly in the channel and at the Western flats).

The main sediment transport patterns after a full-year simulation are depicted in Figure 5.6. As external forcings such as river discharge and atmospheric forcing show a significant variation during the year, sediment transport patterns during the year may vary as well. Separate simulations were run for each season (Autumn: Oct-Nov, Winter: Dec-Feb, Spring: March-Mar, Summer: Jul-Sep) to assess the main sediment fluxes during each season. The network diagrams for each season in Figure 5.9.a show the top 5% largest gross sediment fluxes. North Bay patterns were chosen to be left out so their magnitude will not overshadow inter-Bay fluxes.

Largest fluxes are mostly located in the northern part of South Bay. Segments in Lower South Bay mainly show interconnectivity during the year, with only outgoing fluxes towards the more southern flats and the channel in South Bay. In Winter gross fluxes show the same pattern as in Autumn. In Spring the gross fluxes are significantly larger compared to Autumn and Summer. The eastern part of South Bay is very dynamic with large incoming and outgoing fluxes for the eastern flats and the channel, and there is a high connectivity with

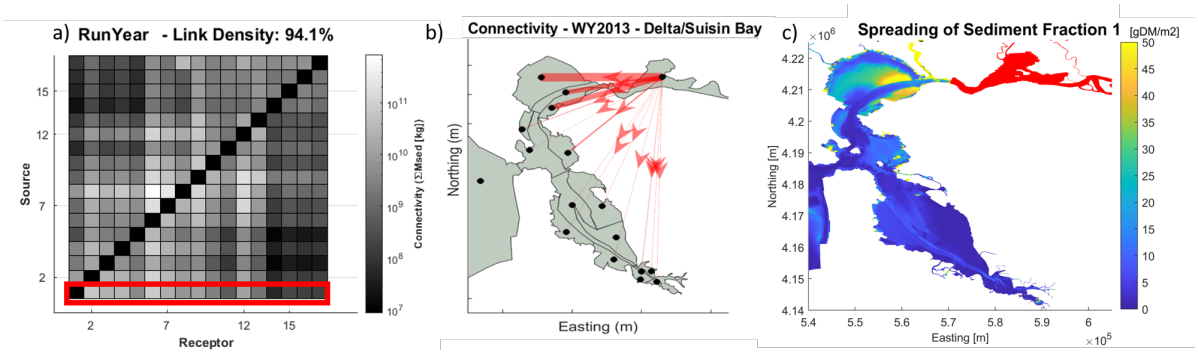

Figure 5.8: a) Adjacency Matrix of one simulation with only the row 1 and column 1 related to segment 1 highlighted. b) Network Diagram of sediment fluxes originating from segment 1 based on the first row of the adjacency matrix. The red arrows indicate the direction with their thickness corresponding to the strength of the connection in proportion to the largest observed connection in the network.c) The amount of mass of fraction 1 found in the bed at t=end.

Central Bay. In Summer the northern segments are still dynamic and exchange strong fluxes with each other. Strong fluxes from Central Bay towards both the channel and north-eastern flat are observed.

Overall, the largest fluxes in the Bay are located in the Northern part of South Bay and connect South Bay with Central Bay. Whether the largest fluxes are incoming or outgoing differs per season, with the largest fluxes during Spring and Summer and smaller fluxes during Autumn and Winter. A network diagram of the top 5% of largest sediment fluxes normalized by the originating area can be found in Appendix B, which shows more sediment mobility in the southern located segments in South Bay and most incoming fluxes towards Lower South Bay in Autumn. In the other seasons smaller incoming fluxes are observed.

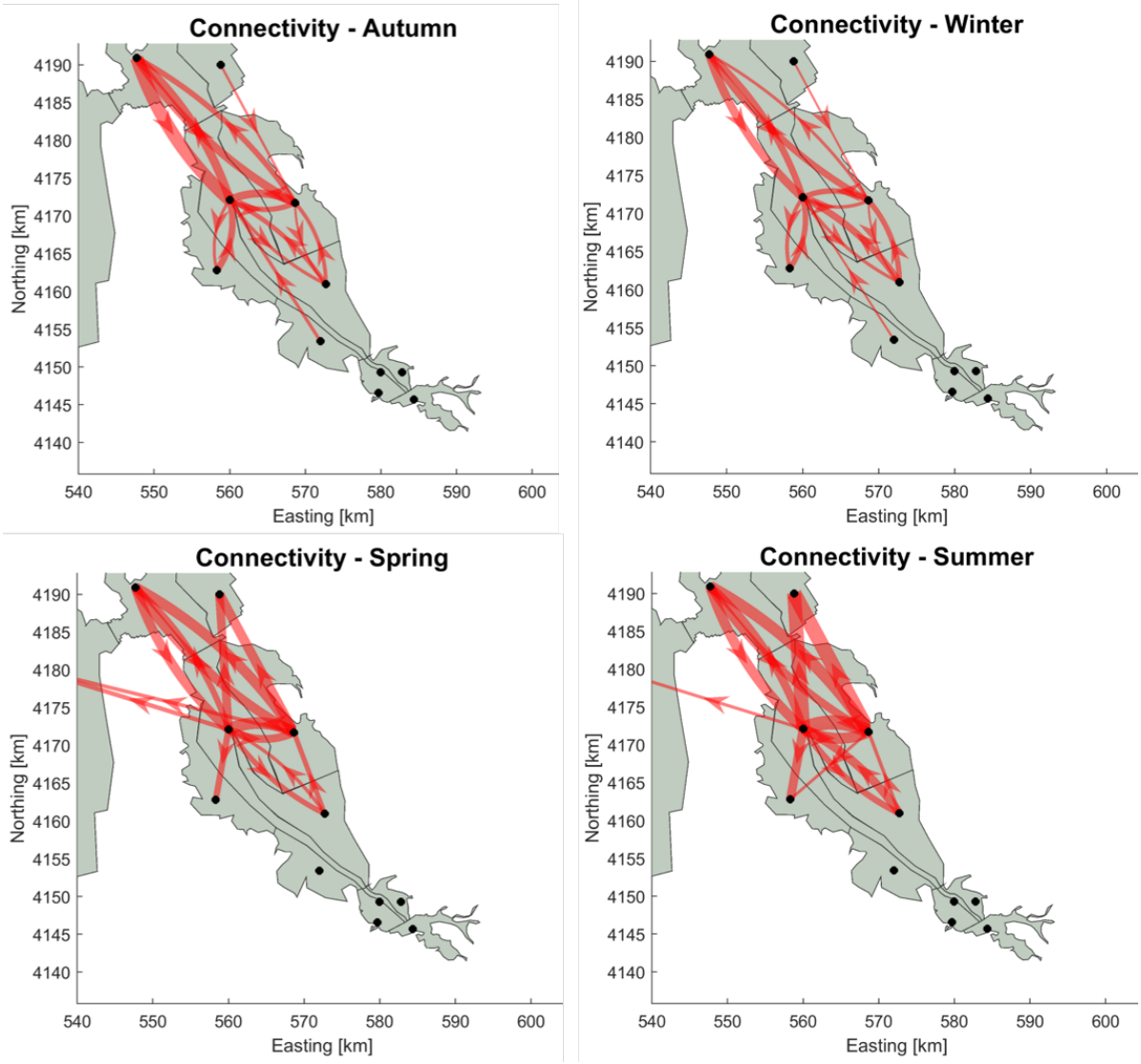

Figure 5.9: Network diagram for the top 5% of connections in the network within South Bay for the four seasons of the year. Red arrows indicate the direction with their thickness corresponding to the strength of the connection in proportion to the largest observed connection in the network. Arrow thickness scaling is consistent across seasons.

5.4.2. Net Transport in South Bay

Long-term trends in morphologic evolution and suspended sediment concentrations result from net fluxes instead of the gross sediment fluxes. Net fluxes tend to be only a small proportion of the gross fluxes moving up and down an estuary each tidal cycle. Patterns of net transports can be discovered by analysing asymmetry of the adjacency matrix. Net transports passing through the cross-section at Bay Bridge during WY2013 and through the Dumbarton Narrows are displayed in Figure 5.10. All sediment mass originating from the South Bay segments but found in exterior segments, which thus must have left South Bay via the cross-section at Bay Bridge is subtracted by the sediment mass found in South Bay originating from exterior segments, which thus must have entered at Bay Bridge (see Figure 5.10.d). The same method was applied to calculate net transport for Lower South Bay and the South Bay shoals, for the latter mass in the channel was not taken into account. In this research a negative net flux out of South Bay means it is exporting.

Figure 5.10 shows the cumulative transport during the year, as well as the net transport compared to the previous output time step of 1 day (instant import/export in the figure). South Bay is importing sediments during most of the year with exception of the period from the end of March until mid-July when strong summer breezes blow over South Bay. The cumulative transport is still positive, so over the whole year South

Bay is importing. In January and February, the import rate tones down, which coincides with the period of reverse estuarine circulation. Furthermore, Lower South Bay is gradually importing during the entire year. A large peak of import is observed during an autumn storm at the end of October. The adjacency matrix shows Lower South Bay is mainly receiving sediment from South Bay, Central Bay, and the Central Bay Flat, and less is coming from North Bay segments. Conversely Lower South Bay is not donating much sediment to North Bay either. The South Bay shoals show the same patterns as Figure 5.10.a though the spring-neap cycle is less present in the signal. As the time-series plots do not give insight into the behaviour of single segments within South Bay, Figure 5.10.f shows the total import/export over the year for each segment. It shows that while South Bay is net-importing overall, this is mainly due to 10 and 11 (west flats) while segments 12 and 13 (east flats) are exporting(Figure 5.11).

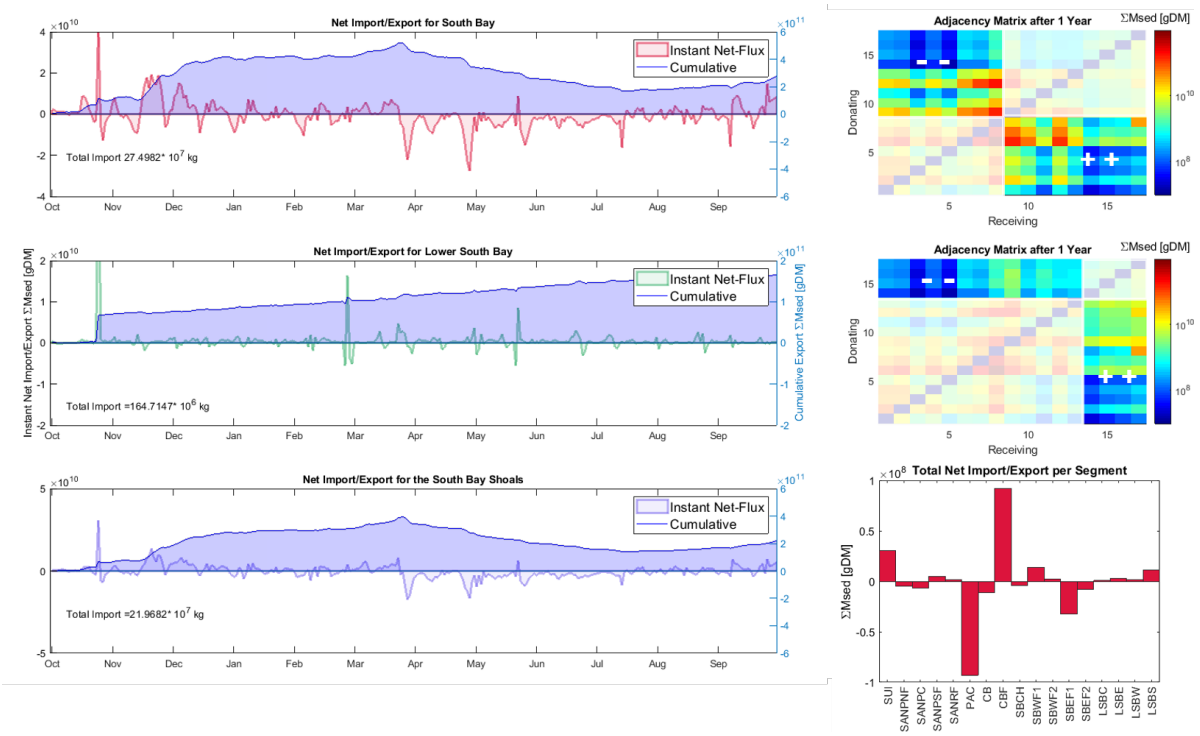

Figure 5.10: Time series of net exchange of sediments at the entrance of South Bay and at the Dumbarton Narrows showing the cumulative net transport during the year and net transport compared to the previous output time step (δt = 3 days). a) Time series of the net exchange of sediments at the entrance of South Bay and b) Dumbarton Narrows. Based on the adjacency matrix, respectively d)&e) by subtracting incoming fluxes by outgoing fluxes. Fluxes within the considered area and North Bay are excluded (in white). c) Time series of the net exchange of sediments at the entrance of South Bay excluding the channel. f) Total net transport per segment.

Whereas Figure 5.10 and B.4 show the net-exchange between respectively South Bay and Lower South Bay in its entirety, net transport between individual nodes can give a more detailed understanding of which segments are eroding or where accretion can be expected. Net transport pathways between nodes are computed by subtracting the in and outgoing flux from a certain node C_i to node C_j, which results in the net sediment flux for the link between node C_i and node C_j. The top 5% of net fluxes are displayed in Figure 5.12 for each season.

In Autumn, net fluxes are directed towards the Pacific from the channel and the West Flat. Within South Bay, net fluxes are directed towards the channel. An incoming net flux is observed from the Central Bay flat to the channel and South Bay east-flat. In Winter, South Bay is importing from Central Bay whereafter sediment is mainly transported from the channel to the eastern flats. Net fluxes from the western flat are directed towards the north-east. In Spring net fluxes significantly increase. Strong net fluxes are directed towards the Ocean and Central Bay from the channel and the eastern flat. Within South Bay, net fluxes are directed towards the western flats. In Summer, South Bay is still receiving net fluxes from Central Bay. Within South Bay, net fluxes are mostly directed in east/south-eastern direction.

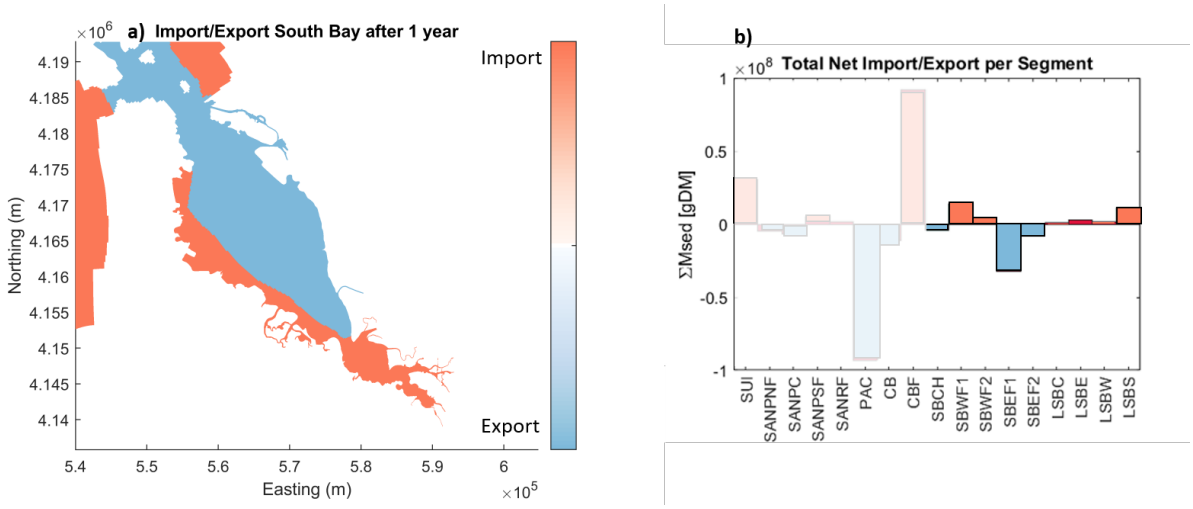

Figure 5.11: Figure a) indicating whether South Bay segments are importing or exporting after a one year simulation. b) Histogram indicating the import or export for each segment after a one year simulation, equal to Figure 5.10.f

. The segments outside of South Bay are faded in colour.

5.4.3. Net Transport in South Bay under different forcings

Three main forcings are identified for fine sediment transport in South Bay being wind, tide, and baroclinic circulation. A changing climate is expected to alter the forcings with higher peak discharges from the Delta, increasing tidal energy due to a rising sea-level and changing wind patterns. Understanding the influence of each forcing to the sediment transport patterns observed throughout the year can help to develop a prognosis on what kind of issues the Bay may deal with in the future. The effects of wind, tide, and spatial salinity differences are analysed by comparing the quantities and trends of cumulative fluxes for separate periods (further referred to as scenarios), when a forcing was either dominant or weak. An overview of the analysed periods is given in Table 5.1. For each forcing analysis two or three scenarios were compared. The results of all conducted analyses are summarized in Table 5.2. The results of the influence of the tide and wind are discussed in more detail in this section. Details of the analysis for the other forcings can be found in Appendix B.

Table 5.1: The different scenarios for which the sediment connectivity have been assessed were based on the different conditions in tides (water levels), the salinity difference between Central Bay and South Bay and the modelled wind velocities in the Bay.

Name	Simulation Time	Duration	Wind speed	Tide	Circulation regime
Year	01-10-2013/01-10-2013	365 days	-	-	-
Wind_Low	27-10-2012/07-11-2012	12 days	Low	Neaptide	Well-Mixed
Wind_High	21-05-2013/31-05-2013	12 days	High	Neaptide	Well-Mixed
Tide_low	22-02-2013/01-03-2013	7 days	Moderate	Neaptide	Well-Mixed
Tide_high	04-03-2013/10-03-2013	7 days	Moderate	Spring tide	Well-Mixed
Tide_low 2	04-11-2012/11-11-2012	7 days	Moderate	Neaptide	Well-Mixed
Tide_high 2	13-11-2012/20/11/2012	7 days	Moderate	Spring tide	Well-Mixed
Reverse Circulation	05-12-2012/24-01-2013	50 days	-	-	Reversed
Classic Circulation	25-01-2013/01-04-2013	67 days	-	-	Classic
Well-Mixed	25-07-2013/30-09-2013	67 days	-	-	Well-Mixed

Tidal influence

Two periods in the first half of November were selected to be analysed, being one lasting a week surrounding a neaptide and the second a week surrounding a spring tide. Winds were relatively low to moderate during the first part of both simulation periods and the Bay was well-mixed. Figures B.6a&b show a time series of the cumulative net import and export for South Bay and Lower South Bay respectively. South Bay experiences import during both neaptide and spring tide, with comparable import rates. These scenarios also show the

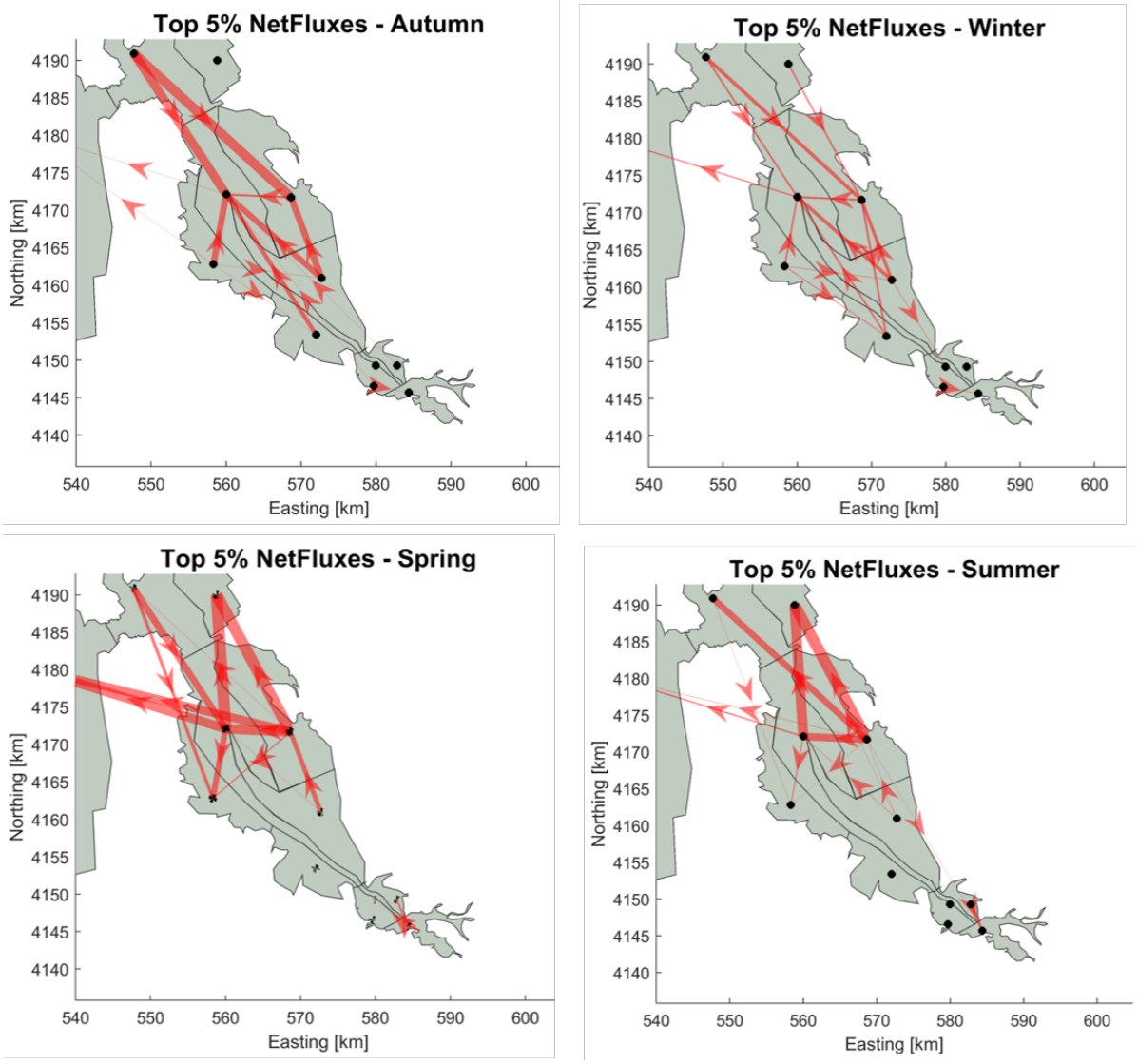

Figure 5.12: Network diagram for the top 5% of net fluxes in the network within South Bay and Central Bay for the four seasons of the year (a-d) and the total WY2013 (e). Red arrows indicate the direction with their thickness corresponding to the strength of the connection in proportion to the largest observed connection in the network. Arrow thickness scaling is consistent across seasons.

Table 5.2: Summarized results of the analysis of the impact of each forcing to the net-fluxes for South Bay and Lower South Bay.

Forcing	Included Scenario	Outcome
Wind	Wind_Low; Wind_High	Wind_Low: Importing Wind_High: Exporting
Tide	Tide_Low; Tide_High	Both importing, strongly increased import during strong northerly winds
Baroclinic	Reverse Circulation; Classic Circulation; Well-Mixed	No clear difference between the reverse and well-mixed regime. Slightly more import during the classic circulation.
Baroclinic & Tide	Tide_Low2; Tide_High2	SB: Stronger import during neaptide LSB: Stronger import during spring tide

importance of wind, as once wind speeds increase in both scenarios around day 5, the amount of import increases for both scenarios. During these scenarios strong northerly winter winds induced import into South Bay. In Lower South Bay no clear net import or export is observed during the spring tide simulation. Lower

South bay initially imports during neaptide, but as the wind speeds go up, peak exports are observed after ebb periods.

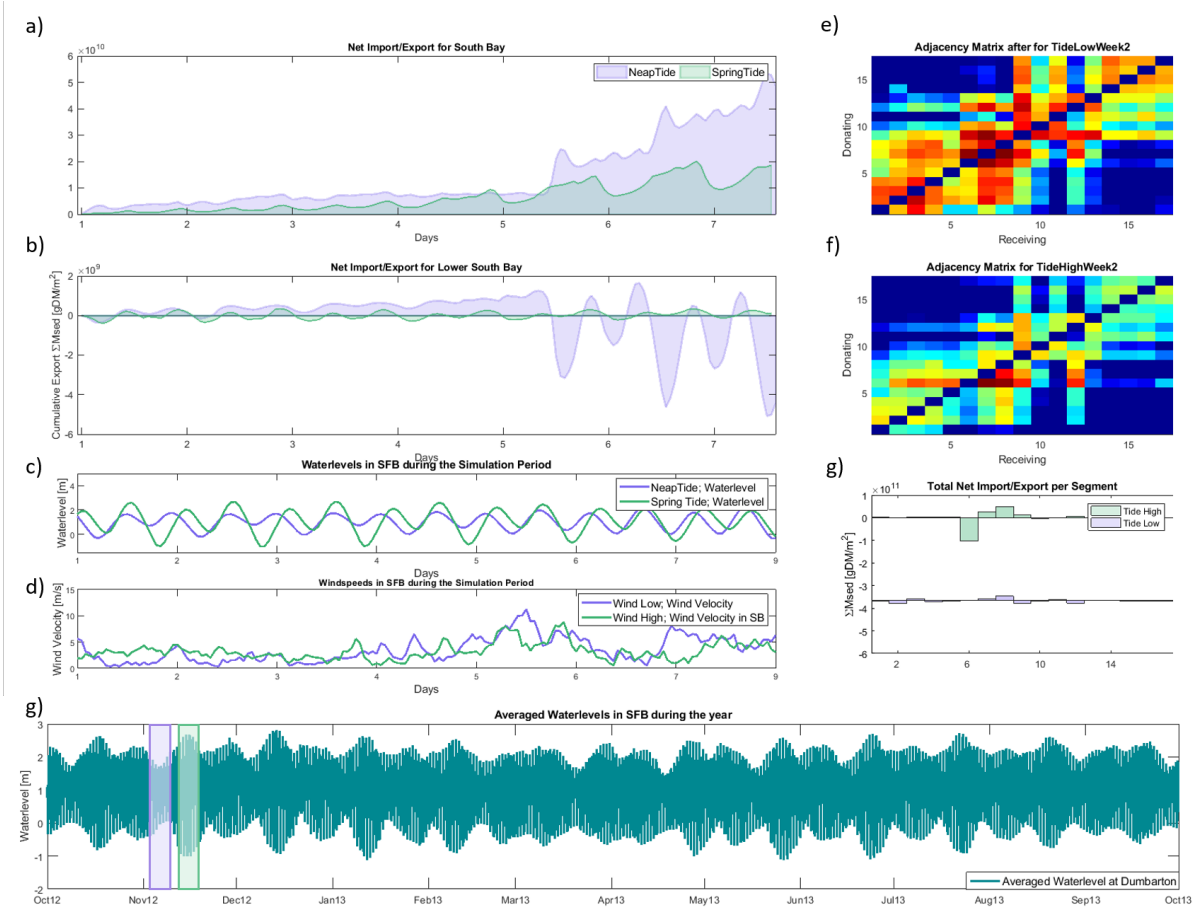

Figure 5.13: Time series of net exchange of sediments at the entrance of South Bay (a) and at the Dumbarton Narrows (b) showing the cumulative net transport during the year and net transport with respect to the previous output time step (δt = 1h03min). Based on the adjacency matrix for a week surrounding neaptide (TideLow) and spring tide (TideHigh), respectively d)&e) by subtracting incoming fluxes by outgoing fluxes. c) Representation of the modelled water level at Dumbarton Bridge. g) Water levels at Dumbarton Bridge with the considered time periods in green(spring tide) and purple (neaptide). e)Indication of difference in total net transport per segment.

Wind influence

Two separate weeks during WY2013 were selected with either strong or weak winds in respectively June and November. Figure 5.14 shows a time series of the simulation periods with the cumulative net import and export for South Bay and Lower South Bay respectively. Tidal conditions were comparable for both simulation periods (see Figure 5.14) and both fall in the well-mixed regime when baroclinic processes are barely noticeable. South Bay is importing sediment for the low wind scenario and exports during the high wind simulation. Winds during the high wind scenario are in south-westerly direction instead of northerly, which was the case for the previous tidal influence analysis. Lower South Bay shows the earlier observed export during the stronger wind simulation yet shows an import for the weaker wind simulation.

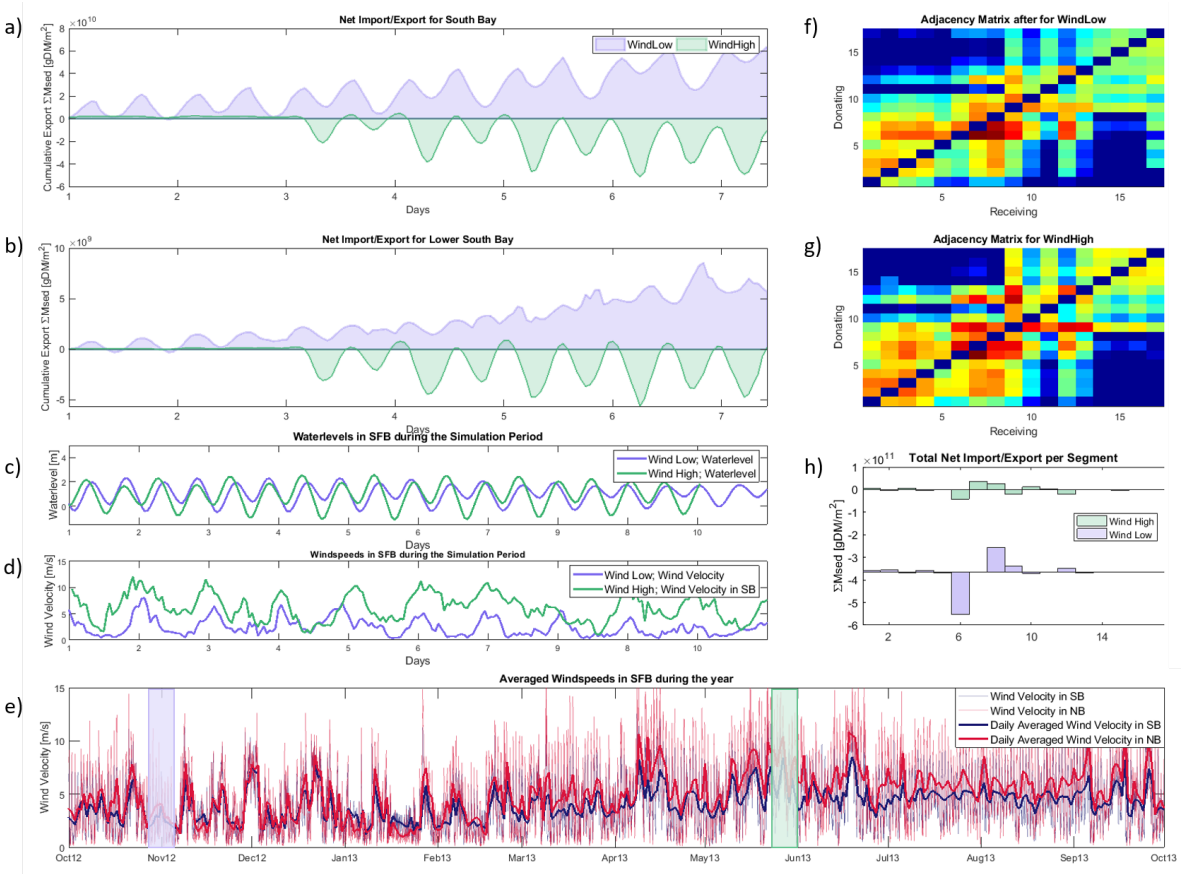

Figure 5.14: Time series of net exchange of sediments at the entrance of South Bay (a) and at the Dumbarton Narrows (b) showing the cumulative net transport and net transport with respect to the previous output time step (δt = 6h00min). Based on the adjacency matrix for a week of strong winds, respectively f)&g) by subtracting incoming fluxes by outgoing fluxes. c) Representation of the modelled water level at Dumbarton Bridge. d) Modelled wind speeds during simulation periods. e) Water levels at Dumbarton Bridge with the considered time periods in green (strong winds) and purple (weak winds). h) Total net transport per segment.

5.5. Correlation Analysis

To further evaluate the influence of different forcings on sediment transport in South Bay, wind conditions and salinity differences were compared to the net sediment fluxes at Bay Bridge and the Dumbarton Narrows in a correlation analysis. The daily net fluxes across each cross-section were derived in Section 5.4.2 and were subsequently averaged over a week for this analysis. Wind forcing was found to have the most correlation with the net fluxes at both cross-sections. In Figure 5.15 the correlation between both wind speed and wind direction and the net fluxes is shown. Before averaging the wind speeds were divided by the cosine of the wind directions. All wind directions relate to the longitudinal axis of South Bay as a reference, which corresponds to the wind direction with the longest fetch. The colour of the scattered dots in Figure 5.15 corresponds to one of the four categories of wind direction. Northerly winds are indicated as yellow, westerly as blue, easterly as green and southerly as red.

Strongest correlation can be found for the cross-section of Bay Bridge with a negative correlation coefficient of r=0.45. Stronger northerly winds in Autumn and Winter (yellow) were more likely to coincide with a positive (importing) net flux for South Bay. For the diurnal south-westerly to westerly winds prevailing in Spring (blue), net fluxes were more likely to be negative (exporting) than for northerly winds. For the net flux across the Dumbarton Narrows, the correlation is less strong with a positive correlation coefficient of r=0.09. Though the points are quite scattered, the highest positive net fluxes (import) occur for stronger westerly winds and the largest negative net fluxes (export) occur for stronger northerly winds.

Additional correlation analyses were conducted and the results are summarized in this paragraph and in Table 5.3. Corresponding figures and graphs can be found in Appendix B. A comparison of only winds speeds and net fluxes resulted in a correlation coefficient of r=-0.30 for Bay Bridge and r=0.14 for the Dumbarton Narrows. With respect to the correlation coefficients including the impact of wind direction, the correlation decreased for Bay Bridge and increased for the Dumbarton Narrows. Hence the combination of strong winds and wind direction influences net fluxes at Bay Bridge, while for the Dumbarton Narrows the wind speeds are more of influence than the wind direction. The influence of salinity gradients on the net fluxes was also analysed. The analysis resulted in a relatively strong correlation for the horizontal salinity at both cross-sections. At Bay Bridge, higher negative fluxes (export) are more likely to occur under a higher horizontal salinity difference between Central Bay and South Bay. At Dumbarton Narrows, a negative correlation is found with a positive net flux (import) during higher salinity differences. Yet, both stronger import and export fluxes occur at lower horizontal salinity differences. The sign of the correlation coefficient for the vertical salinity difference reverses at both cross-sections compared to correlation coefficients of the horizontal salinity difference.

Table 5.3: Correlation coefficients between weekly averaged net fluxes over Bay Bridge and the Dumbarton Narrows and different forcings included in the correlation analysis.

Forcing	Coefficients	
	Bay Bridge	Dumbarton Narrows
Wind speed & wind direction	-0.45	0.09
Wind Speed	-0.30	0.14
Horizontal Salinity	0.20	-0.16
Vertical Salinity	0.05	-0.11

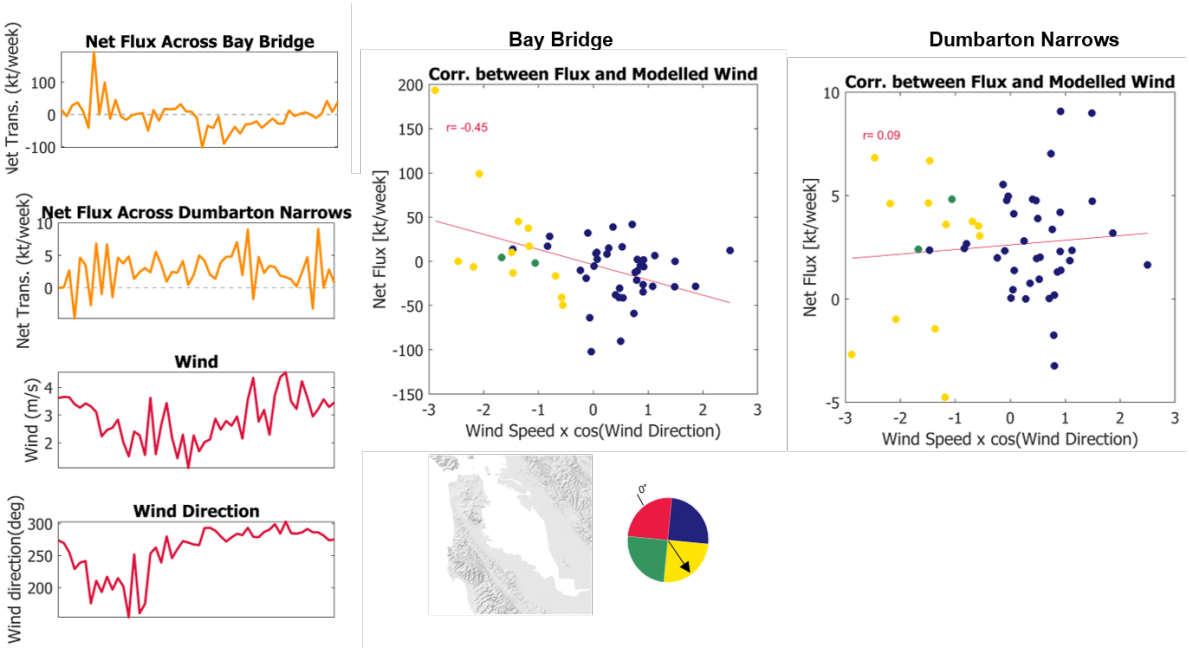

Figure 5.15: Figure showing the results of the correlation analysis between net fluxes at Dumbarton Narrows, Bay Bridge and combined wind speed and direction. The right panels show the scatter plots for wind speeds multiplied by the cosine of the wind direction against the net fluxes at respectively Bay Bridge and the Dumbarton Narrows. The left panels show time-series during the simulation period of: the net flux at Bay Bridge, at the Dumbarton Narrows, wind speed, wind direction and the wind rose oriented along the longitudinal axis of South Bay (from top to bottom).

6

Discussion

6.1. Modelling Fine Sediment Dynamics in South Bay

This research is a combination of model improvement based on comparing modelled and measured SSCs, and the analysis of sediment pathways by applying the approach of sediment connectivity. The integration of information on modelled SSCs that was obtained during calibration efforts and on the net fluxes resulting from sediment connectivity analysis leads to a more thorough understanding of sediment dynamics in South Bay. The calibration procedure provided insight in the seasonal and spatial SSC patterns, which in combination with local flow patterns can help explain the modelled net fluxes. Most research and fieldwork in San Francisco South Bay is focused on locally measuring SSCs during a weekly or monthly period(eg. Lacy and MacVean (2016), Brand et al. (2010), Schoellhamer (1996)). This research can support our results of SSCs by the model, though little literature is available about sediment pathways and sediment budgets in the area.

Key pathways during the year were located between the northern South Bay segments and Central Bay. Large seasonal differences in magnitudes of sediment fluxes were observed, with strongest fluxes in Spring and Summer. This increase in fluxes can be explained by the increase of modelled SSCs in South Bay, a trend which agreed with measurements and is also observed for other years (Shellenbarger et al., 2013). These results support the conventional belief that most sediments enter SFB during Winter, which are then resuspended and redistributed during Spring (Brand et al., 2010). Analysis of the sediment from segment 1 (Suisin Bay) revealed sediment pathways from the most northern segment to South Bay. Hence, the Delta sediment input finds its way to South Bay. Furthermore, most sediment pathways pass through the channel, making it a potential bottle-neck in the system. The net flux across the inlet of South Bay (Bay Bridge) shows a strong seasonal variability, but over the entire year South Bay ended up having a net import for WY2013, which is in compliance with the result from Foxgrover et al. (2004) (See Table 6.1). Gradual imports occurred during Autumn and Winter and the late Summer, with peak imports during winter storms. South Bay was exporting sediments from Spring until mid-Summer.

The gradual sediment import during calmer periods can be explained by the flood asymmetry in South Bay (Brennan et al. (2002),Conomos, T. J. Walters and Cheng (1985),Barnard et al. (2013a)). During windy periods, the wind can influence sediment dynamics in SFB by stirring up sediments at shoals exposed to wind-waves and by transporting sediment by wind-induced residual currents. Winter storms tend to be northerly and inline with the longitudinal axis of the Bay, which induces an inward residual current for South Bay (Conomos, T. J. Walters and Cheng, 1985). This can explain strong imports during Winter. During Spring and Summer, strong diurnal south-westerly summer breezes start to blow over South Bay, which stirs up sediment at the East Flat. Due to the short fetch for these summer breezes, residual currents are weak. Yet, Brand et al. (2010) found that most of the sediment resuspended at the shoal ended up in the channel, after which it may leave South Bay during ebb. Apparently, not all sediment finds it way back to South Bay during flood again. In Section 5.5 a negative correlation was found for net flux and the combined wind speed and wind direction. It showed import was more likely to occur during strong northerly winds, while export was more likely to occur during strong south-westerly winds.

South Bay is believed to receive most sediment and freshwater input during Spring, due to a classic estuarine circulation following the freshening of Central Bay in Winter by inflow at the Delta(Barnard et al., 2013a). Yet for WY2013, this effect was only observed during March during neap tides when tidal mixing can be suppressed by the stratification (Brennan et al., 2002). However, this year was found to be less wet than other years such as WY2011 and WY2017. In WY2017, peak discharges were six times as high as those of WY2013. Therefore, though baroclinic effects were weak in WY2013, they are still presumed to be important for the other years.

Table 6.1: Overview of studies of sediment budgets in South Bay and Lower South Bay and their results.

Study	Result	Region	Studied Years	Based on
Foxgrover et al. (2004)	Import	SB	1858-1983	Bathymetry; volume study
Shellenbarger et al. (2013)	Import: moderate-dry years Export: wet years	LSB	2009-2011	SCC measurements; flow discharges
Gartner et al. (1997)	Import: moderate-dry years Export: wet years	LSB	March 1995	SSC measurements

The net flux across the inlet of Lower South Bay (Dumbarton Narrows) was mostly positive throughout the year. All segments of Lower South Bay had imported sediment by the end of the year, though there was some seasonal variation per segment. A study by Shellenbarger et al. (2013) estimated the sediment budget of Lower South Bay for the years 2009–2011, based on measured SSCs and local flow conditions. They found that environmental conditions in Spring were a very dominant factor in determining whether the sediment budget of a year was positive or negative (See Table 6.1). Lower South Bay showed import for years when less freshwater entered South Bay and export for a higher freshwater input. This result is supported by the correlation analysis performed for the net flux across the Dumbarton Narrows and the horizontal salinity difference between Central Bay and South Bay. During WY2013, export only occurred for a smaller salinity differences, which corresponds to a freshwater input at South Bay. As wet years occur less often than dry to moderate years, Lower South Bay is expected to import over the long run (Shellenbarger et al., 2013). Winds were found to be of little influence to the net flux across the Dumbarton Narrows, which also agrees with the findings of Shellenbarger et al. (2013). In periods when the tide is the main active forcing, Lower South Bay is gradually importing, which can be explained by tidal asymmetry Conomos, T. J. Walters and Cheng (1985).

The main results of this research for seasonal net fluxes are schematized into four concept diagrams in Figure 6.1. It provides information on the main net fluxes, dominant forcings and the regions of sedimentation or erosion. Net-fluxes in Autumn and Winter were mainly directed towards the south-west. The channel and the northern part of the South Bay East Flat imported sediment while most of the other segments lost sediment. In Spring and Summer, the main observed patterns reversed with export at the channel and the East Flat and import at the West-Flat.

Even though a positive cumulative flux is measured for both Bay Bridge and the Dumbarton Narrows, the volume of import should be put in perspective by considering the surface areas and expected deposition of each section of the Bay. The cumulative flux was computed in this study for WY2013 and is divided by the total area of the importing segment (see Figure 6.1) multiplied by the average bulk density derived from core samples in the region (Caffrey and Miller (1995); Love et al. (2003)). Importing South Bay segments would on average experience a deposition of 2.637 mm/year, and the segments of Lower South Bay experience an average deposition of 4.604 mm/year (Table 6.2). These values are hardly measurable, but as it is likely that sediment accumulates more at some location, deposition might be measurable locally. If these deposition rates are representative for other years, deposition would be measurable after longer period. Mean sea level rise for San Francisco Bay is estimated to be 2.17 mm/yr at San Francisco (E. et al., 2003). This amount of import would potentially accommodate for sea level rise and in Lower South Bay additional sediment could be provided for the restoration of salt marshes.

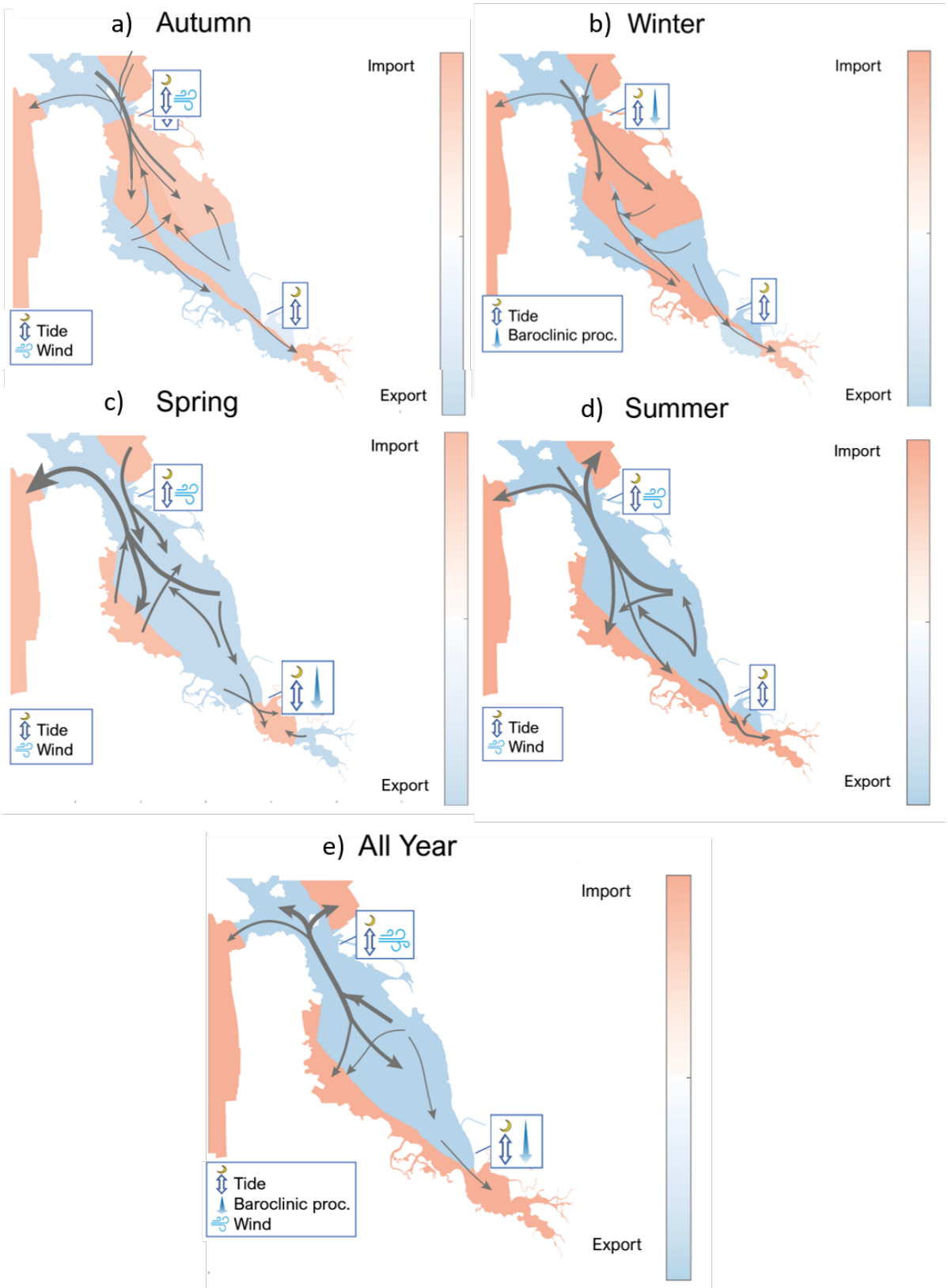

Figure 6.1: Conceptual representation of the research results on net-transports and sediment pathways in South Bay for (a) Autumn, (b) Winter, (c) Spring, (d) Summer and (e) for the entire year. Import denotes sediment accumulation in a given cell, and export indicates net sediment depletion.

Table 6.2: Sediment Budget Analysis for the cumulative flux across the inlet of South Bay and Lower South Bay. Average deposition was calculated
* From Foxgrover et al. (2004)
** From Figure 6.1
*** An average bulk density from seven core samples collected in South San Francisco Bay during two different studies: Caffrey (1995); Love et al.(2003)

Surface Area South Bay*	410	km^2
Surface area of accreting areas **	150	km^2
Surface area of accreting areas for Lower South Bay **	58	km^2
Bulk Density ***	617	$kg\,m^{-3}$

	Cumulative Flux		Deposition	
South Bay	2.75E+08	m^3	+2.962	mm
Lower South Bay	1.647E+08	m^3	+4.604	mm

6.1.1. DELWAQ Model Calibration

Fine sediment transport models are often calibrated against observed suspended sediment concentrations in the considered model domain (van Maren and Cronin, 2016). In most estuaries, the lack of sufficient measurement data inevitably leads to the acceptance of a high level of uncertainty in the model performance. Fortunately, continuous data collection of sediment concentrations started at the end of the previous century in San Francisco Bay. The DELWAQ-Model of San Francisco Bay was calibrated against observed SSCs provided by three data sources, leading to a uniquely high spatial and temporal coverage of the estuary compared to most estuaries in the world. The two main issues in model performance were (1) an underestimation in SSCs in South Bay during Spring and (2) the absence of strong gradients in the model leading amongst others to an underestimated amplitude in the SSC on a tidal scale in North Bay.

Calibration scenarios were developed and their individual and combined effect on model performance was analysed. The resulting final parameter set is a combination of increasing vertical gradients by increasing fall velocities and decreasing the deposition efficiency during the entire year and the local decrease of settling velocities in South Bay during Spring. This parameter set increases model performance compared to the measured data with respect to earlier model versions.

To increase SSCs in Spring in South Bay three scenarios were developed including temporarily decreasing settling velocities, increasing resuspension parameters and decreasing the critical shear stress for the buffer layer. All three scenarios led to increased performance and there was no clear best-performing data set. In combination with scenario C1 which increased the vertical gradients in SSCs, the scenario with the reduction of falling velocities could more distinctly be selected as best-performing scenario on account of statistics and visual inspection. Scenario S1 and C1 are both altering the falling velocities and therefore are oppositely affecting the same process. This interdependency may be the reason why S1 has the best performance in combination with C1. Yet, with the currently available information it is difficult to draw a conclusion regarding which process in Spring is responsible for the increased SSCs. As all three scenarios have promising results it might also be the combination of wind shear and bio-activity which is responsible for the increased SSCs. To avoid overcomplicating the model, only one process is held responsible in this case.

A correct computation of resuspension at the San Francisco shoals during windy periods his very important to obtain correct turbidity levels in the Bay. More information on local conditions regarding bioactivity and wave attenuation at the shoals is required to be able to draw conclusions on which process is responsible. The required additional information is further described in Section 6.3.2.

Model results for WY2017 (indicated as "wet year") were shown in Chapter 4.3, but did not score well. While the station in North Bay scored reasonably well, measured SSCs at Dumbarton Bridge were strongly overestimated by the model during the period of Delta peak discharges in Winter. Due to the large discharges of freshwater, South Bay becomes more stratified with respect to WY2013 and a large amount of sediment is imported. Further analysis of measured and modelled SSCs at Mallard Island, which is located near the inflow points of the Delta rivers, has caused doubts regarding to the correctness of the supplied time series of SSCs of the Delta rivers for WY2017. Modelled SSC are strongly overestimated at Mallard Island, indicating

that river SSCs applied to the model are much larger than they would have been in reality. If river SSCs would be corrected and set to lower levels found in the measurements, the performance of the model would likely improve significantly in other parts of the Bay.

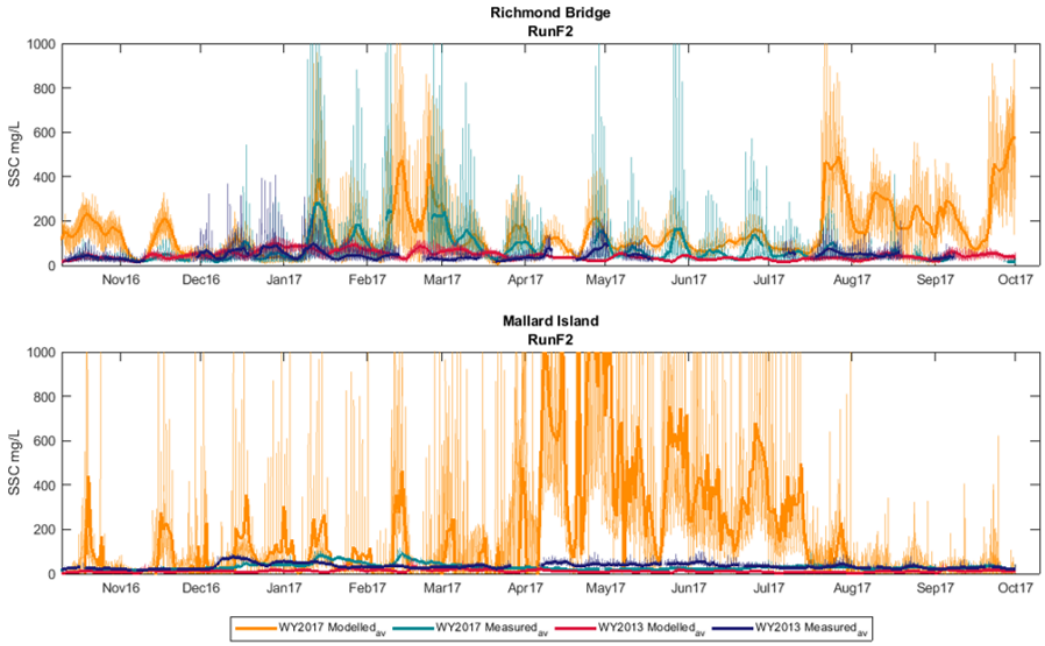

Figure 6.2: Results of model runs for WY2013 (in red) plotted with WY2017 (in orange) and the measured SSCs for WY2013 (in blue) and WY2017 (in green) for a station in North Bay (Mallard Island) and a station in South Bay (Dumbarton Bridge). Together with a scatter plot of the modelled SSCs plotted against the measured SSCs for WY2013 in green and WY2017 in pink.

Calibrating a large model domain with varying dominant forcings varying spatially and temporally has proven to be complex. The calibration efforts have improved model performance on seasonal variations and the amplitude of tidal variations of SSC is captured better. A more adequate computation of SSC variations during the tidal cycle for the entire Bay was found to be unfeasible without locally specifying temporally varying sediment parameters.

6.1.2. Sediment Connectivity in South Bay

The method of sediment connectivity provides a framework to analyse complex coastal systems in a more structural way. Large data sets of spatial and temporal output of sediment transport in San Francisco Bay were reduced to a 17x17 adjacency matrix permitting a more straightforward analysis and the application of different statistical metrics unavailable in more traditional approaches(eg. analysing mean transport vectors).

While schematization of a complex system into a simple network provides the argument to apply graph theory, the schematization should be carried out with care or one may oversimplify the system too much. In this research the large San Francisco Bay estuary was schematized into 17 segments on basis of morphological function with a higher resolution of segments in South Bay. Though this division took into account the important characteristic of comparable sediment dynamics within a segment, increasing the number of segments might unveil new pathways. Yet, introducing new sediment labels to the DELWAQ-Model to increase resolution would increase the simulation time too much. Though it is believed that the main sediment pathways are captured, a higher resolution of segments will likely reveal local differences of accretion rate or erosion rate within a segment as most segments are still quite large.

Though no conventional method or algorithm to divide the model domain into segments is available in literature, one method applied by Rossi et al. (2014) could be applied in future connectivity analysis. In this study connectivity analysis is applied to investigate larval dispersal and they define so-called "hydrodynami-

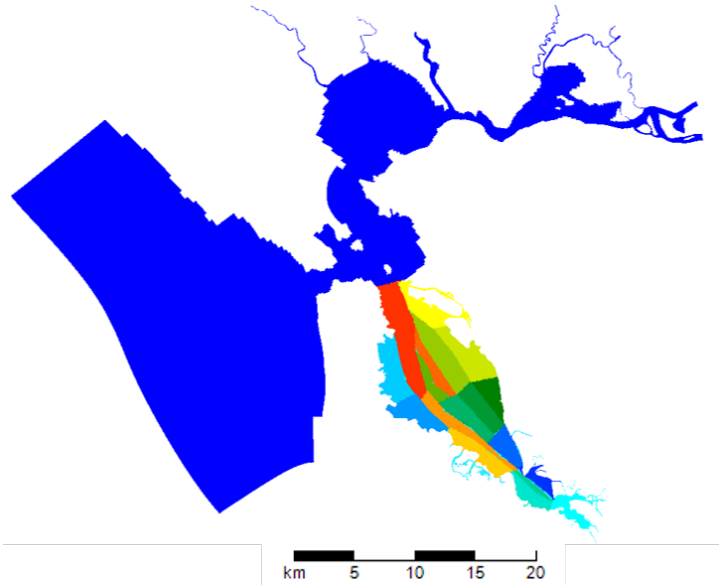

Figure 6.3: Potential division of South Bay into 17 segments in, by dividing the shoals and considering the distance from the channel.

cal provinces" based on earlier developed connectivity matrices. In San Francisco Bay one short test simulation could be run with a higher amount of segments (such as 50-100). Due to the short simulation period, the simulation time would still be acceptable. The analytical metric of modularity could be used to find the sediment sharing communities, consisting out of segments that have relatively uniform transport within them. Another potential approach to divide San Francisco Bay, is to only focus on South Bay and increase the amount of segments locally. Apart from dividing the segments by morphological function, the shoals could be further split up by taking into account the distance from the channel. Hydrodynamic energy is lower further away from the channel, so sediments are likely to behave differently at these locations from areas closer to the channel. A potential division is displayed in Figure 6.3.

Comparing asymmetry analysis with cross-sections in DELWAQ

As a final check, the cumulative net fluxes derived with the Sediment Connectivity approach are compared to the results of the method used by van Kempen (2017) and Gostic (2018). In their approach, the cumulative net-transport was calculated by defining transects at Bay Bridge and the Dumbarton Narrows in the DELWAQ-Model. The cumulative transport of sediment across Bay Bridge, with positive numbers representing net import into South Bay (Figure 6.4) is showing similar trends of a net-import as computed with the Sediment Connectivity approach. Both show an import in Autumn and Winter, a slight export in January and February and a strong import during March. Once south-westerly winds start to blow in Spring both approaches show an export for South Bay. Bathymetry studies by (Foxgrover et al., 2004) showed South Bay has been importing in the 20_{th} century, so the results from both approaches are in agreement with literature. The cumulative transports for Lower South Bay calculated by both approaches agree well with each other. Studies by Gartner et al. (1997) and Shellenbarger et al. (2013) show import for moderate-dry years, which is how WY2013 qualifies (see also Table 6.1).

In the case of Bay Bridge, the results from both approaches deviate from each other during the time-series. The difference in outcome can be explained by the different nature of both approaches. DELWAQ computes the cumulative transports across the cross-sections every hour. Due to the large size of the domain and long simulation period, a smaller time step than 12 hours is not feasible in the sediment connectivity approach. When the output time step is this large, aliasing of the tidal signal can become a problem. The effect of aliasing is discussed further in Appendix B.

Another important source to the difference is the computation method of transport along a transect in DELWAQ. An average level at the transect is used to compute transport over the entire water column (Deltares, 2019). Due to the presence of vertical gradients in SSCs in South Bay and the seasonal presence of strong

vertical shear in velocity over the water column, averaging over the water column is not always suitable. The results of both approaches compare well for the Dumbarton Narrows. Both are showing a gradual net-import during the WY2013. Vertical gradients in SSCs are less present in the area of Lower South Bay, and wind-induced residual currents or estuarine circulations are barely measurable. This may explain why the results of both approaches are more in agreement at this location.

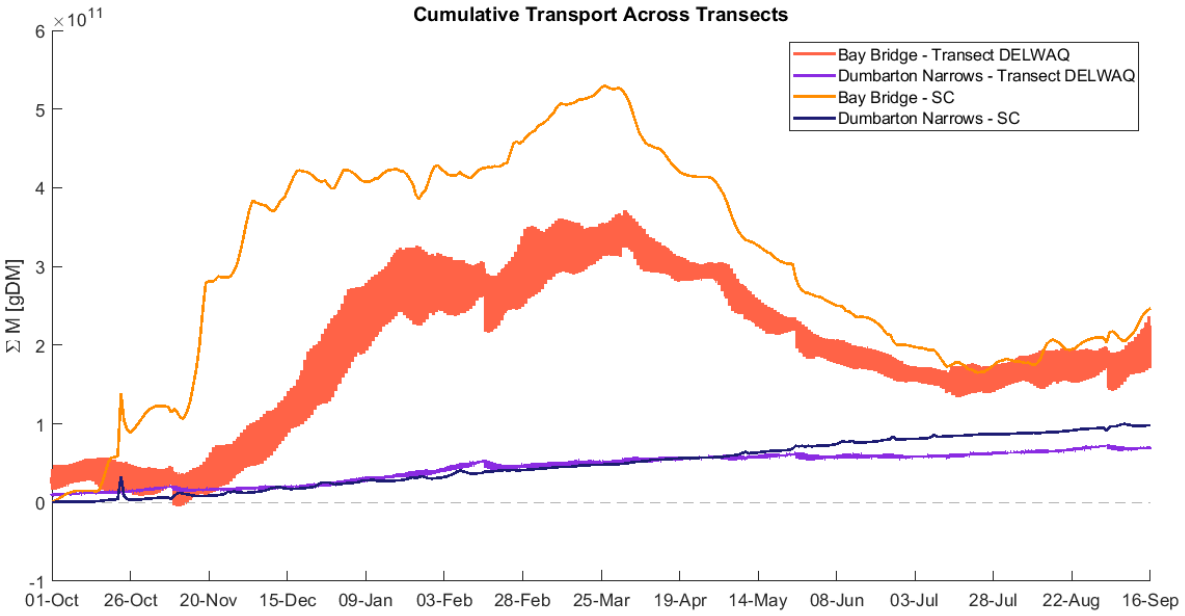

Figure 6.4: Cumulative Transport across the cross sections of Bay Bridge (red) and Dumbarton Narrows (purple), hourly calculated by DELWAQ compared with the daily calculated Cumulative Transport with the sediment connectivity approach with Bay Bridge (orange) and Dumbarton Narrows (blue).

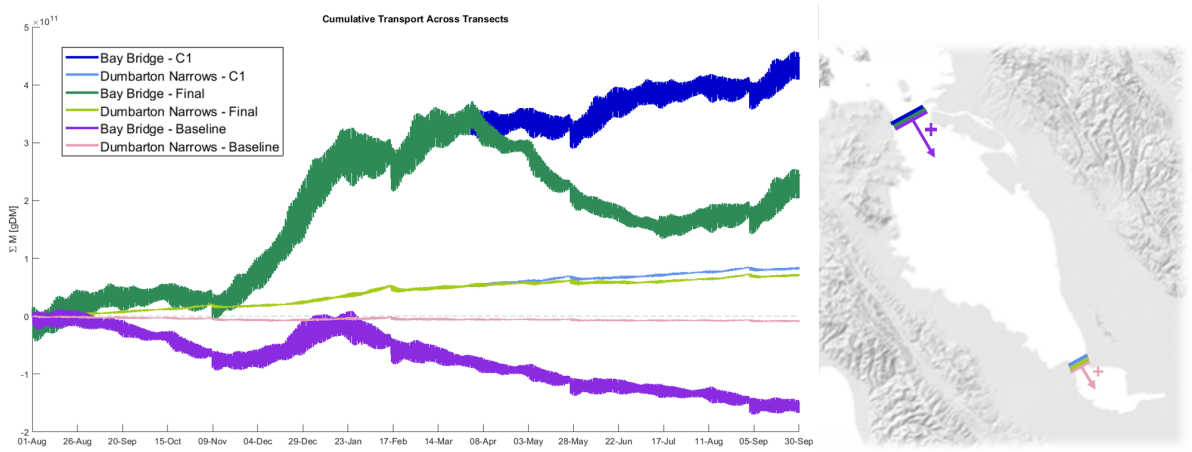

Figure 6.5: Cumulative Transport across the cross sections for the Final run with Bay Bridge (dark green) and Dumbarton Narrows (light green); for the Calibration run C1 (only increased vertical gradients) with Bay Bridge (dark blue) and Dumbarton Narrows (light blue); for the Baseline run with Bay Bridge (purple) and Dumbarton Narrows (pink)

Influence of Model Calibration on Net-Exchanges

To investigate the influence of the model calibration on the net transports two additional simulations were run for calibration scenario C1 and the Baseline run. Calibration scenario C1 is similar to the Final run, except that sediment parameters are not adjusted in Spring(Figure 6.5). With respect to the Baseline run, calibration scenario C1 has increased vertical gradients in SSC.

Compared to the Final run, there is still a slight export from April-July in South Bay for scenario C1. Yet, while South Bay remains to export until July for the Final run, South Bay is importing from May until the end of the simulation. Therefore, South Bay ends up to export twice as much sediment as for the Final run. The import rates for Lower South Bay do not differ as much, though scenario C1 shows a slightly higher import than the Final run. The Baserun is showing a totally opposite signal of export for both South Bay as Lower South Bay, with only import to South Bay during the regime of residual circulation. Yet, conventional belief for San Francisco Bay is that South Bay experiences export in this period as bottom currents are directed seaward. This signal of export in South Bay is in agreement with the model study conducted by White (2019) was also focused on WY2013 and equal parameter settings were used as for the Baserun of this study. Though sediment fractions and parameters equal to White (2019) were used in the model study of Gostic (2018), it resulted in an importing signal for South Bay for WY2015. In WY2015 the reverse and classic estuarine circulation were much stronger due to the larger influx of freshwater. This probably led to the difference in net transport between Gostic (2018) and White (2019) and this study's Baseline run, while similar sediment parameters were used.

Suspended sediment concentrations seemed to be quite uniform over depth in South Bay for the Baserun with respect to the final calibrated model run. This difference shows the vertical gradient is very important in obtaining import into South Bay as a model result. The only available study on sediment budgets focusses on Lower South Bay and predicts import for Lower South Bay (Shellenbarger et al. (2013)). No studies are available to validate the import volumes of calibration scenario C1 or the Final run. However, modelled SSCs in South Bay of the Final run compared better to the local measured SSCs than those of scenario C1 (See Chapter 4).

6.2. Limitations

The analysis result while using the sediment connectivity approach is still only as good as the data or model used to derive it. This section will highlight the most important limitations to the application of the DELWAQ-Model in this study. The Sediment Connectivity Approach also has some limitations.

6.2.1. DELWAQ-Model Limitations

Process-based numerical models have proven to be a very useful tool to analyse the complex processes involved in sediment transport. However, as models are in the end always a schematization of reality and therefore there is a limit to which end a model can reproduce it. Especially with a large model domain as San Francisco Bay, a compromise must be made in the number of detailed processes that can be included while the simulation time remains feasible. Hence, the results from the DELWAQ-Model should be interpreted with these limitations in mind.

Time and spatially varying sediment parameters

Sensitivity Analysis in Section 4.2 has shown that the model performance in North Bay and South Bay sometimes responded oppositely to varying constant sediment parameters in the model domain. The model performance increased more often for parameter changes when separate parameters were set to North Bay and South Bay. North Bay and South Bay are indicated as two hydrologically distinctive sub-embayments in literature (Barnard et al., 2013a), which is in line with the choice of separate sediment parameters. Furthermore, the Baserun in Chapter 4 showed that a fall velocity constant in time in South Bay performed well during Autumn and Winter, yet lead to a significant underestimation of the SSCs in Spring. Setting a new fall velocity during Spring in calibration scenario S1 has improved the model performance in Spring. However, the abrupt change in fall velocity that was applied in this research does not resemble reality, which might lead to some peaks in the model response as it has to adjust to the abrupt changes. A period of transition to change sediment properties would be advisable, yet was not feasible to apply during this research due to time restriction.

Studies by Gartner (2004) and Allen et al. (2019) involving fieldwork in South Bay and North Bay respectively show seasonal and spatial variations on seasonal,spring-neap and daily tidal cycles. Allen et al. (2019) found hydrodynamic roughness and bed erodibility to fluctuate on seasonal and spring-neap time scales, while the floc size fluctuated on a tidal scale. Also, Schoellhamer et al. (2003) mentions calibration in San Francisco Bay is site and time-dependent. Introducing temporal and spatial variables may enable the model to capture local dynamics better, but a high number of model parameters will complicate the model significantly. Including

a large number of variables can lead to several combinations that can reproduce measured values. However, the user will remain uncertain which combination is correct and therefore which processes are dominant. If the wrong combination is selected, the sediment properties do not represent the dominant processes and therefore will likely not produce accurate results for the simulations of other years.

Settling Velocity and vertical profile

The vertical profile of SSCs can be very important when analysing sediment transport due to vertical shear in the flow velocity. The vertical profile in SSCs is a combination of settling, resuspension and turbulence in the water column. All three processes are simplified in the DELWAQ-Model and its implication will be described here. The fall velocity of mud particles is a dynamic parameter, influenced by several time-varying processes. Hence in reality, falling velocity for sediment in the model does not exist. The settling velocity depends on the shape of the particle and the size. The process of flocculation determines these characteristics but is also very complicated. The consolidation of the bed is also not taken into account in the model. A consolidated bed is less likely to resuspend than a freshly deposited bed, hence the modelled resuspension flux while applying constant erosion parameter in time may deviate from reality. Next to that, the presence of bioactivity may have an influence on the erodibility, which can vary spatially and temporally. Furthermore, the formation of flocs depends on factors such as shear stresses, salinity, availability of organic material, temperature and turbulence density, which are not included in the flocculation application of the DELWAQ-Model. The variability of floc sizes is taken into account by including two sediment fractions, though these are not variable in time. This prevents the model of accurately simulating seasonal and tidal variations in SSCs.

Correct computation of the bed shear stresses is essential for calculating the right resuspension flux. The study of Egan et al. (2019) attempted to characterize the mean and turbulent properties of the boundary layer for the location in South Bay. The measured shear stresses in the study could not be approximated well by various estimation methods. The bottom shear stresses in DFLOW are simply calculated by adding the bottom shear stresses due to currents and waves assuming the velocity profile follows the logarithmic profile. This more traditional approach is likely to overestimate mean current-induced shear stress, but to underestimate the total bed shear stress during strong waves. Furthermore, critical shear stresses are regarded as constant in DELWAQ, yet the critical shear stress is also a variable parameter. Critical bed shear stress is influenced by the history of erosion. Suggestions to reduce the uncertainty in the bed shear stresses in the model are described in Section 6.3.1.

6.2.2. Limitations to the Sediment Connectivity Approach

In the literature about Sediment Connectivity, a clear distinction is made between structural connectivity and functional connectivity. In reality, functional connectivity (sediment fluxes) is likely to lead to a change in structural connectivity (morphology) which in turn will influence the functional connectivity(Wainwright et al., 2011). However, this version of the DELWAQ-Model is morphostatic so the feedback loop between functional and structural connectivity is not incorporated. For the considered timescale of this project, the morphostatic character of the model does not have a significant influence on the model results. Nonetheless, when longer timescales are simulated the structural connectivity should be adjusted in time.

In the current implementation of sediment connectivity in the DELWAQ-Model by sediment labelling at the start of the simulation, information about the route the sediment is taking (for instance from Lower South Bay to the ocean) is lost. As this is very interesting information, it would be beneficial to explore other methods to trace sediments were this information is not lost. In the Lagrangian approach of sediment particle tracking models(eg. Soulsby et al. (2011)) the detailed pathway is preserved.
Though each tidal cycle strong gross sediment fluxes move back and forth in San Francisco Bay, resulting net fluxes are responsible for morphologic change and changes in turbidity. Therefore an accurate computation of net fluxes are essential in order to understand observed trends and develop adequate management strategies. In the approach of Sediment Connectivity, the net flux is computed by assessing the displacement of sediment in the bed in comparison to the previous time step. Net fluxes are generally of an order smaller than the gross fluxes. Due to the relatively large and constant daily output time step, the effect of tidal aliasing can lead to the inclusion of gross fluxes. To accurately describe net transports the inclusion of gross fluxes should be minimized, hence output time steps preferably occur during the same moment of tidal phase. Though the tidal signal is semi-diurnal on a basic level, tidal harmonics are highly variable in South Bay and Lower South Bay due to its shallowness and semi-enclosed nature. Several output frequencies were compared and

the 24h50min output frequency resulted in the least shifting in the tidal phase for the model output. The effect of tidal aliasing was found to cancel itself out over a longer simulation period. Yet, for shorter monthly or weekly simulation periods tidal aliasing led to more smoothed gradients in the results. More details on the effect of tidal aliasing can be found in Appendix B.

6.3. Directions for Future Research

6.3.1. Recommendations for further Model Improvement

The calibration efforts in this study enabled the model to better capture signals of seasonal and episodic variations in SSCs across the Bay. However, episodic peak values observed in South Bay in the Polaris Cruise Data and the USGS High-Frequency Data are occasionally still underestimated by the model by 50%. The ability to capture ebb-flood cycle variations and wind-wave events in the SSC signal varies spatially in the Bay and over time. Further calibration is needed if SSC fluctuations are required to be reproduced more accurately. Several topics to focus on are highlighted in this section.

Sediment input from the Delta and local tributaries

Both sediment input from the Delta and local tributaries are hypothesized to be an important source to South Bay (Barnard et al., 2013a). To investigate which sediment source is dominant and how it relates to the Bay's ocean export, an accurate representation of sediment concentrations and river discharges should be applied to the model's boundaries. A study performed by White (2019) provided an indication of sediment concentrations and water discharges of local tributaries, yet it also revealed the large uncertainty in the estimates. Though there is more certainty in the time-series of the water discharges of the Delta rivers due to measurements of the USGS, an error in the initial file for the sediment concentrations applied to the model for WY2013 required the development of new SSC time series. The new time-series was simply created by deducing the relationship between river discharge and sediment concentrations in WY2015 and applying this relationship to WY2013 (see Section 4.2 and Appendix A for more details on the procedure). Due to time restrictions a more thorough research on SSCs in the Delta rivers in WY2013 was not feasible. A correct relation between sediment concentrations and river discharge is essential in accurately estimating the sediment load entering the Bay. By including data of SSCs and water discharges of other years to analyse the relationship or by executing new measurement campaigns at the Delta and local tributaries, the sediment load entering the Bay could be better predicted.

Calculation of Bed Shear Stresses

As highlighted in Section 6.2.1, the calculation of bed shear stresses is highly schematized in the DELWAQ-Model. However, the adequately modelling of bottom shear stresses is an important factor in the modelling of mud resuspension and therefore sediment transport (Lacy and MacVean (2016), Egan et al. (2019)). The currently used D-FLOW Hydrodynamics model computes total bed shear stress by adding the bottom shear stresses due to currents and waves, while assuming a logarithmic velocity profile. This simple and traditional approach is likely to overestimate mean current-induced shear stress, but to underestimate the total bed shear stress during strong waves due to their non-linear interactions. In situ estimates of bottom shear stresses are available from studies in South Bay (Cheng et al., 1999), San Pablo Bay (Lacy et al., 2017b) and Suisin Bay (Brennan et al., 2002) (see Figure 6.6.a). Additional suggestions for bed shear stress measurements are included in the figure. These new measurement locations are located at the flats, near the channel and near shore to be able to investigate the effect of wave dissipation. These estimates could be used to calibrate and validate generated local bed shear stresses to obtain more convincing estimates of the bed shear stresses in the model domain. Or if the model is not adjusted, comparisons of the measured and modelled bed shear stresses might explain deviations of the modelled SSCs from the measured SSCs.

6.3.2. Resuspension and settling at the shoals of San Francisco Bay

Though the model used in this study is calibrated against a relatively good spatial coverage of measurements of SCCs, there was no information included of SSCs at the shoals at the beginning of this research. An extra dataset of SSCs at the shoals was provided by SFEI in the later stage of this thesis. Due to time restrictions, only two locations in South Bay were included during calibration. A significant increase in SSCs was observed at both the West Flat and the East Flat. There might also be an increase in SSC at the North Bay shoals, though no increase in SSCs was observed at nearby USGS measurement stations in the channel. Though SSC observations at other shoals were not taken into account, they could prove valuable in future calibration efforts.

a)

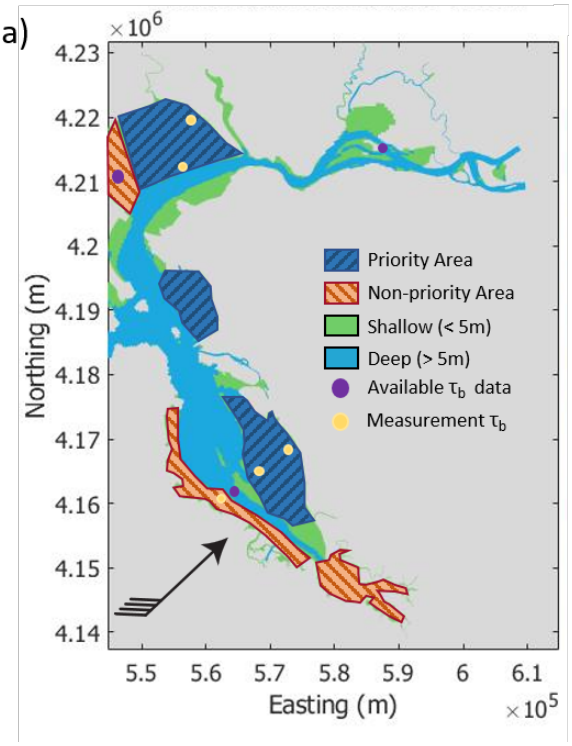

b)

Parameter	Location
Bottom Shear Stresses	San Pablo Bay • Near channel • Near coast
Bottom Shear Stresses	South Bay East Flat • Near channel • Near coast
Bottom Shear Stresses	South Bay West Flat
SSCs	Eastern Flats (in line of wind fetch)
SSCs	Western Flats (in line of wind fetch)

Figure 6.6: Overview of a suggestion of measurement locations with a) An overview of (non-)priority areas for SSC measurements and an overview of available τ_b data and suggestions of locations for measurements. b. Table overview of the suggested measurement locations.

Furthermore, the shoal measurements were only two-weekly conducted and information on the evolution of SSCs during a tidal cycle or spring-neap cycle would be very valuable to accurately calibrate the model. Figure 6.6.a shows a suggestion of locations for additional SSC measurements. The eastern flats are indicated as priority areas as these are most prone to wave resuspension during Spring as they are in line of the fetch of the south-westerly summer sea breezes. A measurement period of a week or month during Spring and one outside this period of strong winds, could provide valuable information on the effect of wind waves on sediment resuspension in San Francisco Bay.

To avoid over-calibrating the model to episodic peaks in SSCs occurring during the WY2013, SSCs observations of other years should be included. The time-series of WY2015 used in the study of Gostic (2018) shows a similar increase at Dumbarton Bridge in Spring. Yet, it would be interesting if this increase in Spring can be observed in all years. Though the study of Shellenbarger et al. (2013) shows similar peaks during Spring for 2009-2011, which indicates the high SSCs in Spring are not a one-off event.

6.3.3. Different hydrodynamic scenarios

With only the hydrodynamics of WY2013 available, it is difficult to fully identify the separate influence of the tide, wind and baroclinic processes on sediment pathways and net-transports in South Bay. In this study, the best approach was to find weeks in the simulation period where different forcings were dominant and to compare them. However, as the tide is always present and the wind regularly blowing in the Bay, their individual effects cannot be isolated. Applying the DELWAQ-Model to different hydrodynamic scenarios could support the findings during this study and provide a conclusive answer to the effect of tides on fine sediment dynamics in South Bay. Yet, these scenarios also do not provide the effects of each forcing in reality as forces often enhance or work against each other due to non-linear interaction. WY2017 would be a good candidate for a wet year simulation to analyse the effects of baroclinic processes as long as the sediment influx from the Delta is correctly quantified. Furthermore, a scenario without wind could provide more information on the wind effect on sediment dynamics.

6.4. Model Applicability to the issues of San Francisco Bay

6.4.1. Habitat restoration as measure against sea level rise

The global threat to coastal communities of the predicted sea-level rise due to climate change is amplified in the Bay Area due to local land subsidence. It is expected that almost all municipalities along the South Bay shores will eventually be at risk of inundation due to sea-level rise (Knowles, 2010). Some of the most valuable corporate real estate of the country is situated around the periphery of South Bay, thus inundation of these areas will have both significant economic as social consequences.

Salt marshes can act as a defence against the flooding of communities along the Bay's coast as their shallow slope and vegetation dissipate wave energy. The South Bay Salt Pond Restoration Project is an ongoing initiative in South Bay of salt marsh restoration (Hobbs et al., 2015). Recent reports (De La Cruz et al. (2018), Hobbs et al. (2015)) show that salt marsh restoration efforts are fruitful. Essential for the development of salt marshes are calm abiotic conditions and sufficient sediment supply. However, under the current trend of decreasing SSCs in South Bay (Schoellhamer, 2011) and a potential increase in tidal energy due to sea-level rise, it remains uncertain if conditions in the future will still be adequate for salt marsh development and conservation. This research has shown that for the year 2013, both the importing segments in South Bay and Lower South Bay could keep up with sea-level rise (see Table 6.2), under the assumption that all incoming sediment would be equally distributed over the importing segments.

A riposte of opposition to the Salt Pond Restoration Project is the possible consequence of the loss of intertidal flats, as a sediment sink is created by opening the salt ponds (Jaffe and Foxgrover, 2006). In this research, the DELWAQ-Model in combination with the method of Sediment Connectivity can improve understanding of the sediment input to South Bay through both Bay Bridge as the Dumbarton Narrows. Analysis of net sediment transport in South Bay has provided an indication of the locations of sedimentation. and therefore promising sites for salt marsh restoration. This information can support develop fitting managing strategies by providing the opportunity to focus attention in the promising areas.

6.4.2. Assessing Future Climate Change Impacts

As discussed in the previous section, South Bay communities risk inundation due to the projected sea-level rise. In addition to the risk of flooding of the built environment, sea-level rise can also increase salt intrusion, drown tidal habitats, accelerate coastal erosion and change the level of tidal energy (Shirzaei and Bürgmann, 2018). Changing precipitation patterns can alter river discharge intensities and together with increasing temperatures increase stratification. Research has predicted dryer summers and wetter Springs (Grenier and Davis, 2010). Drier summers with higher temperatures may increase the water demand in the upstream agricultural region of Central Valley. With the use of the upstream river dams, the already low river discharge might be used for irrigation, resulting in less freshwater inflow for San Francisco Bay. Ganju and Schoellhamer (2010) analysed the influence of different scenarios of climate change for San Francisco Bay and found that the changes will undoubtedly impact stratification and circulation patterns. The DELWAQ-Model can be used to assess the influence of the different predicted circulation patterns on sediment input and sediment pathways in South Bay. Information on projected sediment budgets can help develop large-scale management decisions in river water regulation and inspire local measures to mitigate impact due to climate change. The model can also be used as a tool to investigate which local measures are most promising and help select the most suitable location.

6.4.3. Dealing with contaminants

San Francisco Bay has been dealing with poor water quality since mercury used for hydraulic mining has found its way to the SFB through the river discharge from the Delta. An additional source of mercury for South Bay was the Guadeloupe River, along which shores a mercury factory was located. As mercury tends to attach itself to fine sediments, the spreading of sediments can provide an indication of the distribution mercury. Although there are limitations to determining the exact spreading of mercury by tracing sediments, information on regions of erosion can indicate the potential redistribution of mercury buried in the bed over time. Oppositely a region of sedimentation could function as a mercury sink. For WY2013, connectivity analysis showed strong erosion for the eastern flats of South Bay, which could indicate the redistribution of formerly buried mercury if it is present in the bed. The western flats and Lower South Bay experience import and could therefore be a mercury sink. This information can provide a better foundation for the management

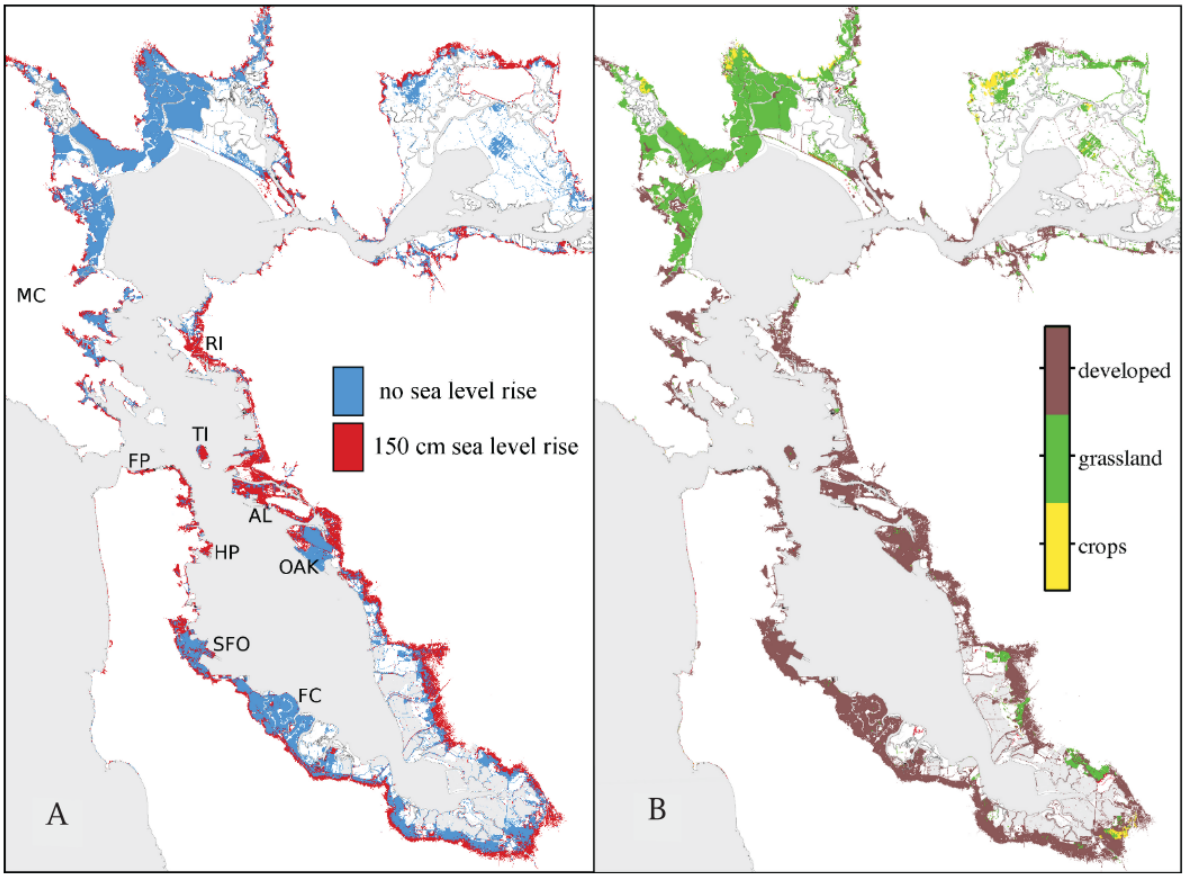

Figure 6.7: Figure from Knowles (2010) indicating A) the areas at risk of inundation with either no sea level rise (blue) or 150cm sea level rise (red) B) the high amount of developed area around the periphery of South Bay. Highly developed city areas of Oakland, San Francisco and San Jose become at risk when sea level rises with 150 cm.

of mercury contamination in the Bay (David et al., 2009).

6.4.4. Future of toxic algae blooms

South Bay and especially Lower South Bay are vulnerable to water quality issues such as toxic algae blooms due to the increased amount of sewage discharge following urban development and the little freshwater flushing. The high level of turbidity in the last century following the sediment pulse during the period of hydraulic mining has been of great importance to South Bay as the turbidity has regulated the algae outbreaks by limiting light penetration. Yet as water in South Bay has been clearing up over the last decades, San Francisco Bay changed from a low-productivity estuary to a level of primary production typical of temperate-latitude estuaries (Cloern et al., 2007). The DELWAQ fine sediment model could be coupled with the DELWAQ-BLOOM module to investigate the relation of SSCs and algae outbreaks. A increased comprehension of the mechanisms controlling the algae outbreaks in South Bay might ignite stricter regulations on water management to limit the entering of nutrition for algae or highlight the necessity of improved education to local residents on the dangers of residential fishing or swimming as it increases exposure to harmful toxins.

6.4.5. Applicability in a larger context

Estuarine tidal mudflats tend to form unique and valuable habitats as they flood and dry during a tidal cycle. They accommodate meio- and macrobenthos and act as feeding grounds for fish and birds. Hence estuaries are fragile systems under the influence of many natural and anthropogenic forcings Cloern and Jassby (2012). Due to the presence of fertile grounds and good navigational connections, estuaries tend to be densely populated. In the wake of the industrialisation and urbanization of coastal areas, water quality within estuaries has deteriorated as estuarine systems need to deal with chemical discharges and sewer input. Contaminants tend to attach themselves to these long residing fine sediments in the estuary, harming the estuary's ecosystem

with their presence. Besides giving rise to water quality issues, industrial development has altered freshwater input and sediment supply by the construction of river dams. This reduction in sediment input can cause a sediment deficit in the estuary and lead to erosion within the estuary and along the adjacent coasts. This global trend of deterioration of estuarine conditions and their ecosystems can be observed in most densely populated estuaries in the world.

To improve estuarine and deltaic conditions, it is important to understand these estuarine systems. An important ecological factor in estuaries is suspended sediment as affects the water quality in numerous ways (Brand et al., 2010). It determines the distribution of heavy metals like mercury, organic pollutants and other chemical contaminants as these tend to attach themselves to fine sediments. Furthermore it regulates primary production as increased turbidity limits required light penetration and it functions as a building source for mudflats. Both quantitative and qualitative information of suspended sediment dynamics can support to develop fitting managing strategies in salt marsh restoration and coastal erosion (McKee et al., 2013).

This study has acted as a proof of concept for the method of Sediment Connectivity to discover sediment pathways and net-transport in complex estuarine systems all over the world. The additional analytical methods introduced by the method may reveal patterns conventional analysis techniques do not. In this study, connectivity analysis of separate segments with connectivity revealed that while South Bay was importing, there was a large difference between eastern and western shoals. Furthermore, one can easily identify the most dynamic regions of the domain with the help of the metric of strength. Applying the framework of connectivity enables coastal engineers to collaborate with experts of other disciplines as ecology and social sciences in the same framework. The opportunity of collaboration and the addition of new analytical methods makes connectivity a powerful tool that can help to solve the contemporary problems that threat our estuaries.

7

Conclusions

South Bay is a sub-embayment of the hydrodynamic complex San Francisco Bay (SFB), which is one of the biggest estuaries of the North West Pacific Coast of the US. South Bay does not have a significant freshwater input from the upstream end, making South Bay unique as both saline and freshwater enter from Central Bay through the same entrance. South Bay is dealing with increased risk of inundation due to the combination of sea-level rise and land subsidence and deteriorating water quality. Particularly in human-altered estuarine systems, it is essential to understand and identify the dominant pathways of sediment (net) fluxes to establish adequate sediment management strategies (Knowles and Cayan, 2004). In this thesis, a DELWAQ-Model was used to simulate sediment fine transport in San Francisco Bay. First of all the model was calibrated, after which model results were analysed with the method of Sediment Connectivity. It revealed the main sediment pathways in South Bay, net-transport patterns during the different seasons in the year and the different net-transports during different dominant forcings. The main advances and findings of this research are described in this research.

7.1. Main Advances

Model Calibration

The research builds on the earlier calibration efforts of DELWAQ-Model by van Kempen (2017) and Gostic (2018). The DELWAQ-Model was calibrated against newly available data of SSCs. The number of locations of measured SSCs increased from one single point High-Frequency station in South Bay to 8 spread throughout the Bay and additional depth varying SSC measurements across the entire 145 km length of the Bay. This improved the overview of the model performance throughout the Bay, revealing new issues in space and time where the model under delivered. In this research, an important step was taken in developing a model that captures the main signals of SSC variations measured throughout the Bay. While using the same set of sediment parameters but a different initial bed, White (2019) shows an overestimation of averaged SSCs and tidal variations. Gostic (2018) shows an underestimation during Spring in average SSCs and an underestimation on tidal variations for WY2015. After calibration in this research, tidal variations are more of the same magnitude and the daily averaged SSCs are not underestimated as much in Spring. The focal points that were tackled during calibration are described below.

- **Inclusion of Waves**
  In earlier research, the applied hydrodynamic model did not include waves in the computation. Due to the shallowness of the Bay excluding flood channels, incorporating waves is advised as it enables the model to capture peak SSCs due to seasonal winds and storms.

- **Change in Numerical Scheme**
  The previously used upwind scheme was not suitable for a model domain where strong horizontal and vertical gradients are observed in the field due to numerical mixing of steep gradients. It was replaced by a central differences scheme, which resulted in stronger gradients in the model results, while sediment parameter settings were kept equal.

- **Larger vertical gradient**
  A larger vertical gradient in sediment concentrations was obtained in the model by decreasing the de-

position efficiency and increasing settling velocities. This way less sediment is lost to the bed and available for resuspension, which makes the model respond better to tidal variations.

- **Increased SSCs in Spring**
  Increased SSCs were measured in South Bay in this study for WY2013. These higher values were captured after reducing fall velocities in Spring for South Bay.

The model domain is very large and covers almost the entire San Francisco Bay area, including two hydrologically distinctive sub-embayments with a different response to varying sediment parameters. A compromise must be made between preventing to over-complicate the model and increasing the model's ability to capture local and episodic peaks or dips in SSCs. Over-complicating the model introducing many varying parameters and over-calibrating the model on a specific water year is non-advisable, as it makes the model less comprehensible and less applicable to other water years.

Sediment Connectivity

To apply the approach of sediment connectivity to analyse sediment pathways San Francisco Bay was divided into 17 segments. New techniques introduced by graph theory and network analysis provide a new way of analysing sediment dynamics in San Francisco Bay. Net-transports found by analysing asymmetry of the adjacency matrix, agree with net-transports found with the more conventional method of introducing transects in the DELWAQ-model. Furthermore, the application of Sediment Connectivity to analyse sediment pathways in San Francisco Bay functions as a case study of the framework for Coastal Sediment Connectivity developed by Pearson et al. (2020). Uniquely in this research, net fluxes in the model were quantified and seasonal trends were analysed and found with the use of sediment connectivity. This method could function as a structured way of analysing sediment pathways and provide new insights in other estuaries around the world.

7.2. Findings

This research aimed to investigate pathways of fine sediments in South Bay with the help of the approach of Sediment Connectivity. The main pathways of fine sediment, intra-Bay and extra-Bay net-transports were computed for the entire year and for the separate seasons. Furthermore, the the net-transport was found to be under the influence of different dominant forcings.

7.2.1. Sediment Pathways South Bay

Sediment pathways show strong seasonal variations in South Bay. Relatively smaller sediment fluxes are observed in the colder Autumn and Winter months, with the exception of an occasional winter storm. Stronger fluxes emerge during the warmer months of Spring and Summer, when summer sea breezes stir up sediments at the shoals. Throughout the year, the largest sediment fluxes are between the northern segments of South Bay and Central Bay.

7.2.2. Net-Transports in South Bay

Net-transport varies in both magnitude and direction for Autumn/Winter and Spring/Summer. In Autumn and Winter, South Bay and Lower South Bay are importing sediment, with intra-Bay net fluxes being mainly in a south-easterly direction. This leads to accretion at the East Flat, the channel and in the southernmost segment in Lower South Bay. In Spring and Summer strongest net fluxes are observed, which are directed towards the Ocean from the channel and the East Flat. South Bay is exporting sediment, yet Lower South Bay is still importing. Within South Bay, net fluxes are mainly in a south-westerly direction. The East Flat of South Bay is eroding, but the West Flat is gaining sediment. Though gross-fluxes are still strong in Summer, the net sediment exchange between South Bay and Central Bay has decreased with respect to Spring. Eventually, South Bay is slightly importing again in August and September. At the end of the year, South Bay has imported sediment with respect to the beginning of the simulation. However, a clear distinction is visible between the importing west flats and Lower South Bay and the eroding east flats and the channel.

7.2.3. Net-Transport in South Bay under different forcings

During the entire year, the neap-spring tidal signal is observed in net-transports into South Bay. South Bay is showing a stronger import during neap tides than spring tides, though it is importing for both scenarios. The wind is presumed to have a large influence on the net-transports in South Bay. It showed peak rates of import

during autumn and winter storms, while in Spring SSCs increase and South Bay starts to export. In Autumn and Winter, strong northerly winds were observed, while winds were south-westerly in Spring and Summer. This influence of wind speed and direction on the net flux was supported by a correlation analysis. Increased rates of import were perceived during the annually observed period of classic estuarine circulation. However, this year was found to be a dry to moderate year in terms of freshwater inflow from the Delta. Therefore, the classic circulation of WY2013 is presumed to be less strong in WY2013 than in the other years. Lower South Bay experienced a steady rate of import during the entire year. With the exception of a clear peak in import during an autumn storm in November. Wind-generated waves and resulting residual currents during Spring and the early Summer did not seem to influence the net flux.

7.3. Impact of research results

While keeping the limitations of the DELWAQ-Model and the Sediment Connectivity in mind, the research results can be used to predict the impact of current sediment dynamics on the issues of South Bay. Understanding this impact can help to develop current management strategies and future policies to acquire and retain a healthy and safe estuary. As South Bay is dealing with the risk of turbidity-depended algae blooms in Spring and Summer increased values for SSCs are favourable. Lower South Bay is importing sediment throughout the year so turbidity levels are expected to remain high as long as sediments remain in suspension. Intra-Bay net-transport has shown that the west flats of South Bay and Lower South Bay are importing sediment and hence are more suitable for salt marsh restoration than the east flats and the channel of South Bay as these are eroding.

San Francisco Bay is one of the first estuaries where the method of Sediment Connectivity is applied. The Bay has already been the topic of much research regarding hydrodynamics and (fine) sediment dynamics. This makes it a perfect case study for testing a new method as the results can be validated against the results found in literature where different approaches are used. Connectivity results agreed with the sediment patterns described in literature while providing new insights by using analytical metrics that are not available in other research methods. The development of adequate strategies regarding salt marsh restoration and water quality management is often a combination of ecology, hydrodynamics and sediment supply. Connectivity creates a structural framework that enables collaboration with other disciplines that use connectivity to tackle the problems of South Bay.

Many other estuaries around the world are dealing with issues similar to the ones of San Francisco Bay. This study has shown that Sediment Connectivity provides a suitable framework to analyse fine sediment patterns and has highlighted the limitations and sensibilities. With this study as a proof of concept, Sediment Connectivity could be applied to other estuaries around the world.

A

Sensitivity Analysis of the DELWAQ-Model

A.1. Previous calibration efforts

This research builds on the calibration efforts by Gostic (2018) for WY2015 and White (2019) for WY2013. They applied equal sediment parameters in their models runs. However applied a different initial bed with White (2019) applying a fluff layer containing over 10x more sediment per m$\hat{2}$ with respect to Gostic (2018). This large difference is likely due to the fact that unlike Gostic (2018), White (2019) did not include waves in the model and required more available sediment to bring enough sediment into resuspension. The sediment parameters and initial beds used by both studies are applied to the combination of the DELWAQ-Model with the hydrodynamic model for WY2013. Results are shown in Figure A.1 for White (2019) and in Figure A.2 for **?**. White (2019) calibrated her model against one week of model observations in March at Dumbarton Bridge. The model performed reasonably well with a skill score of 0.6 at that specific location in that specific week. However in the bigger model domain over the entire year, SSCs are very much overestimated. Applying the initial bed used by Gostic (2018) provided better results, which leaded to the conclusion that too much sediment was available in the bed used by White (2019). The results from Gostic (2018) showed quite some underestimations in the model domain and scored poorly statistically with SS scores below zero for WY2013. Also the model performance in the entire model domain in WY2015 is analysed. Figure A.3 shows the model results against the Polaris Cruise measurements for a single cruise sailed in August 2015. Gostic (2018) only calibrated the model for measurements obtained at Dumbarton where both measured as modelled SSCs are of the same order. However in the rest of the model domain the model is underestimating the model significantly.

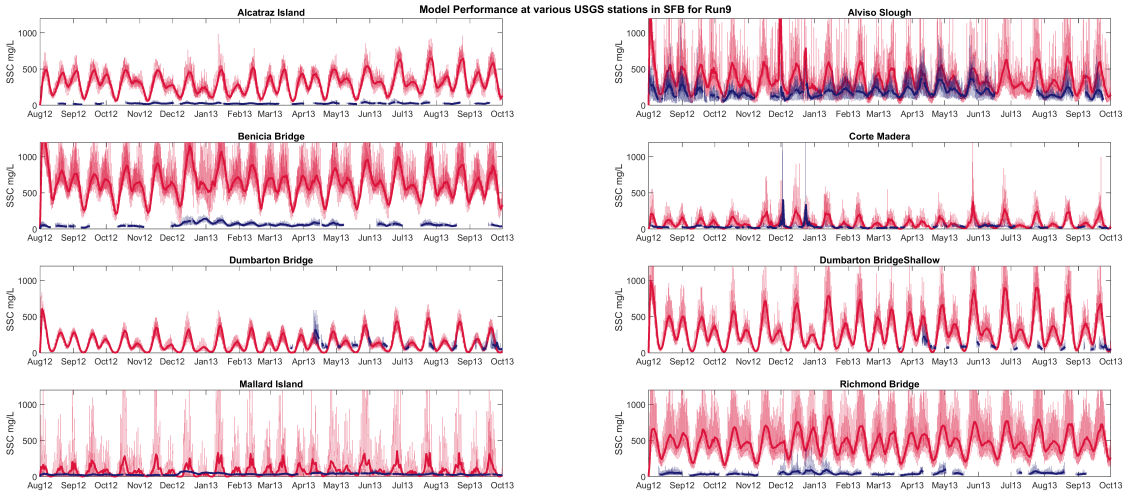

Figure A.1: Results for the Run with sediment parameters and initial bed used by White (2019) for the High-Frequency USGS-stations during for stations in North Bay (Richmond Bridge) and South Bay (Dumbarton Bridge). With the daily averaged modelled SSCs in thick red lines red and the measured SSCs in blue for the 8 USGS stations. Instantaneous measurements are shown in the thinner transparent lines.

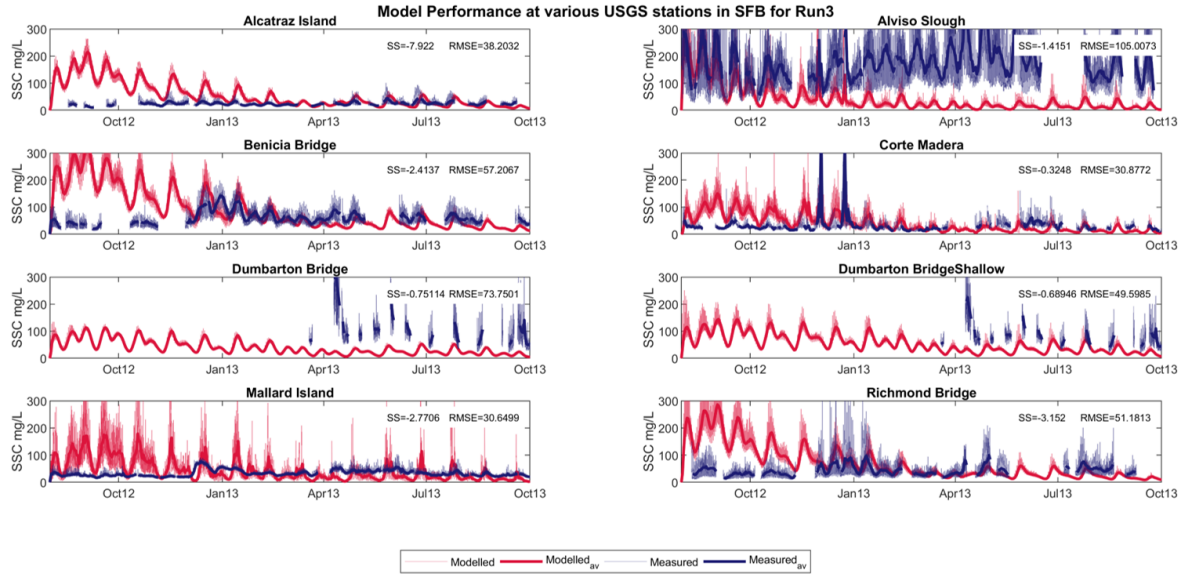

Figure A.2: Results for the Run with sediment parameters and initial bed used by Gostic (2018) for the High-Frequency USGS-stations for stations in North Bay (Richmond Bridge) and South Bay (Dumbarton Bridge). With the daily averaged modelled SSCs in thick red lines red and the measured SSCs in blue for the 8 USGS stations. Instantaneous measurements are shown in the thinner transparent lines.

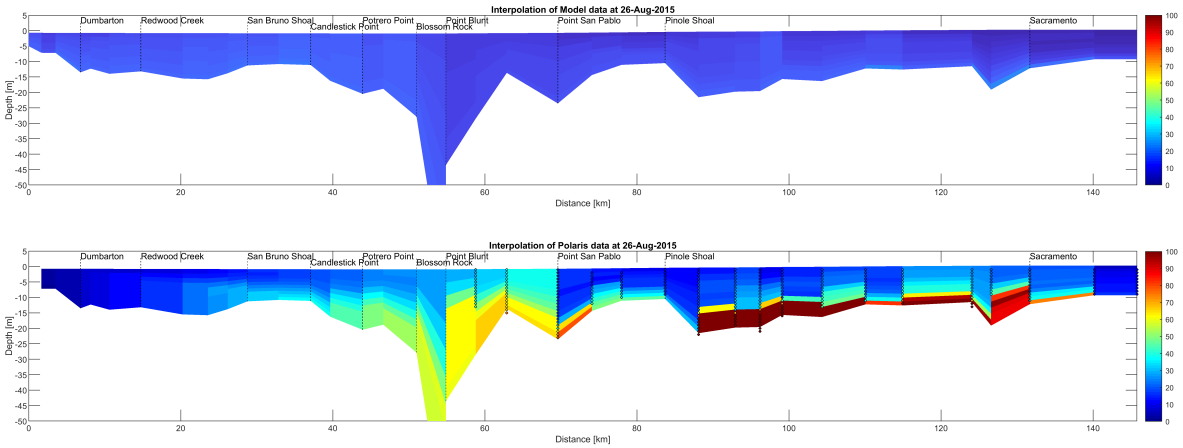

Figure A.3: Results for the Run of WY2015 for with sediment parameters and initial bed used by Gostic (2018) for the Polaris Data with the modelled SSCs as a top-plot and measured SSCs as the bottom plot.

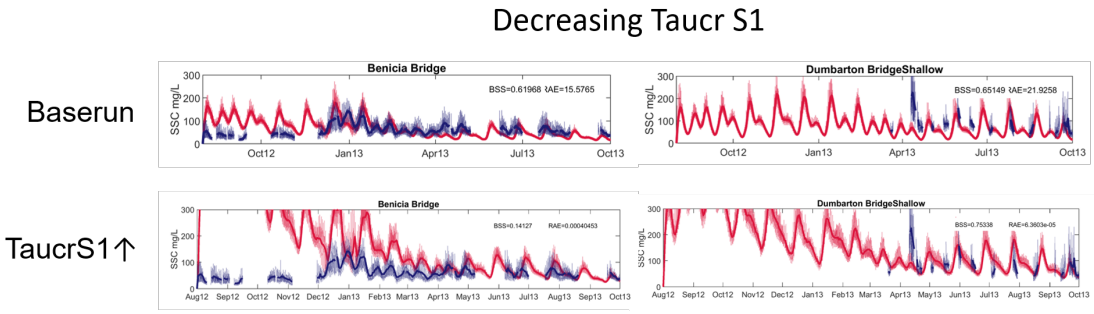

Figure A.4: Results of increasing of TauCr of the fluff layer for two stations in Benicia Bridge (NB) and Dumbarton Bridge (SB).

A.2. Sensitivity Analysis

The initial bed from Gostic (2018) was selected to perform further sensitivity analysis on. Sensitivity to changing falling velocities, $M_0, M_1, \tau_{cr,S1}, \tau_{cr,S1}$, burial parameter α and the effect of changing vertical dynamics in the water column was analysed. Both often sub-embayments responded oppositely to changes in sediment parameters of settling velocities, resuspension parameters. This is further explained in Section A.2. The model was not sensitive to changes in the burial parameter. Both sub-embayments responded positively to changes in $\tau_{cr,S1}$ and $\tau_{cr,S2}$. The results are shown in Figures A.4 and A.5. Reducing both critical shear stresses lead to a higher tidal variability in SSCs in both the sub-embayments. In Figure A.6 modelled bottom shear stresses are compared to the critical shear stress of the fluff layer which is almost always exceeded. The critical shear stress of the buffer layer is varied in the analysis from 0.6-0.9 N/m$\hat{2}$ which was only occasionally exceeded during strong spring tides.

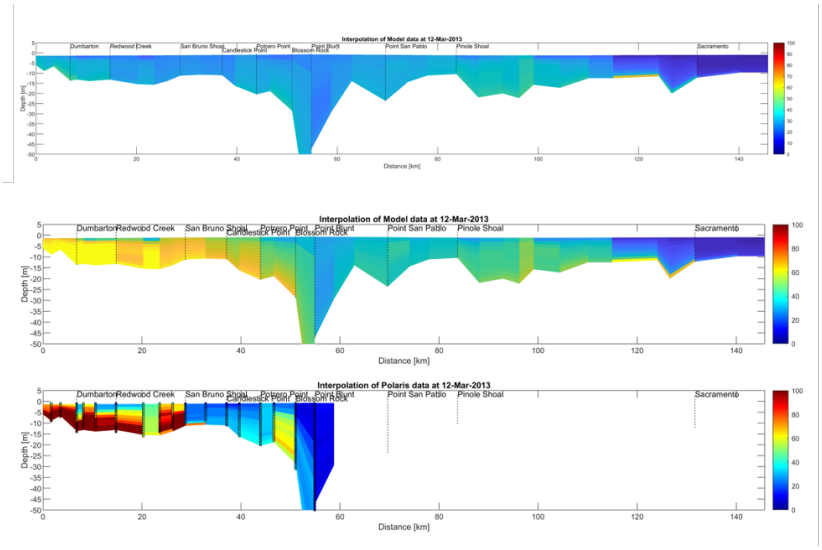

Figure A.5: Results of increasing of TauCr of the buffer layer for two stations in Benicia Bridge (NB) and Dumbarton Bridge (SB).

Difference between NB/SB

As mentioned before, both sub-embayments were found to respond differently to changes in sediment parameters. This effect is displayed in Figure A.7. While the parameters of settling velocities and resuspension parameters were either all divided by 2 to reduce vertical dynamics or increased North Bay and South Bay responded differently. Therefore the choice was made to treat North Bay and South Bay separately by applying different sediment parameters. From the sensitivity analysis varying $\tau_{cr,2}$ seemed most promising and different values were applied to both sub-embayments in different scenarios (See FigureA.8).

A.3. Changing Delta sediment input

While results of changing $\tau_{cr,2}$ were analysed, sediment concentrations in North Bay were lower than expected in Winter. During the peak sediment input in Winter higher SSCs were expected and the SSC boundary conditions applied to the Delta rivers were consulted. There appeared to be an error in the SSCs of the Delta rivers during Winter (see Figure A.9) as SSCs were expected to increase with the water discharge. The SSCs of the water entering via the main Delta rivers San Joaquin River and Sacramento River were corrected by applying the relationship found between the water discharge and SSCs of these rivers in WY2015. The corrected time series of SSCs and water discharges are displayed in Figure A.10. After this correction the model better captured peaks in SSC observed in North Bay (Figure A.11).
After this alteration of the model and reducing the $\tau_{cr,2}$ in South Bay the model was occasionally already able to capture SSC signals in San Francisco Bay (Figure A.12). However gradients in the model were too weak and measured peak values were never modelled. Further decreasing $\tau_{cr,2}$ or $\tau_{cr,1}$ would make the model overestimate average SSC during the year. Up until now waves were not included in the model although most of the model domain consists out of flats. Applying waves to the model has large effects on the SSCs and required $\tau_{cr,2}$ to be increased from 0.6 to 0.9 N/m$\hat{2}$ in North Bay and from 0.4 to 0.9 N/m$\hat{2}$ in South Bay to obtain equal SSC levels as before including waves. The resulting set of parameters functioned as a Baseline scenario for the calibration efforts in the main body of this thesis.

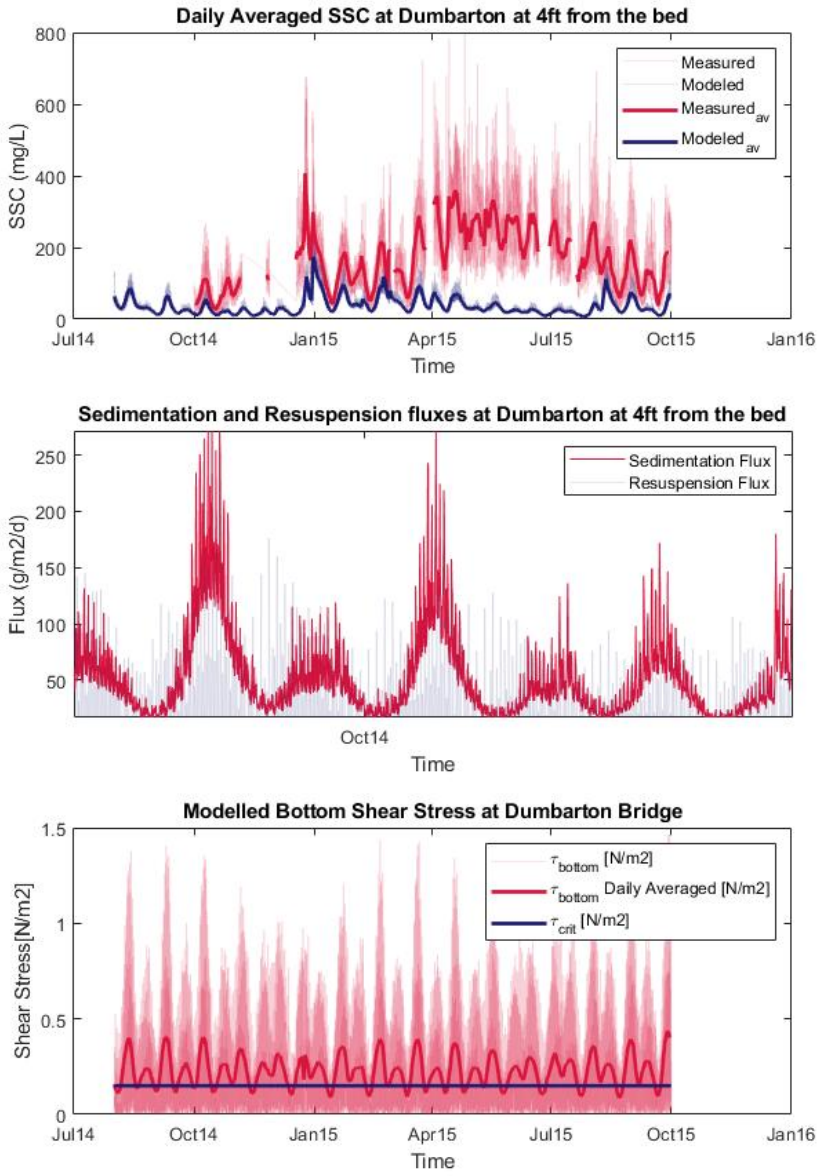

Figure A.6: Top-plot: Modelled and measured SSCs at Dumbarton Bridge (SB), mid-plot resuspension and sedimendation fluxes modelled at the bed, bottom plot : modelled bottom shear stresses against the critical shear stress for the fluff layer.

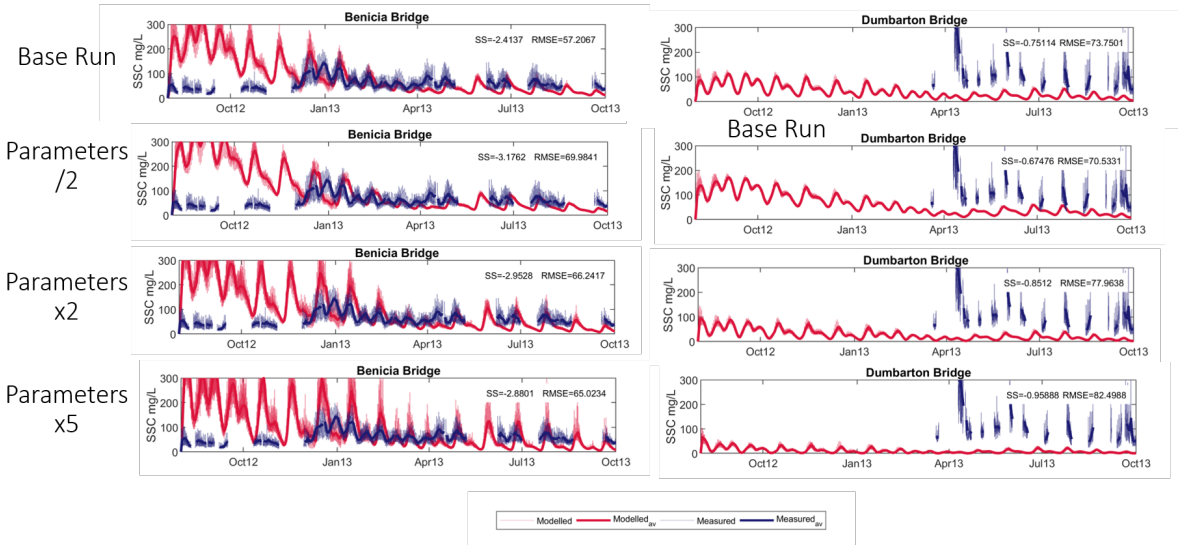

Figure A.7: Results of changing vertical dynamics of the High-Frequency USGS-stations for stations in North Bay (Richmond Bridge) and South Bay (Dumbarton Bridge). With the daily averaged modelled SSCs in thick red lines red and the measured SSCs in blue for the 8 USGS stations. Instantaneous measurements are shown in the thinner transparent lines.

Run	τ_{cr} NB	SB
A1	S2↑	S2↓
A2	-	S2↓
A3	S2↑	-

Overview calibration scenarios

Parameter	Symbol	Baseline	A1	A2	A3
Settling Velocity	ws	0,5/0,1	0,5/0,1	0,5/0,1	0,5/0,1
Critical Shear Stress S1	τ_{c1}	0,15	0,15	0,15	0,15
Critical Shear Stress S2	τ_{c2}	0,6	0,4/1,2	0,4/0,6	0,6/1,2
0th Order Resuspension Flux S1	M0	0,0006	0,0006	0,0006	0,0006
1st Order Resuspension Flux S1	M1	0,0006	0,0006	0,0006	0,0006
1st Order Resuspension Flux S2	M2	0,000003	0,000003	0,000003	0,000003

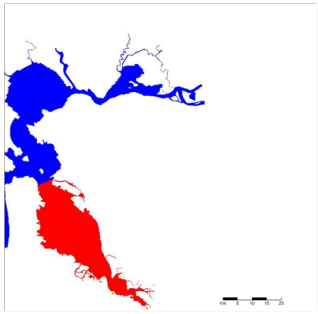

Figure A.8: Calibration scenarios applied for the first calibration round with different hydrodynamics. A division was made between sediment parameters applied to North Bay and South Bay as shown at the right.

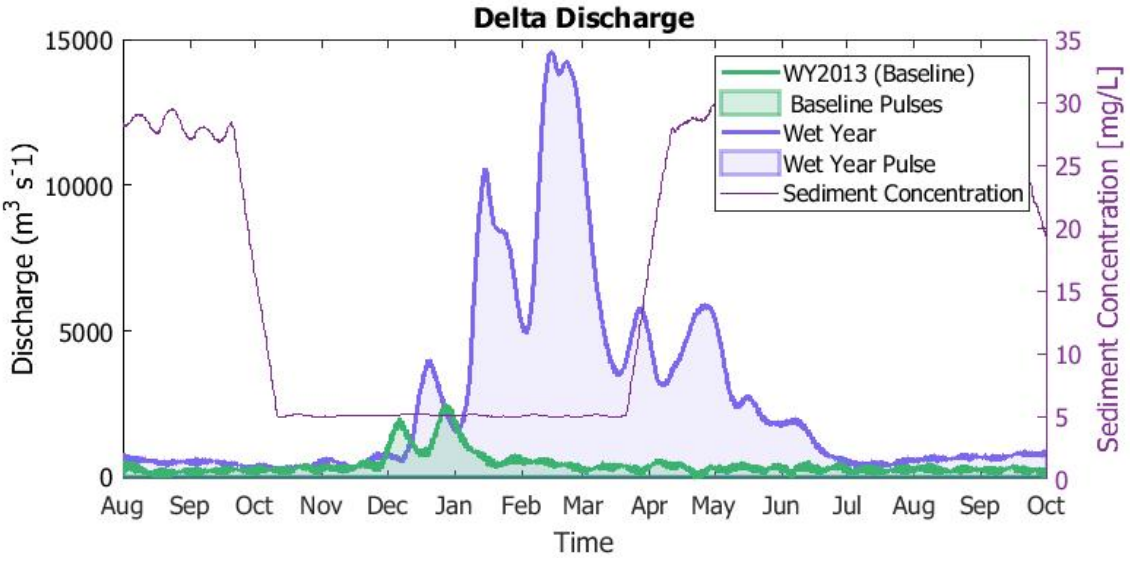

Figure A.9: Rate of combined discharge from the San-Joaquin and Sacramento rivers entering the SFB estuary through the Delta for WY2013 and the wet year WY2017.

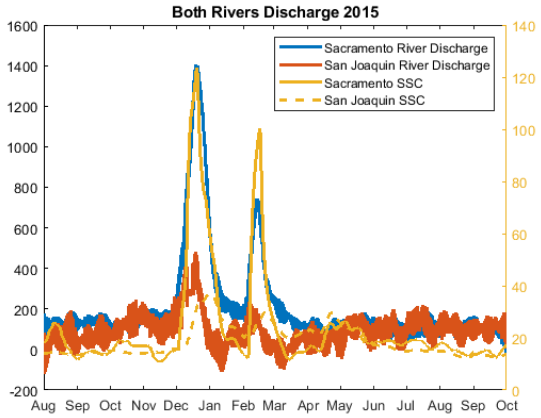

Figure A.10: River discharges from the San-Joaquin and Sacramento rivers of the Delta together with the corrected signal of sediment concentrations for each river.

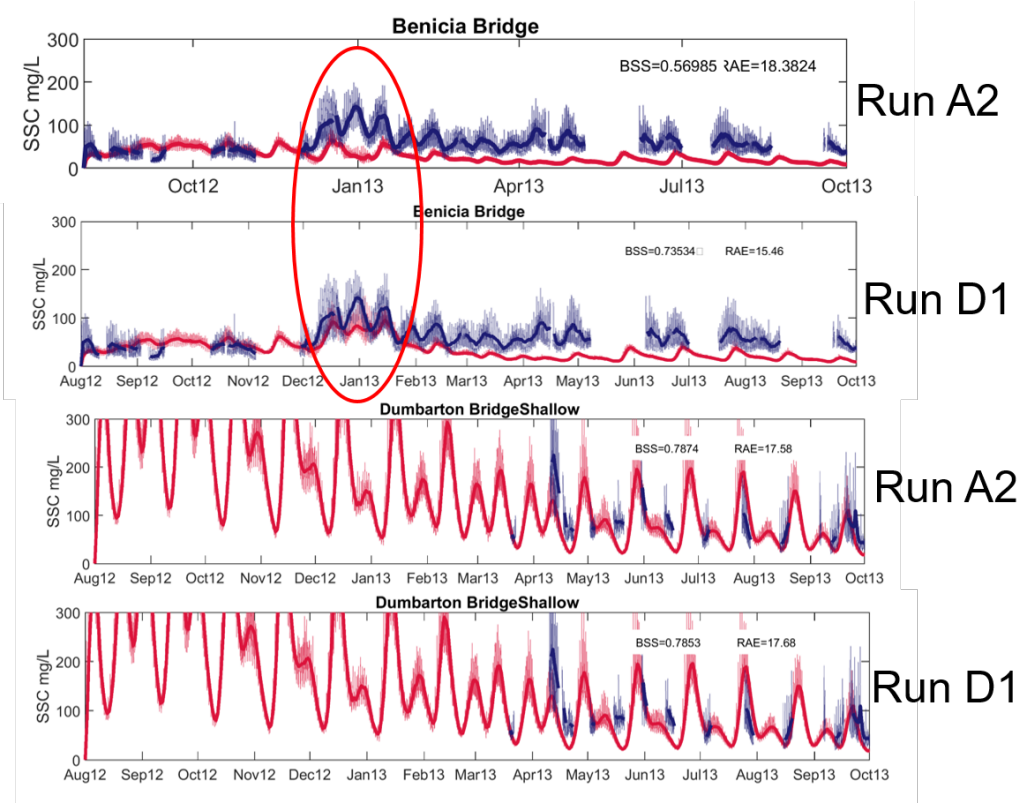

Figure A.11: Results of correcting the sediment input from the Delta Rivers for two stations in Benicia Bridge (NB) and Dumbarton Bridge (SB). With A2 before the correction and D1 after the correction.

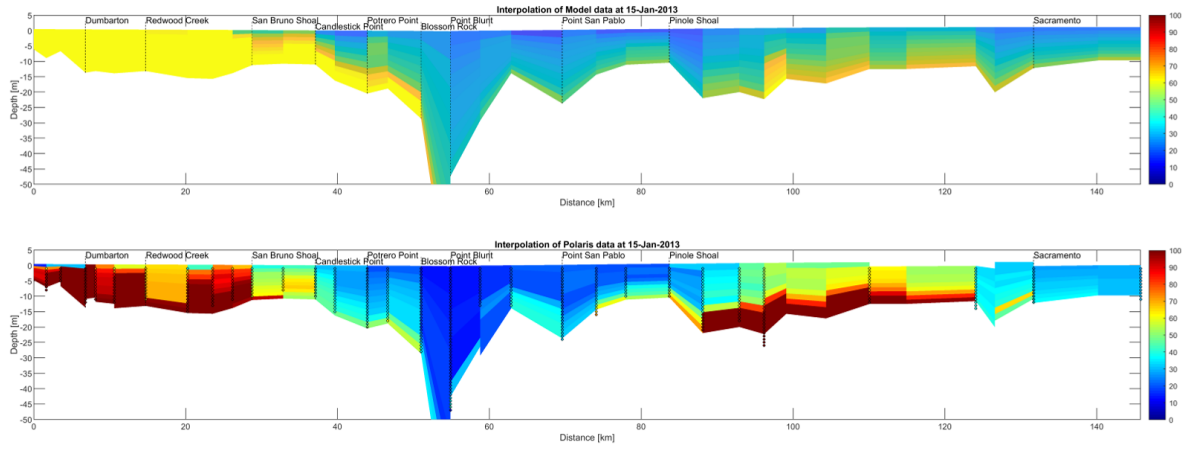

Figure A.12: Results for the Run of WY2015 for with sediment parameters and initial bed used by Gostic (2018) for the High-Frequency USGS-stations during Autumn/Winter and Spring/Summer for stations in North Bay (Richmond Bridge) and South Bay (Dumbarton Bridge). With the daily averaged modelled SSCs in thick red lines red and the measured SSCs in blue for the 8 USGS stations. Instantaneous measurements are shown in the thinner transparent lines.

B

Sediment Connectivity Results

B.1. Sediment Pathways in SB

Whereas in Chapter 5 the matrices show the combined sediment mass in the bed layer and in the water column, Figure B.1 shows the matrices for suspended sediments only. For these matrices, the difference in connectivity between the lighter (IM2) and the heavier (IM1) segment is even clearer. Fraction IM2 has a far stronger degree of connectivity.

In addition to the results discussed in Chapter 5 more analyses were conducted. To account for the difference in surface area between all the segments, the sediment transport pathways of Figure B.2 were created by dividing the gross fluxes by the surface area of the originating segment. What immediately stands out is that the conglomeration of important fluxes shifts from the northern segments to the southern segments. Though their gross fluxes are not that large, the southern segments are very dynamic relative to their size. The main direction of the fluxes are in southward direction.

The same holds for the net transport pathways normalized by the originating surface area of Figure B.3. Main pathways are located in the southern part of South Bay with the main fluxes directed towards the south. This is pattern is equal for all seasons, with exception of the fluxes located near the Bay Bridge inlet of South Bay. These fluxes are inward for Autumn and Winter but are reversed in Summer.

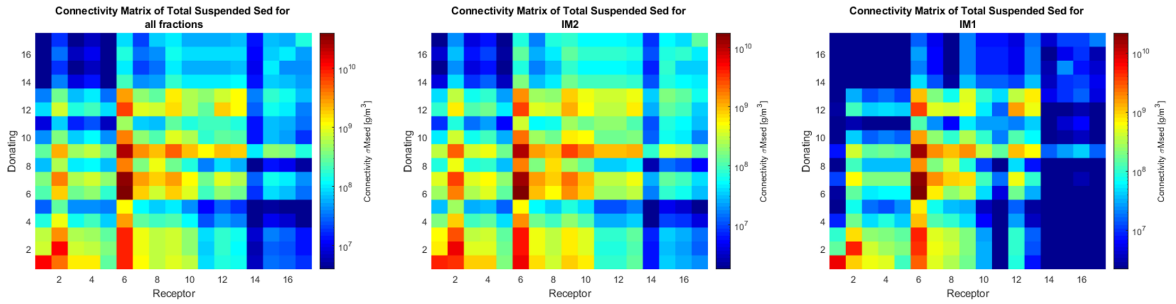

Figure B.1: Adjacency matrices for the displaced sediment mass found in suspension for all or individual sediment fractions, with rows representing the donating units and columns the receiving units. With a) the connectivity matrix for all fractions with histograms where each bar represents the sum of the corresponding row/column, b) the connectivity matrix for the larger fraction IM1 and c) the connectivity matrix for the smaller fraction IM2. A clear emerging pattern is the net transport towards the ocean (column 6). Furthermore a clear difference can be observed between the displacement of IM1 and IM2, where the smaller fraction IM2 to disperse more.

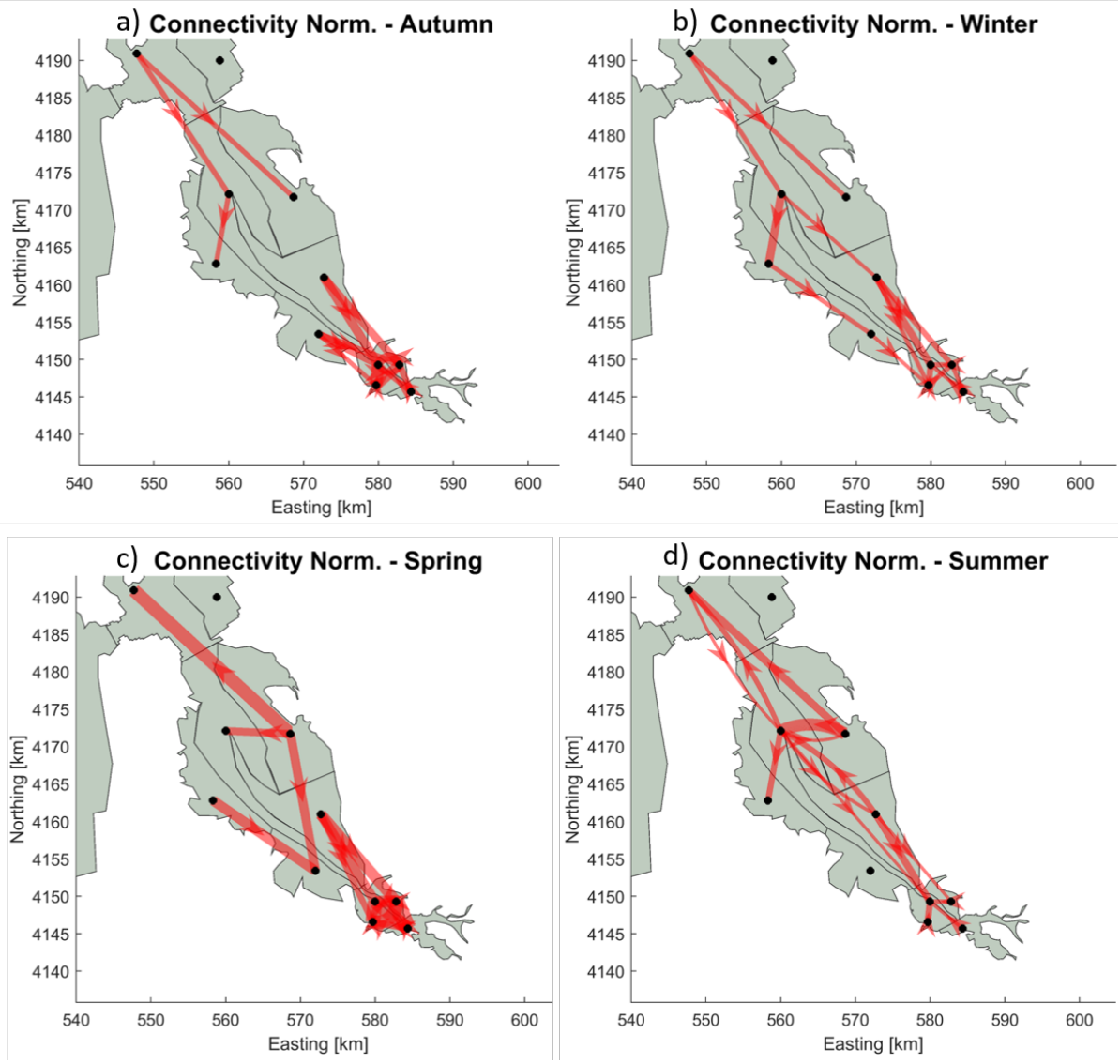

Figure B.2: Network diagram for the top 5% of connections in the network within South Bay for the four seasons of the year. The sediment fluxes are normalized by the area of the originated segment. Red arrows indicate the direction with their thickness corresponding to the strength of the connection in proportion to the largest observed connection in the network.

B.2. Ocean Exchange

The exchange of South Bay with the ocean is investigated in more detail in Figure B.4. Using the same approach to analyse incoming and outgoing sediment fluxes as in Figure 5.10 the net flux between South Bay-Ocean, is calculated. However, the modelled sediment exported by the Ocean is set to zero as in reality rarely any sediment enters the Bay from the Ocean. This plot is aimed to show the trends of export of South Bay to the Ocean during the entire year. Highest export rates are observed during Autumn and from April to mid-June. Least export is observed during Summer.

B.3. Net transport in South Bay under different forcings

Baroclinic influence

Every year three different regimes of density driven flow can be distinguished in South Bay: well-mixed from June-November, residual estuarine circulation from December-January and a classic estuarine circulation for

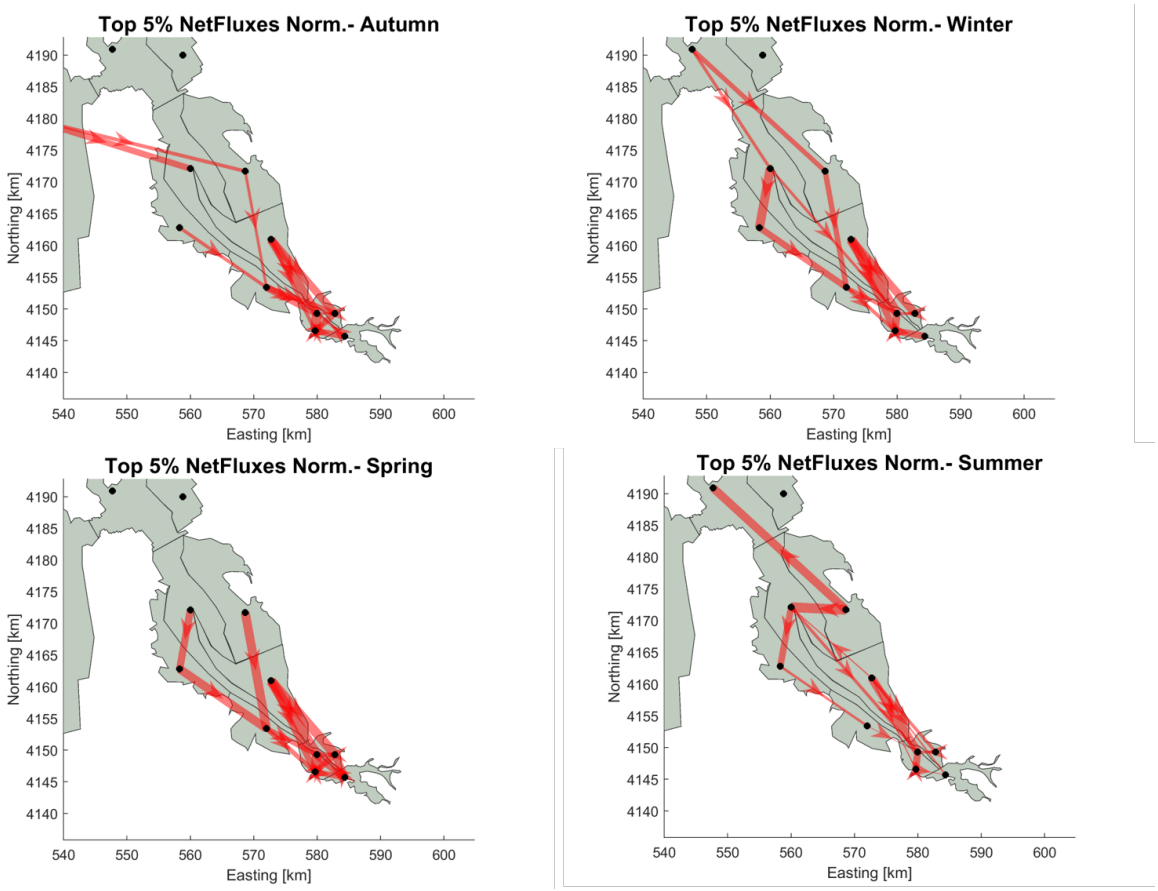

Figure B.3: Network diagram for the top 5% of net fluxes in the network within South Bay for the four seasons of the year. The sediment fluxes are normalized by the area of the originated segment. Red arrows indicate the direction with their thickness corresponding to the strength of the connection in proportion to the largest observed connection in the network.

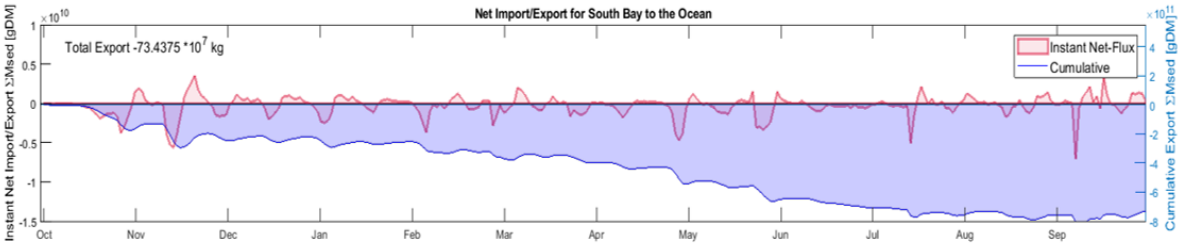

Figure B.4: Net-exchange between the Ocean and South Bay with the cumulative net transport during the year and net transport with respect to the previous output time step (δt = 1 day).Derived from the adjacency matrices with similar approach as described in Figure 5.10. A positive flux indicates transport towards the Bay and negative values indicate transport towards the ocean.

February-May. Three simulation periods of approximately 2 month duration were selected to compare net fluxes during the three different circulation regimes. As longer time periods are considered wind and tidal conditions are not exactly the same. Occasional winter storms occur during the time slot of reverse circulation, yet the period strong summer breezes from April was not selected. Figure B.5 shows the time series of the different regimes with the cumulative net-exchange for South Bay, Lower South Bay and the South Bay shoals respectively. In the right column histograms are plotted of the total net flux per segment for each circulation regime. South Bay is importing for all scenarios, though most import is observed for the scenario during the classic estuarine circulation. Most exporting seems to occur during the reversed circulation. Lower South Bay is showing an oscillating signal of import and export but turns out to be exporting for all scenarios due to an asymmetry in the signal. The histogram plots show most sediment is displaced during the scenario of classic estuarine circulation with high import in segment 6 (ocean) and export for Central Bay(segment 7) and the

Delta (segment 1).
Additionally the effect of the tide on the import during the classic circulation is analysed. Both simulation periods depicted in Figure B.6 occur during the classic estuarine circulation and tide and wind conditions are as similar as possible. The import during the classic circulation is strongest in the week surrounding neap tide. A probable explanation is that increased tidal energy of spring tides prevents stratification from developing, thereby minimizing the baroclinic effects.

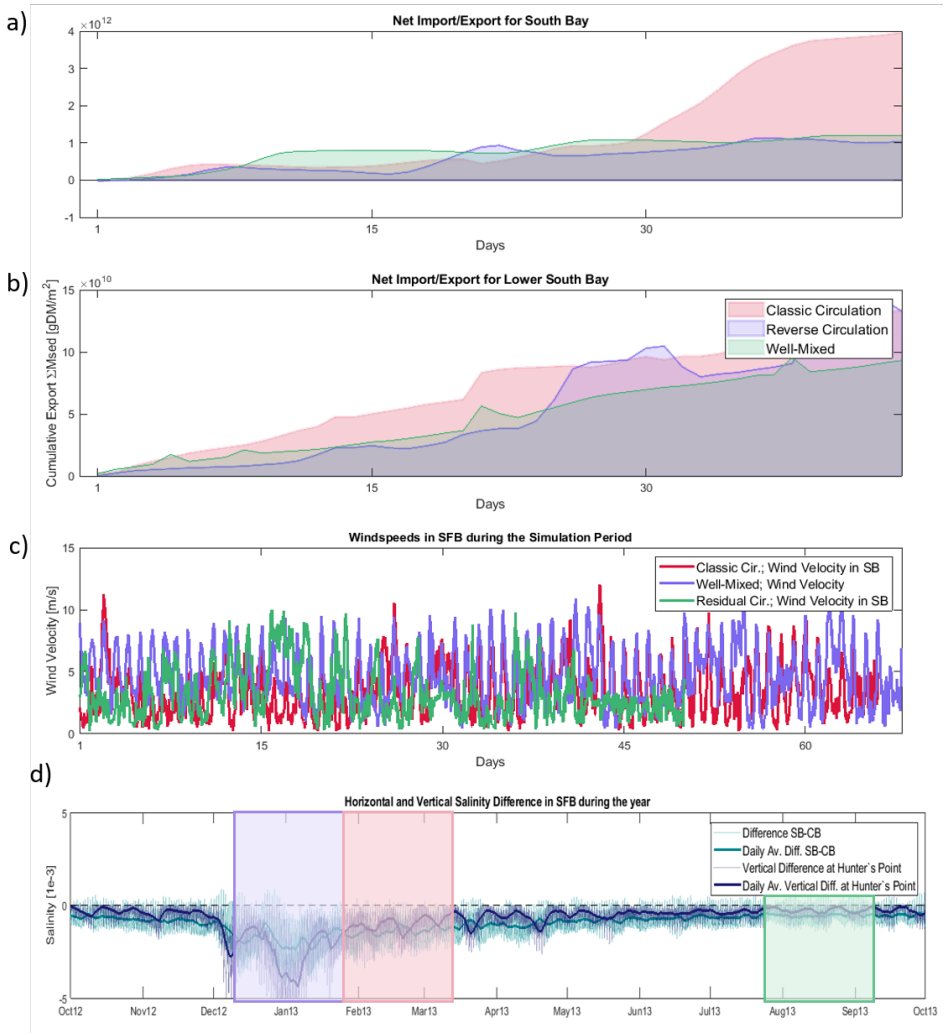

Figure B.5: Time series of net exchange of sediments at the entrance of South Bay(a), at the Dumbarton Narrows(b) and c) South Bay excluding the channel showing the cumulative net transport and net transport with respect to the previous output time step (δt = 1h03min) for three scenarios. g) Time series of horizontal and vertical salinity differences in South Bay with simulation scenarios in green(residual circulation) and purple (well-mixed) and pink(classic circulation). d,e,f)Total net transport per segment for the simulation scenario of respectively well-mixed, residual circulation and classical circulation.

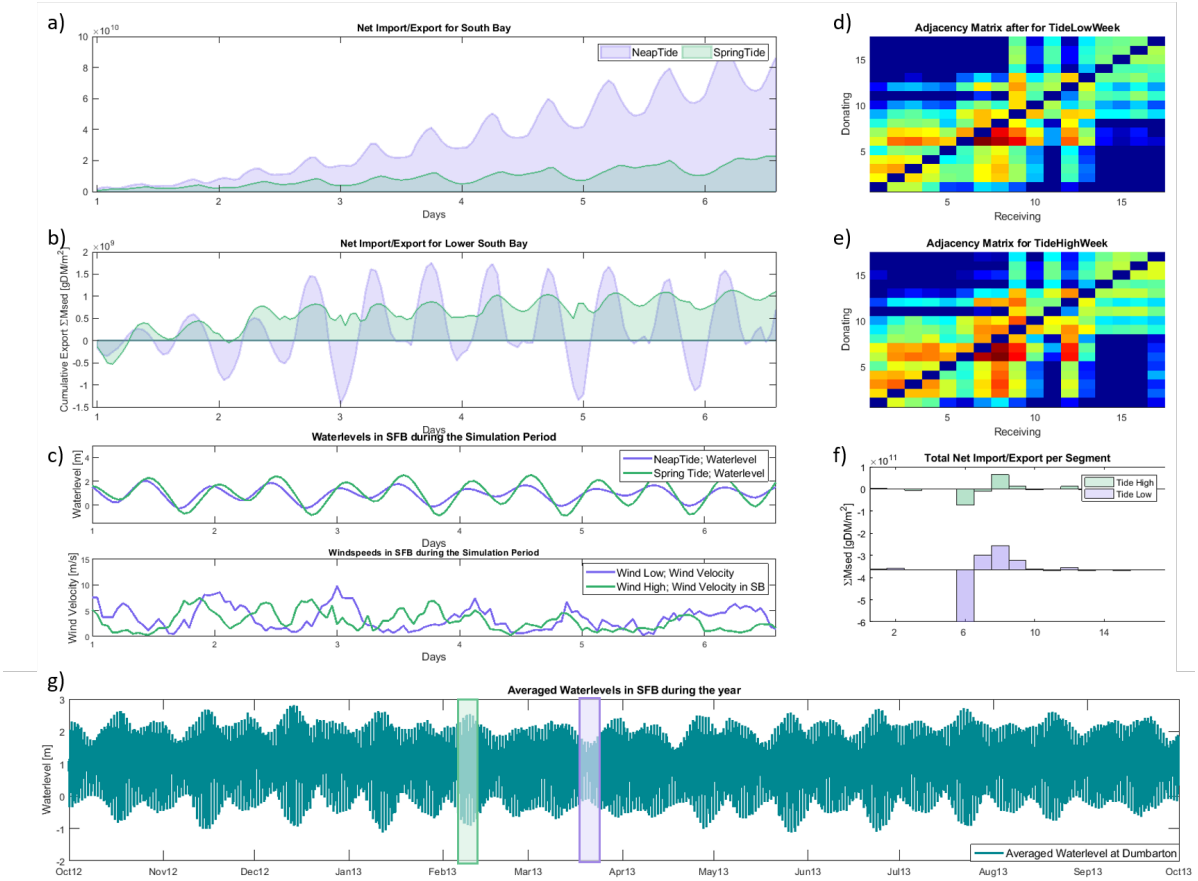

Figure B.6: Time series of net exchange of sediments at the entrance of South Bay(a) and at the Dumbarton Narrows(b) showing the cumulative net transport during the year and net transport with respect to the previous output time step (δt = 1h03min). Based on the adjacency matrix for a week surrounding neaptide(TideLow) and spring tide(TideHigh), respectively d)&e) by subtracting incoming fluxes by outgoing fluxes. c) Representation of the modelled water level at Dumbarton Bridge. g) Waterlevels at Dumbarton Bridge with the considered time periods in green(spring tide) and purple (neaptide). e)Total net transport per segment.

B.4. Correlation Analysis

Apart from the correlation analysis between the net flux and the combination of wind speed and wind direction, the correlation between net flux and respectively wind speed, horizontal salinity difference and vertical salinity difference was analysed.

Figure B.7.a shows the correlation between the net flux at Bay Bridge(sub-figure a) and Dumbarton (sub-figure b). It shows a similar correlation as for the combined wind direction and wind speed, though the precise values vary. Correlation decreased for Bay Bridge when only wind speed was considered, indicating that wind direction has an influence in determining net fluxes at Bay Bridge. The correlation coefficient increased for the Dumbarton Narrows when only wind speed was considered, indicating wind speed is more of influence than wind direction.

A correlation coefficient of r= 0.20 was found for the correlation between the net flux and the horizontal salinity gradient at Bay Bridge. Based on the physical process behind the horizontal salinity difference (classic estuarine circulation) one would expect a negative correlation coefficient. During high salinity differences and the prevailing classic circulation regime, one would expect import in stead of export. However, the period of classic estuarine circulation coincides with the period of strong south-westerly winds which are linked to the export. The forcing of wind is probably overruling the baroclinic circulations. Figure B.9 shows little correlation between the net flux and the vertical salinity gradient at both cross sections. Though salinity gradients seem to have little correlation with the net fluxes at in WY2013, this year did not experience a high freshwater water discharge from the Delta compared to other water years.

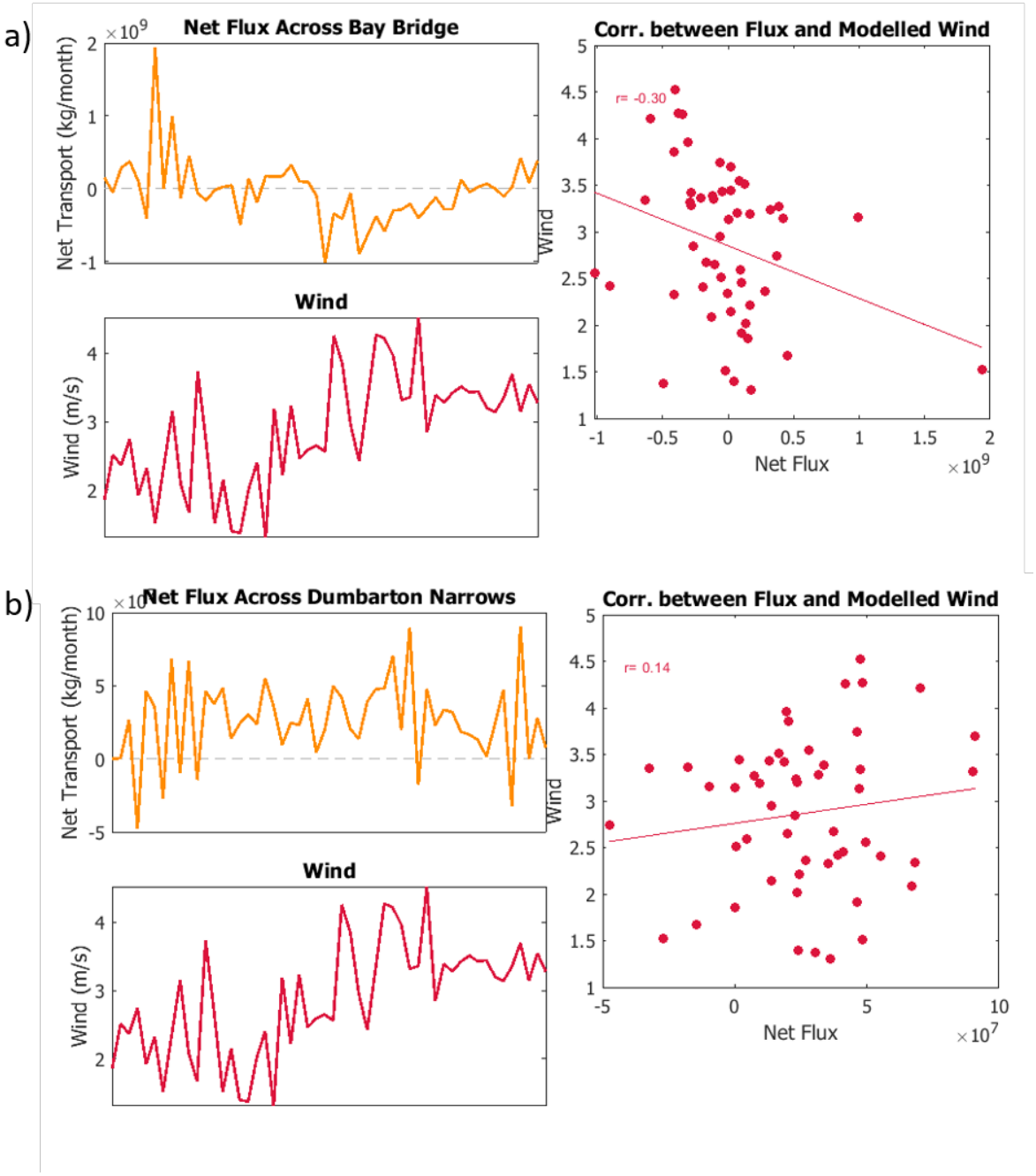

Figure B.7: Figure showing the results of the correlation analysis between net fluxes at Dumbarton Narrows, Bay Bridge and wind speed. The right panels show the scatter plots for wind speeds against the net fluxes at respectively Bay Bridge and the Dumbarton Narrows. The left panels show time-series during the simulation period of: the net flux at Bay Bridge, at the Dumbarton Narrows, wind speed.

B.5. Effect of tidal aliasing

Capturing seasonal net-transports

Tidal currents in San Francisco Bay result in large gross sediment fluxes moving back and forth each tidal cycle. Net fluxes are generally of an order smaller than the gross fluxes. Apart from errors in sediment transport due to limitations in the model, an error in gross flux might be of the same order as the net-flux. With the approach of sediment labelling, the position of all sediments is recorded at t=0 and t=end the simulation time the distribution of the sediment is retrieved. To retrieve net transports one should match the tidal phase of t=0 with that at t=end or the retrieved sediment redistribution is partially due to gross fluxes instead of solely the net-flux. Though limited by the model's output time step, the tidal phases at the start and end of

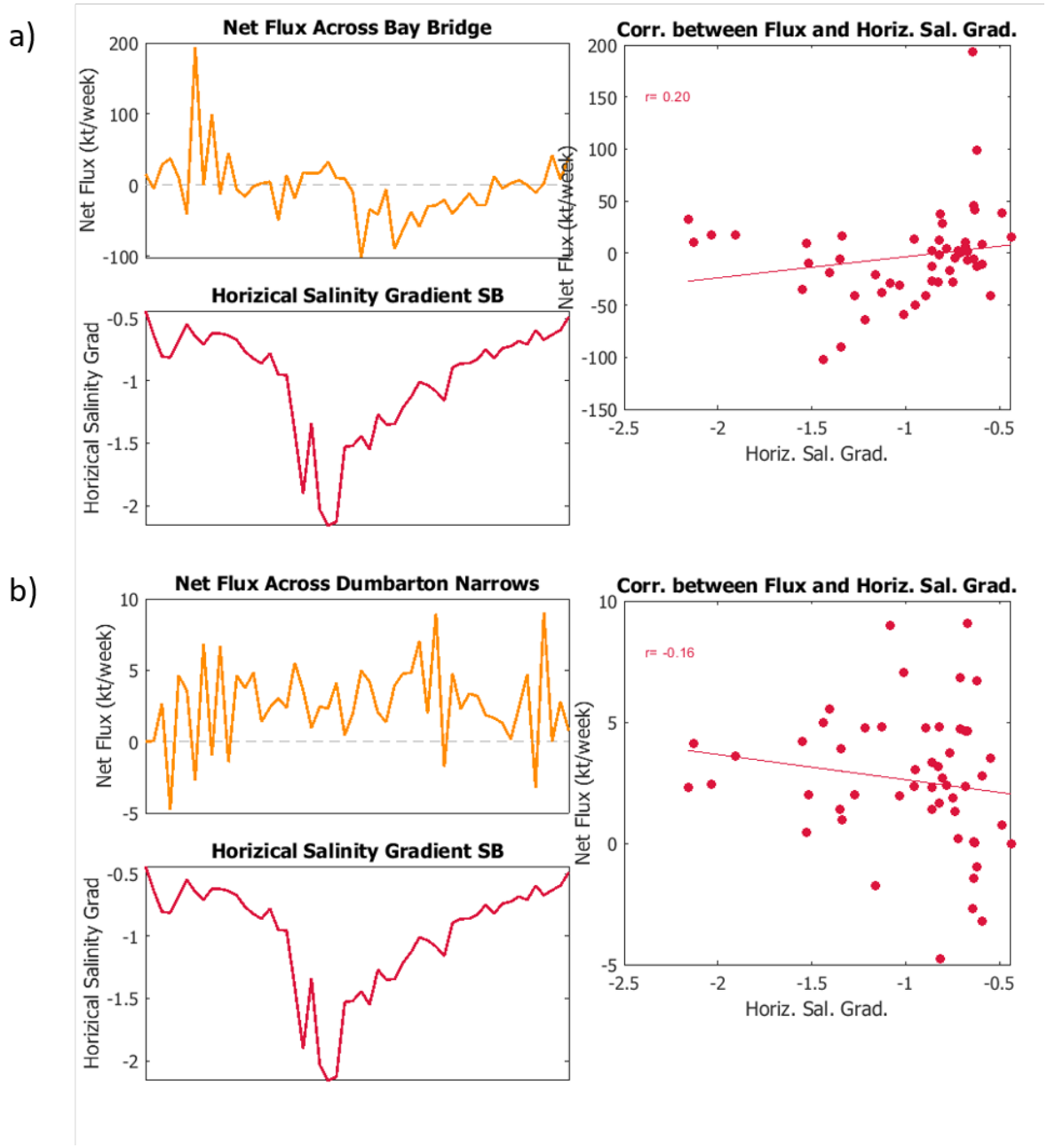

Figure B.8: Figure showing the results of the correlation analysis between net fluxes at Dumbarton Narrows, Bay Bridge and the horizontal salinity gradient. The right panels show the scatter plots for wind speeds against the net fluxes at respectively Bay Bridge and the Dumbarton Narrows. The left panels show time-series during the simulation period of: the net flux at Bay Bridge, at the Dumbarton Narrows and the horizontal salinity gradient .

each simulation are most matched as possible. As example the tidal cycles for the seasonal simulations can be found in Figure B.12 in Appendix B.

Aliasing in continuous output time steps

Though the tidal signal is semi-diurnal on a basic level, tidal harmonics are highly varying in South Bay and Lower South Bay due to its shallowness and semi-enclosed nature. As described above timing of model output and tidal phase is essential to obtain convincing estimates for net-transports. The principle semi-diurnal M2 tide (flood and ebb) has a period of about 12 h and 25 min. This consequently results in a shift of the same tidal phase being a little later each next dayEleveld et al. (2014). However, the output time step of the DELWAQ-model was specified by default as 6 full hours, completing one simulation day after 4 output time

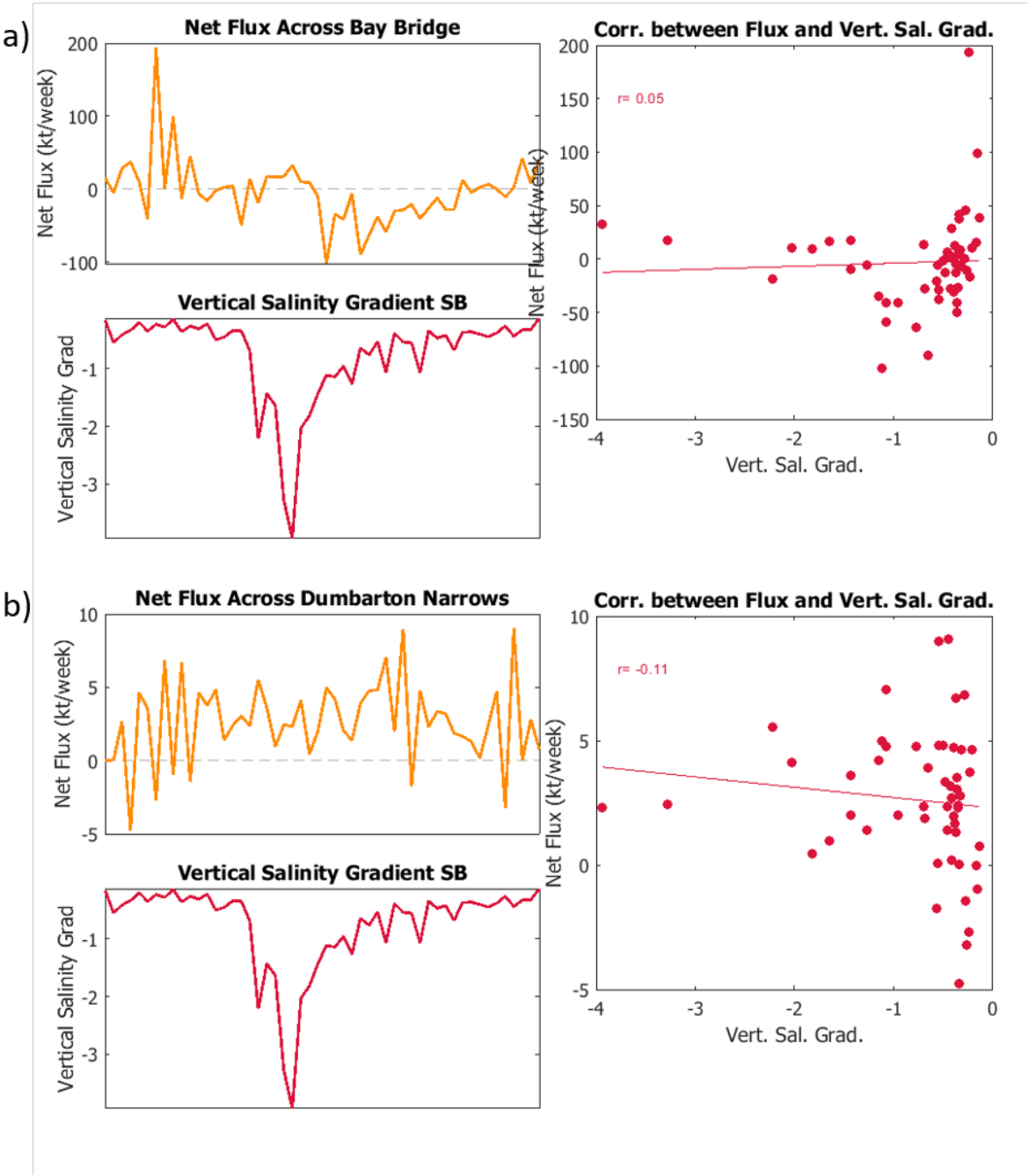

Figure B.9: Figure showing the results of the correlation analysis between net fluxes at Dumbarton Narrows, Bay Bridge and the vertical salinity gradient. The right panels show the scatter plots for vertical salinity gradients against the net fluxes at respectively Bay Bridge and the Dumbarton Narrows. The left panels show time-series during the simulation period of: the net flux at Bay Bridge, at the Dumbarton Narrows and the vertical salinity gradient.

steps. As a consequence, the model output is reported at a shifting tidal phase. Figure B.10 shows the tidal levels in January 2013 for measuring stations near Bay Bridge and the Dumbarton Narrows. To accurately describe net transports the inclusion of gross fluxes should be minimized, hence output time steps preferably occur during the same moment of tidal phase. Water levels at both Bay Bridge as the Dumbarton Narrows show a clear tidal semi-diurnal signal. In Figure B.10 the water levels are displays with the water level during the first output step displayed in black as a reference, in red the tidal level for a 24h output frequency and in blue the 24h50min output frequency. Results are based on the 24h50min output frequency, which results in only slight shifting in the tidal phase for the model output. For an output time step of 24h model output is

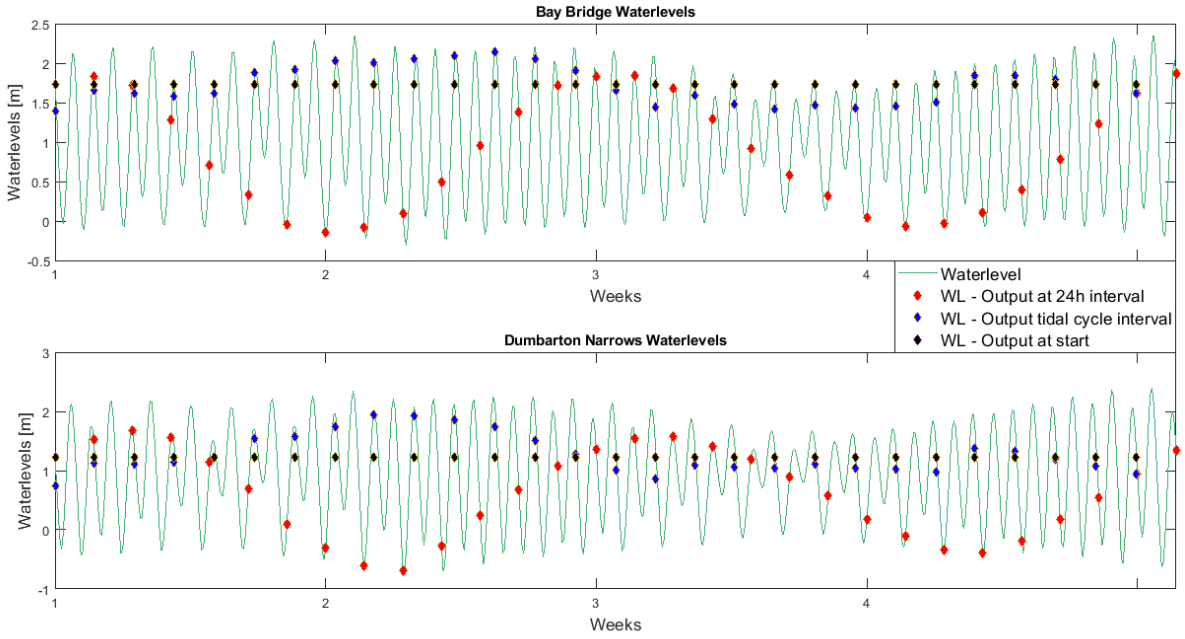

Figure B.10: Water levels at Bay Bridge (top-plot) and the Dumbarton Narrows (bottom-plot) with the water level at several optional output time steps plotted as diamonds. In red: water level and time for a 24h time step, blue: 24h50min time step, black: water level at t=0 of the tidal cycle as a reference.

generated during both flood and ebb phases. When a output frequency of 24h50min is applied the output is always generated during ebb though the precise tidal phase slightly shifts. When considering cumulative net-transport based on continuous model output during the simulation period, results with a 24h50min output time step are more trustworthy. However the results for both a 24h and a 24h50min output step are displayed in Figure B.11. Also the difference of decreasing the output time step to 12h is included in the figure. Though the smaller output time step causes small oscillations on the short timescale, the large seasonal trends are similar. Therefore on the time scales of a year, it does not make a big difference which time step is chosen, though on smaller timescales such as a week it will make difference.

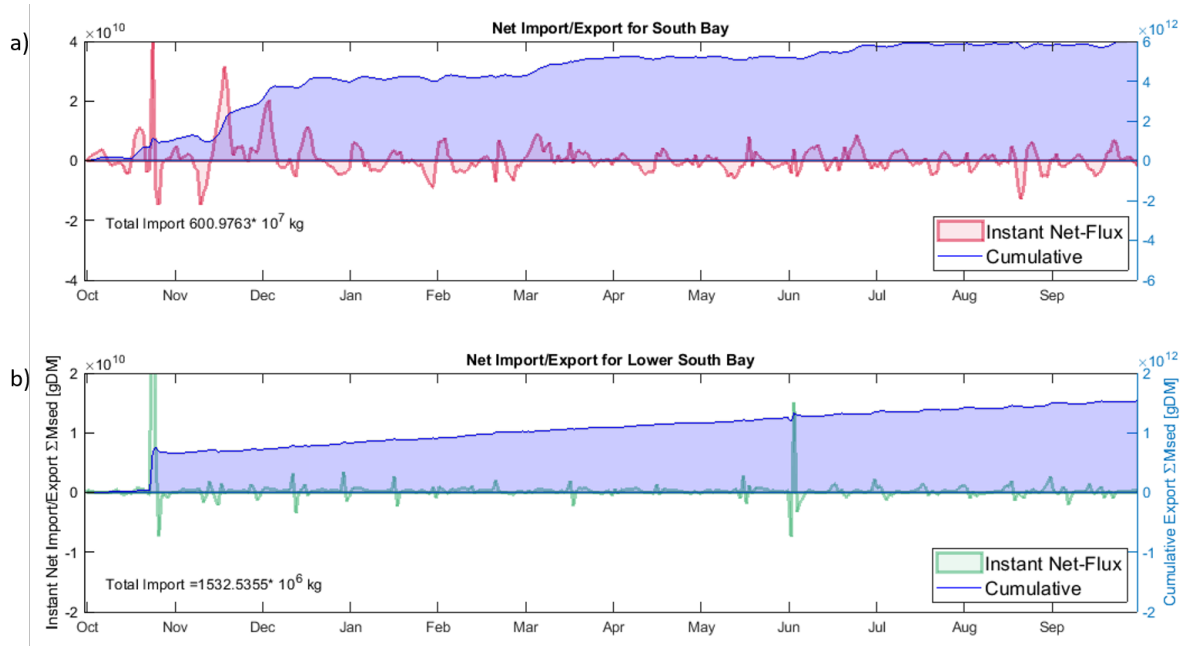

Figure B.11: Time series of net exchange of sediments at the entrance of South Bay showing the cumulative net-transport during the year and net-transport with respect to the previous output. a) time step (δt = 12h) b)time step (δt = 24h50min)

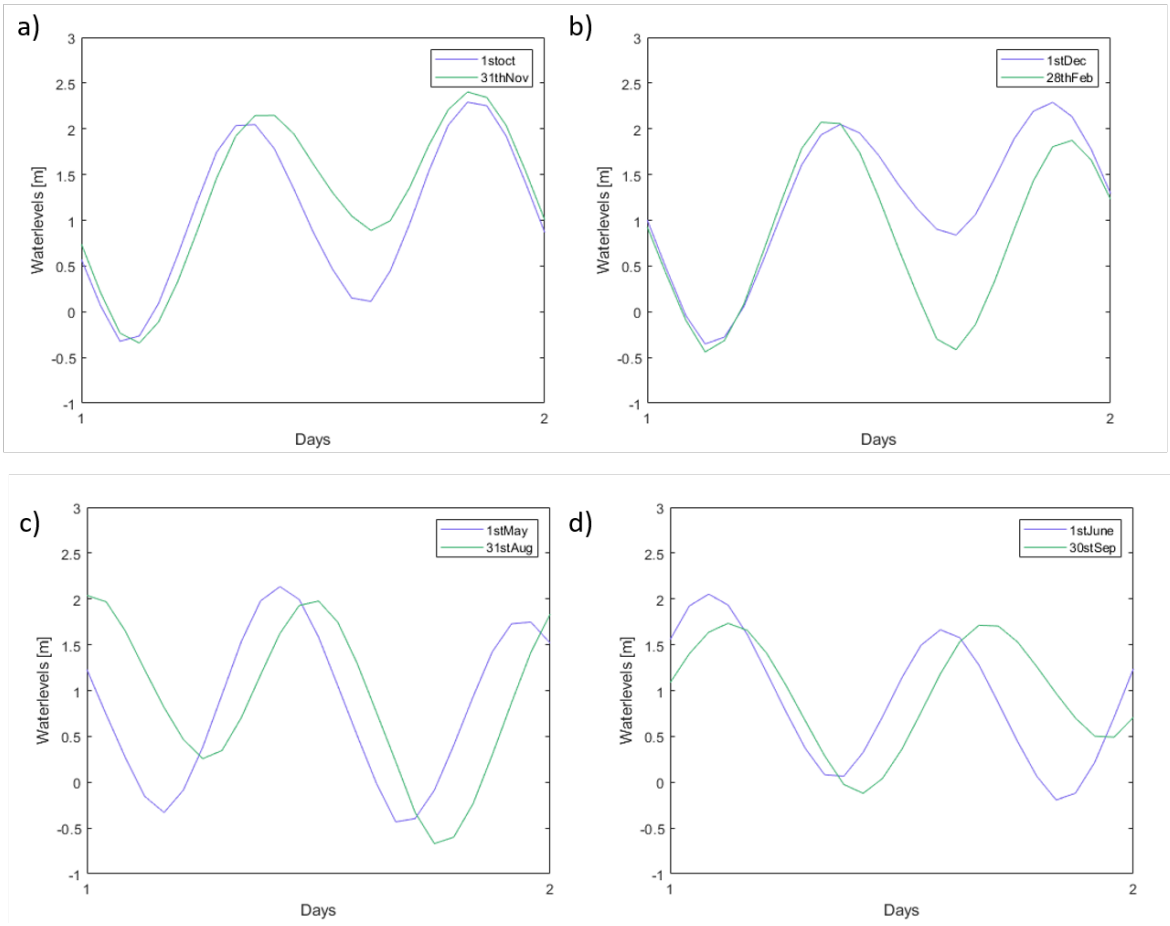

Figure B.12

Bibliography

F. M. Achete, M. Van Der Wegen, D. Roelvink, and B. Jaffe. A 2-D process-based model for suspended sediment dynamics: A first step towards ecological modeling. *Hydrol. Earth Syst. Sci.*, 19(6):2837–2857, 2015. ISSN 16077938. doi: 10.5194/hess-19-2837-2015.

Rachel M Allen, Jessica R Lacy, Mark T Stacey, and Evan A Variano. Seasonal , spring-neap , and tidal variation in cohesive sediment transport parameters in estuarine shallows. *JGR-Oceans*, 124(11):7265–7284, 2019.

I. Austen, T. J. Andersen, and K. Edelvang. The influence of benthic diatoms and invertebrates on the erodibility of an intertidal mudflat, the Danish Wadden Sea. *Estuar. Coast. Shelf Sci.*, 49(1):99–111, 1999. ISSN 02727714. doi: 10.1006/ecss.1998.0491.

Patrick L. Barnard, Li H. Erikson, Edwin P.L. Elias, and Peter Dartnell. Sediment transport patterns in the San Francisco Bay Coastal System from cross-validation of bedform asymmetry and modeled residual flux. *Mar. Geol.*, 345:72–95, 2013a. ISSN 00253227. doi: 10.1016/j.margeo.2012.10.011. URL http://dx.doi.org/10.1016/j.margeo.2012.10.011.

Patrick L. Barnard, Amy C. Foxgrover, Edwin P.L. Elias, Li H. Erikson, James R. Hein, Mary McGann, Kira Mizell, Robert J. Rosenbauer, Peter W. Swarzenski, Renee K. Takesue, Florence L. Wong, and Donald L. Woodrow. Integration of bed characteristics, geochemical tracers, current measurements, and numerical modeling for assessing the provenance of beach sand in the San Francisco Bay Coastal System. *Mar. Geol.*, 345:181–206, 2013b. ISSN 00253227. doi: 10.1016/j.margeo.2013.08.007. URL http://dx.doi.org/10.1016/j.margeo.2013.08.007.

Patrick L. Barnard, David H. Schoellhamer, Bruce E. Jaffe, and Lester J. McKee. Sediment transport in the San Francisco Bay Coastal System: An overview. *Mar. Geol.*, 345:3–17, 2013c. ISSN 00253227. doi: 10.1016/j.margeo.2013.04.005. URL http://dx.doi.org/10.1016/j.margeo.2013.04.005.

Tanya M. Beck and Ping Wang. Morphodynamics of barrier-inlet systems in the context of regional sediment management, with case studies from west-central Florida, USA. *Ocean Coast. Manag.*, 177(January):31–51, 2019. ISSN 09645691. doi: 10.1016/j.ocecoaman.2019.04.022. URL https://doi.org/10.1016/j.ocecoaman.2019.04.022.

Louis Bracken, Laura Turnbull, John Wainwright, and Patrick Bogaart. Sediment Connectivity: A Framework for Understanding Sediment Transfer at Multiple Scales. *Earth Surf. Process. landforms*, 44(February):177–188, 2015.

Andreas Brand, Jessica R. Lacy, Kevin Hsu, Daniel Hoover, Steve Gladding, and Mark T. Stacey. Wind-enhanced resuspension in the shallow waters of South San Francisco Bay: Mechanisms and potential implications for cohesive sediment transport. *J. Geophys. Res. Ocean.*, 115(11):1–15, 2010. ISSN 21699291. doi: 10.1029/2010JC006172.

Andreas Brand, Jessica R. Lacy, Steve Gladding, Rusty Holleman, and Mark Stacey. Model-based interpretation of sediment concentration and vertical flux measurements in a shallow estuarine environment. *Limnol. Oceanogr.*, 60(2):463–481, 2015. ISSN 19395590. doi: 10.1002/lno.10047.

Matthew L. Brennan, David H. Schoellhamer, Jon R. Burau, and Stephen G. Monismith. Tidal asymmetry and variability of bed shear stress and sediment bed flux at a site in San Francisco Bay, USA. *Proc. Mar. Sci.*, 5:93–107, jan 2002. ISSN 1568-2692. doi: 10.1016/S1568-2692(02)80010-9. URL https://www.sciencedirect.com/science/article/pii/S1568269202800109.

J M Caffrey and L G Miller. A comparison of two nitrification inhibitors used to measure nitrification rates in estuarine sediments. *FEMS Microbiol. Ecol.*, 17(3):213–219, jul 1995. ISSN 0168-6496. doi: 10.1111/j.1574-6941.1995.tb00145.x. URL https://doi.org/10.1111/j.1574-6941.1995.tb00145.x.

Chen Margeret. Flocculation in turbulent flow – a view into particle network. In *13th Int. Conf. Cohesive Sediment Transp. Process.*, number September, pages 1–33, Leuven, Belgium, 2015. ISBN 9789492043085. doi: 10.1109/icuas.2015.7152437.

Ralph T Cheng and Richard E Smith. a Nowcast Model for Tides and Tidal Currents in San Francisco Bay , California. pages 537–543, 1998.

Ralph T Cheng, Chi-hai Ling, W Gartner, Menlo Park, and P F Wang. Estimates of bottom roughness length and bottom shear stress in South San Francisco Bay, California. *J. Geophys. Res.*, 104(April 1999):7715–7728, 1999.

James E Cloern and Alan D Jassby. Drivers of Change in Estuarine-Coastal Ecosystems : Discoveries from Four Decades of Study in San Francisco Bay. pages 1–33, 2012. doi: 10.1029/2012RG000397.

James E Cloern, Alan D Jassby, Janet K Thompson, and Kathryn A Hieb. A cold phase of the East Pacific triggers new phytoplankton blooms in San Francisco Bay. *Proc. Natl. Acad. Sci.*, 104(47):18561 LP – 18565, nov 2007. doi: 10.1073/pnas.0706151104. URL http://www.pnas.org/content/104/47/18561.abstract.

R. A. Conomos, T. J. Walters and R. T. Cheng. Time scales of circulation and mixing processes of San Francisco Bay waters. *Hydrobiologia*, 129(1):13–36, 1985. ISSN 00188158. doi: 10.1007/BF00048685.

Wendell Cox. Demographia World Urban Areas 15 th Annual Addition. Technical report, 2019. URL http://www.demographia.com/db-worldua.pdf.

Nicole David, Lester J. Mckee, Frank J. Black, A. Russell Flegal, Christopher H. Conaway, David H. Schoellhamer, and Neil K. Ganju. Mercury concentrations and loads in a large river system tributary to San Francisco Bay, California, USA. *Environ. Toxicol. Chem.*, 28(10):2091–2100, 2009. ISSN 07307268. doi: 10.1897/08-482.1.

Susan E W De La Cruz, Lacy M Smith, Stacy M Moskal, Cheryl Strong, John Krause, Yiwei Wang, and John Y Takekawa. Trends and habitat associations of waterbirds using the South Bay Salt Pond Restoration Project, San Francisco Bay, California. Technical report, 2018. URL http://pubs.er.usgs.gov/publication/ofr20181040.

Deltares. *D-Water Quality User Manual*. Deltares, 5.06 edition, 2019.

Flick Reinhard E., Murray Joseph F., and Ewing Lesley C. Trends in United States Tidal Datum Statistics and Tide Range. *J. Waterw. Port, Coastal, Ocean Eng.*, 129(4):155–164, jul 2003. doi: 10.1061/(ASCE)0733-950X(2003)129:4(155). URL https://doi.org/10.1061/(ASCE)0733-950X(2003)129:4(155).

Galen Egan, Marianne Cowherd, Oliver Fringer, and Stephen Monismith. Observations of near-bed shear stress in a shallow , wave- and current-driven flow. *JGR Ocean.*, 124(1):1–39, 2019. doi: 10.1029/2019JC015165.

Marieke A. Eleveld, Daphne Van der Wal, and Thijs Van Kessel. Estuarine suspended particulate matter concentrations from sun-synchronous satellite remote sensing: Tidal and meteorological effects and biases. *Remote Sens. Environ.*, 143:204–215, 2014. ISSN 00344257. doi: 10.1016/j.rse.2013.12.019. URL http://dx.doi.org/10.1016/j.rse.2013.12.019.

EDWIN Elias, G U Y Gelfenbaum, MAARTEN van Ormondt, and HANS R Moritz. Predicting Sediment Transport Patterns at the mouth of the Columbia River. In *Proc. Coast. Sediments 2011*, pages 588–601. World Scientific Publishing Company, apr 2011. ISBN 978-981-4355-52-0. doi: doi:10.1142/9789814355537_0045. URL https://doi.org/10.1142/9789814355537{_}0045.

Amy C. Foxgrover, Shawn A. Higgins, Melissa K. Ingraca, Bruce E. Jaffe, and Richard E. Smith. Deposition, erosion, and bathymetric change in South San Francisco Bay : 1858-1983. Technical Report August 2014, 2004. URL http://pubs.usgs.gov/of/2004/1192/of2004-1192.pdf{%}5Cnhttp://pubs.usgs.gov/of/2004/1192/.

Theresa A. Fregoso, Amy C. Foxgrover, and Bruce E. Jaffe. Sediment deposition, erosion, and bathymetric change in central San Francisco Bay: 1855-1979. Technical Report January, 2008.

Neil K. Ganju and David H. Schoellhamer. Annual sediment flux estimates in a tidal strait using surrogate measurements. *Estuar. Coast. Shelf Sci.*, 69(1-2):165–178, 2006. ISSN 02727714. doi: 10.1016/j.ecss.2006.04.008.

Neil K. Ganju and David H. Schoellhamer. Decadal-timescale estuarine geomorphic change under future scenarios of climate and sediment supply. *Estuaries and Coasts*, 33(1):15–29, 2010. ISSN 15592723. doi: 10.1007/s12237-009-9244-y.

Jeffrey W. Gartner. Estimating suspended solids concentrations from backscatter intensity measured by acoustic Doppler current profiler in San Francisco Bay, California. *Mar. Geol.*, 211(3-4):169–187, 2004. ISSN 00253227. doi: 10.1016/j.margeo.2004.07.001.

Jeffrey W Gartner, Ralph T Cheng, David A Cacchione, and George B Tate. Near bottom velocity and suspended solids measurements in San Francisco Bay, California, 1997. URL http://pubs.er.usgs.gov/publication/70020167.

M. Gostic. *Sediment pathways in San Francisco South Bay*. PhD thesis, TU Delft, 2018.

J Letitia Grenier and Jay A Davis. Water Quality in South San Francisco Bay, California: Current Condition and Potential Issues for the South Bay Salt Pond Restoration Project BT - Reviews of Environmental Contamination and Toxicology Volume 206. pages 115–147. Springer New York, New York, NY, 2010. ISBN 978-1-4419-6260-7. doi: 10.1007/978-1-4419-6260-7_6. URL https://doi.org/10.1007/978-1-4419-6260-7{_}6.

Daniel M Hanes and Patrick L Barnard. Morphological Evolution in the San Francisco Bight. *J. Coast. Res.*, pages 469–472, mar 2007. ISSN 07490208, 15515036. URL http://www.jstor.org/stable/26481634.

Shawn A Higgins, Bruce E Jaffe, and Christopher C Fuller. Reconstructing sediment age profiles from historical bathymetry changes in San Pablo Bay, California. *Estuar. Coast. Shelf Sci.*, 73(1):165–174, 2007. ISSN 0272-7714. doi: https://doi.org/10.1016/j.ecss.2006.12.018. URL http://www.sciencedirect.com/science/article/pii/S0272771407000078.

JA Hobbs, J Cook, and P Crain. Final Report Phase 1: Tidal Marsh Restoration Benefits in South Bay Salt Pond Restoration Project, 2015.

Rusty Holleman, Emma Nuss, and David Senn. San Francisco Bay Interim Model Validation Report Prepared by Interim Model Validation Report. Technical report, 2017.

Bruce E. Jaffe, Richard E. Smith, and Amy C. Foxgrover. Anthropogenic influence on sedimentation and intertidal mudflat change in San Pablo Bay, California: 1856–1983. *Estuar. Coast. Shelf Sci.*, 73(1-2):175–187, jun 2007. ISSN 0272-7714. doi: 10.1016/J.ECSS.2007.02.017. URL https://www.sciencedirect.com/science/article/abs/pii/S0272771407000625.

By Bruce Jaffe and Amy Foxgrover. A History of Intertidal Flat Area in South San Francisco Bay , California : 1858 to 2005. *Usgs*, page 32, 2006. URL http://pubs.usgs.gov/of/2006/1262.

Allie King. Wind Over San Francsico Bay and the Sacramento-San Joaquin River Delta : Forcing for Hydrodynamic Models. Technical report, San Francisco Estuarine Institute, 2019.

N Knowles. Potential Inundation Due to Rising Sea Levels in the San Francisco Bay Region. *San Fr. Estuary Watershed Sci.*, 8(1), 2010.

Noah Knowles and Daniel R Cayan. Elevational Dependence of Projected Hydrologic Changes in the San Francisco Estuary and Watershed. *Clim. Change*, 62(1):319–336, 2004. ISSN 1573-1480. doi: 10.1023/B:CLIM.0000013696.14308.b9. URL https://doi.org/10.1023/B:CLIM.0000013696.14308.b9.

Jessica R. Lacy and Lissa J. MacVean. Wave attenuation in the shallows of San Francisco Bay. *Coast. Eng.*, 114:159–168, 2016. ISSN 03783839. doi: 10.1016/j.coastaleng.2016.03.008. URL http://dx.doi.org/10.1016/j.coastaleng.2016.03.008.

J.R. Lacy, R.M. Allen, M.R. Ferreira, J.C. Foster-Martinez, and A.C. O'Neill. Hydrodynamic and sediment transport data from San Pablo Bay and China Camp marsh (Northern San Francisco Bay), 2013-2016, 2017a. URL https://doi.org/10.5066/F7HM56MX.

J.R. Lacy, R.M. Allen, M.R. Foster-Martinez, J.C. Ferreira, and A.C. O'Neill. Hydrodynamic and sediment transport data from San Pablo Bay and China Camp marsh (Northern San Francisco Bay), 2013-2016. Technical report, 2017b. URL https://doi.org/10.5066/F7HM56MX.

Mikolaj Lewicki and Lester J McKee. New methods for estimating annual and long-term suspended sediment loads from small tributaries to San Francisco Bay. *Sediment Dyn. a Chang. Futur.*, (April 2015):121–125, 2010.

Adam H. Love, Bradley K. Esser, and James R. Hunt. Reconstructing contaminant deposition in a San Francisco Bay Marina, California. *J. Environ. Eng.*, 129(7):659–666, 2003. ISSN 07339372. doi: 10.1061/(ASCE)0733-9372(2003)129:7(659).

R. C. Martyr-Koller, H. W.J. Kernkamp, A. van Dam, M. van der Wegen, L. V. Lucas, N. Knowles, B. Jaffe, and T. A. Fregoso. Application of an unstructured 3D finite volume numerical model to flows and salinity dynamics in the San Francisco Bay-Delta. *Estuar. Coast. Shelf Sci.*, 192:86–107, 2017. ISSN 02727714. doi: 10.1016/j.ecss.2017.04.024. URL http://dx.doi.org/10.1016/j.ecss.2017.04.024.

L. J. McKee, M. Lewicki, D. H. Schoellhamer, and N. K. Ganju. Comparison of sediment supply to San Francisco Bay from watersheds draining the Bay Area and the Central Valley of California. *Mar. Geol.*, 345:47–62, 2013. ISSN 00253227. doi: 10.1016/j.margeo.2013.03.003. URL http://dx.doi.org/10.1016/j.margeo.2013.03.003.

Lester J. McKee, Neil K. Ganju, and David H. Schoellhamer. Estimates of suspended sediment entering San Francisco Bay from the Sacramento and San Joaquin Delta, San Francisco Bay, California. *J. Hydrol.*, 323(1-4):335–352, may 2006. ISSN 0022-1694. doi: 10.1016/J.JHYDROL.2005.09.006. URL https://www.sciencedirect.com/science/article/pii/S0022169405004439.

Robert H Meade. Sources, Sinks, and Storage of River Sediment in the Atlantic Drainage of the United States. *J. Geol.*, 90(3):235–252, may 1982. ISSN 0022-1376. doi: 10.1086/628677. URL https://doi.org/10.1086/628677.

Mick van der Wegen; Bruce Jaffe; Johan Reyns; Amy Foxgrover. Modeling morphodynamic development in the Alviso Slough system , South San Francisco Bay.

A. K. Miles. Science Support for Wetland Restoration in the Napa-Sonoma Salt Ponds, San Francisco Bay Estuary, 2007.

Richard Mooi, Victor Smith, Meg Burke, Terrence Gosliner, Chrissy Piotrowski, and Rebecca Ritger. *Animals of San Francisco Bay: a field guide to its common benthic species.* jan 2007.

M. E.J. Newman. The structure and function of complex networks. *SIAM Rev.*, 45(2):167–256, 2003. ISSN 00361445. doi: 10.1137/S003614450342480.

Jaap H. Nienhuis and Andrew D. Ashton. Mechanics and rates of tidal inlet migration: Modeling and application to natural examples. *J. Geophys. Res. Earth Surf.*, 121(11):2118–2139, 2016. ISSN 21699011. doi: 10.1002/2016JF004035.

S G Pearson, B C Van Prooijen, E P L Elias, and Z B Wang. Sediment Connectivity : A Framework for Analyzing Coastal Sediment Transport Pathways. *Submitt. to J. Geophys. Res. Earth Surf.*, 2020.

Jonathan D Phillips, Wolfgang Schwanghart, and Tobias Heckmann. Graph theory in the geosciences. *Earth-Science Rev.*, 143:147–160, 2015. ISSN 0012-8252. doi: https://doi.org/10.1016/j.earscirev.2015.02.002. URL http://www.sciencedirect.com/science/article/pii/S0012825215000239.

S. Pubben. *3D Mixing Patterns in San Francisco South Bay.* PhD thesis, 2017.

V. Rossi, E. Ser-Giacomi, C. Lòpez, and E. Hernández-García. Hydrodynamic provinces and oceanic connectivity from a transport network help designing marine reserves. *Geophys. Res. Lett.*, 41(8):2883–2891, 2014. doi: 10.1002/2014GL059540.Received.

Mikail Rubinov and Olaf Sporns. NeuroImage Complex network measures of brain connectivity : Uses and interpretations. *Neuroimage*, 52(3):1059–1069, 2010. ISSN 1053-8119. doi: 10.1016/j.neuroimage.2009.10.003. URL http://dx.doi.org/10.1016/j.neuroimage.2009.10.003.

San Francisco Bay Comission. Salt Ponds Staff Report. Technical report, 2005.

D. Schoellhamer, L. McKee, S. Pearce, P. Kauhanen, M. Salomon, S. Dusterhoff, L. Grenier, M. Marineau, and P. Trowbridge. Sediment Supply to San Francisco Bay, Water Years 1995 through 2016: Data, trends, and monitoring recommendations to support decisions about water quality, tidal wetlands, and resilience to sea level rise. Technical Report 842, 2018.

D H Schoellhamer, N K Ganju, J W Gartner, M C Murrell, and S A Wright. Seasonal and longitudinal homogeneity of suspended sediment in San Francisco Bay, California. Technical report, 2003. URL http://pubs.er.usgs.gov/publication/70175035.

David H. Schoellhamer. Factors affecting suspended-solids concentrations in South San Francisco Bay, California. *J. Geophys. Res. C Ocean.*, 101(C5):12087–12095, 1996. ISSN 01480227. doi: 10.1029/96JC00747.

David H. Schoellhamer. Sudden Clearing of Estuarine Waters upon Crossing the Threshold from Transport to Supply Regulation of Sediment Transport as an Erodible Sediment Pool is Depleted: San Francisco Bay, 1999. *Estuaries and Coasts*, 34(5):885–899, 2011. ISSN 15592723. doi: 10.1007/s12237-011-9382-x.

Gregory G. Shellenbarger, Scott A. Wright, and David H. Schoellhamer. A sediment budget for the southern reach in San Francisco Bay, CA: Implications for habitat restoration. *Mar. Geol.*, 345:281–293, 2013. ISSN 00253227. doi: 10.1016/j.margeo.2013.05.007. URL http://dx.doi.org/10.1016/j.margeo.2013.05.007.

Manoochehr Shirzaei and Roland Bürgmann. Global climate change and local land subsidence exacerbate inundation risk to the San Francisco Bay Area. *Sci. Adv.*, 4(3):eaap9234, mar 2018. doi: 10.1126/sciadv.aap9234. URL http://advances.sciencemag.org/content/4/3/eaap9234.abstract.

AB Shvidchenko, RC MacArthur, and BR Hall. Historic sedimentation in Sacramento–San Joaquin Delta. *Interag. Ecol. Progr. San Fr. Estuary Newsl.*, 17(3):21–30, 2004.

R Soulsby, C Mead, Brigitte Wild, and Matthew Wood. Lagrangian Model for Simulating the Dispersal of Sand-Sized Particles in Coastal Waters. *J. Waterw. Port, Coastal, Ocean Eng.*, 137, may 2011. doi: 10.1061/(ASCE)WW.1943-5460.0000074.

Laura Turnbull, Marc-thorsten Hütt, Andreas A Ioannides, Stuart Kininmonth, Ronald Poeppl, Klement Tockner, Louise J Bracken, Saskia Keesstra, Lichan Liu, Rens Masselink, and Anthony J Parsons. Connectivity and complex systems : learning from a multi-disciplinary perspective. *Appl. Netw. Sci.*, 3(11), 2018.

M Van Der Wegen, A Dastgheib, B E. Jaffe, and D Roelvink. Bed composition generation for morphodynamic modeling: Case study of San Pablo Bay in California, USA. *Ocean Dyn.*, 61(2-3):173–186, 2011. ISSN 16167341. doi: 10.1007/s10236-010-0314-2.

O M Oxana van Kempen. Sediment pathways in San Francisco South Bay. *TU Delft*, 2017.

Thijs van Kessel, Joris Vanlede, and Johan de Kok. Development of a mud transport model for the Scheldt estuary. *Cont. Shelf Res.*, 31(10 SUPPL.):S165–S181, 2011. ISSN 02784343. doi: 10.1016/j.csr.2010.12.006. URL http://dx.doi.org/10.1016/j.csr.2010.12.006.

D.S. van Maren and K Cronin. Uncertainty in complex three-dimensional sediment transport models: equifinality in a model application of the Ems Estuary, the Netherlands. *Ocean Dyn.*, 66(12):1665–1679, 2016. ISSN 16167228. doi: 10.1007/s10236-016-1000-9. URL http://dx.doi.org/10.1007/s10236-016-1000-9.

John Wainwright, Laura Turnbull, Tristan G Ibrahim, Irantzu Lexartza-artza, Steven F Thornton, and Richard E Brazier. Geomorphology Linking environmental régimes , space and time : Interpretations of structural and functional connectivity. *Geomorphology*, 126(3-4):387–404, 2011. ISSN 0169-555X. doi: 10.1016/j.geomorph.2010.07.027. URL http://dx.doi.org/10.1016/j.geomorph.2010.07.027.

Richard Walker. Industry builds the city the suburbanization of manufacturing in SFB., 2001.

Sienna R White. *A Numerical Model for Sediment Flux and Flocculation in San Francisco Bay.* PhD thesis, 2019.

S. Wright and D. Schoellhamer. Trends in the Sediment Yield of the Sacramento River , California , 1957 – 2001. *San Fr. Estuary Watershed Sci.*, 2, 2004.